TTI: 2-8-87-1159

PB92-218007

TEXAS TRANSPORTATION INSTITUTE

DETERMINING DEPTH TO APPARENT STIFF LAYER FROM FWD DATA

RESEARCH REPORT 1159-1

COOPERATIVE RESEARCH PROGRAM

TEXAS TRANSPORTATION INSTITUTE
THE TEXAS A&M UNIVERSITY SYSTEM
COLLEGE STATION, TEXAS

TEXAS DEPARTMENT OF TRANSPORTATION

in cooperation with the
U.S. Department of Transportation
Federal Highway Administration

TECHNICAL REPORT STANDARD TITLE PAGE

1. Report Number	2.	3. Recipient's Catalog No.
FHWA/TX-91-1159-1	PB92-218007	
4. Title and Subtitle Determining Depth to Apparent Stiff Layer From FWD Data		5. Report Date October, 1991 6. Performing Organization Code
7. Author(s) G. T. Rohde and R. E. Smith		8. Performing Organization Report No. Research Report 1159-1
9. Performing Organization Name and Address Texas Transportation Institute The Texas A&M University System College Station, Texas 77843		10. Work Unit No. 11. Contract or Grant No. Study No. 2-8-87-1159
12. Sponsoring Agency Name and Address Texas Department of Transportation Transportation Planning Division P.O. Box 5051 Austin, Texas 78763		13. Type of Report and Period Covered 14. Sponsoring Agency Code

15. Supplementary Notes

Research performed in cooperation with USDOT, FHWA.
Research Study Title: The Mechanistic Analysis of Pavement Deflections on Subgrades Varying in Stiffness with Depth.

16. Abstract

Nondestructive deflection testing (NDT) has become an integral part of the structural evaluation of pavements. Interpretation of the measured deflection data is extremely complex, and the analyzed pavement is often modelled as a multilayered elastic system. In this model the subgrade is usually defined as uniformly stiff and infinitely thick or a rigid layer is placed at an arbitrary depth. The actual subgrade on which the tested pavement structure is founded, varies considerably from this model. It is not infinitely thick, and whether the subgrade is sedimentary or residual in nature, its stiffness normally changes with depth. This change in stiffness can be due to shallow bedrock, material differences, the stress history, or an apparent increase in stiffness due to the stress dependant behavior of most soils.

In this study a method to determine the depth to an apparent rigid layer from surface deflections is developed. This method is based on Bousinesq's equation and is related to a three layer linear elastic system through an extensive regression analysis. The procedure is validated using field data. The inclusion of an apparent rigid layer into the pavement model led to considerable improvements in the backcalculated layer moduli.

17. Key Words	18. Distribution Statement
Pavement Analysis Deflection Testing	No restrictions. This document is available to the public through the National Technical Information Service 5285 Port Royal Road Springfield, Virginia 22161

19. Security Classif.(of this report)	20. Security Classif.(of this page)	21. No. of Pages	22. Price
Unclassified	Unclassified	169	

Form DOT F 1700.7 (8-69)

DETERMINING DEPTH TO APPARENT STIFF LAYER FROM FWD DATA

by

Gustav T. Rohde
Roger E. Smith

Research Report 1159-1
Research Study 2-8-87-1159

Sponsored by

The Texas Department of Transportation

in cooperation with

The U. S. Department of Transportation
Federal Highway Administration

Texas Transportation Institute
Texas A&M University
College Station, Texas 77843

October, 1991

METRIC (SI*) CONVERSION FACTORS

APPROXIMATE CONVERSIONS TO SI UNITS

Symbol	When You Know	Multiply By	To Find	Symbol
	LENGTH			
in	inches	2.54	centimetres	cm
ft	feet	0.3048	metres	m
yd	yards	0.914	metres	m
mi	miles	1.61	kilometres	km
	AREA			
in^2	square inches	645.2	centimetres squared	cm^2
ft^2	square feet	0.0929	metres squared	m^2
yd^2	square yards	0.836	metres squared	m^2
mi^2	square miles	2.59	kilometres squared	km^2
ac	acres	0.395	hectares	ha
	MASS (weight)			
oz	ounces	28.35	grams	g
lb	pounds	0.454	kilograms	kg
T	short tons (2000 lb)	0.907	megagrams	Mg
	VOLUME			
fl oz	fluid ounces	29.57	millilitres	mL
gal	gallons	3.785	litres	L
ft^3	cubic feet	0.0328	metres cubed	m^3
yd^3	cubic yards	0.0765	metres cubed	m^3

NOTE: Volumes greater than 1000 L shall be shown in m^3.

TEMPERATURE (exact)

°F	Fahrenheit temperature	5/9 (after subtracting 32)	Celsius temperature	°C

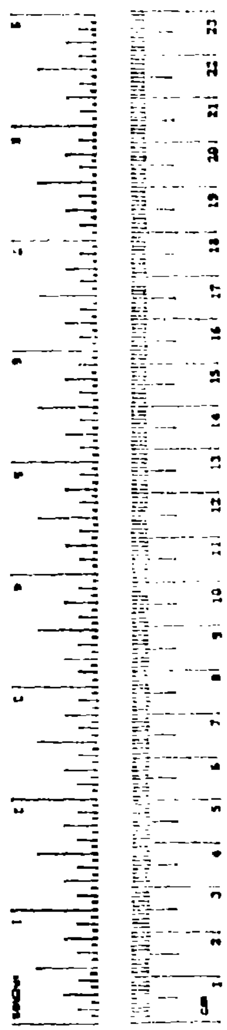

APPROXIMATE CONVERSIONS TO SI UNITS

Symbol	When You Know	Multiply By	To Find	Symbol
	LENGTH			
mm	millimetres	0.039	inches	in
m	metres	3.28	feet	ft
m	metres	1.09	yards	yd
km	kilometres	0.621	miles	mi
	AREA			
mm^2	millimetres squared	0.0016	square inches	in^2
m^2	metres squared	10.764	square feet	ft^2
km^2	kilometres squared	0.39	square miles	mi^2
ha	hectares (10 000 m^2)	2.53	acres	ac
	MASS (weight)			
g	grams	0.0353	ounces	oz
kg	kilograms	2.205	pounds	lb
Mg	megagrams (1 000 kg)	1.103	short tons	T
	VOLUME			
mL	millilitres	0.034	fluid ounces	fl oz
L	litres	0.264	gallons	gal
m^3	metres cubed	35.315	cubic feet	ft^3
m^3	metres cubed	1.308	cubic yards	yd^3

TEMPERATURE (exact)

°C	Celsius temperature	9/5 (then add 32)	Fahrenheit temperature	°F

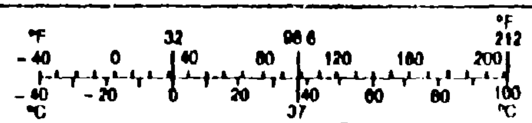

These factors conform to the requirement of FHWA Order 5190.1A.

* SI is the symbol for the International System of Measurements

IMPLEMENTATION STATEMENT

The findings of this study show that a stiff layer below the subgrade will have a significant impact on the moduli values of pavement layers. When deflection testing is used, the depth to this stiff layer must be known before the data can be analyzed to determine accurate in-situ layer stiffnesses. Failure to consider the depth to stiff layers in backcalculation of layer stiffness values can result in unconservative designs of new and rehabilitated pavements.

A method was developed in the study to estimate the depth to a stiff layer below the subgrade from deflection test data. Some subgrade materials have stress sensitive moduli values. This creates a change in the effective stiffness which can act like an equivalent stiff layer. The procedure developed will also address this situation.

The procedure developed in this study should be used to estimate the depth to bedrock, other stiff layer, or apparent stiff layer in all procedures based on elastic layer concepts which calculate moduli values from deflection data, unless the actual depths to stiff layers and changes in apparent stiffnesses are known from test results. This procedure has been implemented in the TxDOT MODULUS 4.0 backcalculation procedure which should be used to backcalculate layer stiffnesses of asphalt concrete pavements from deflection data.

DISCLAIMER

The contents of this report reflect the view of the authors who are responsible for the opinions, findings, and conclusions presented herein. The contents do not necessarily reflect the official views or policies of the Federal Highway Administration. The report does not constitute a standard, specifications, or regulation.

There is no invention or discovery conceived or first actually reduced to practice in the course of or under this contract, including any art, method, process, machine, manufacture, design or composition of matter, or any new or useful improvement thereof, or any variety of plant which is or may be patentable under the patent law of the United States of America or any foreign country. This report is not intended for construction, bidding or permit purposes.

TABLE OF CONTENTS

TABLE OF CONTENTS (Continued)

TABLE OF CONTENTS (Continued)

LIST OF TABLES

LIST OF TABLES

LIST OF FIGURES

LIST OF FIGURES

LIST OF FIGURES

CHAPTER I
INTRODUCTION

GENERAL

The work described in this report is the development of a procedure to address stiff layers in backcalculating layer moduli values from deflection testing. It is based on an analysis of nondestructive deflection data on sections with the subgrade stiffness changing with depth. This change can be due to layered material, rigid layers underlying the subgrade, or an apparent increase in stiffness with depth due to the stress dependent behavior of soils. A procedure to predict the depth to an apparent rigid layer below the subgrade is developed and verified. This apparent rigid layer can be used in a multilayered elastic pavement model to account for rigid layers or an increase in subgrade stiffness with depth.

In recent years flexible pavement design has evolved to a level in which designs are based on mechanistic-empirical procedures (Thompson 1989). In such design procedures, stresses, strains, and deflections induced by a wheel load are theoretically calculated in a multilayered pavement system. These pavement responses are then transformed into pavement performance parameters such as cracking or rutting using performance models and empirical relationships (Rohde et al. 1989). In most existing mechanistic-empirical procedures, the pavement is modelled as a multilayered linear elastic system. To calculate the pavement responses under a wheel load, the thickness and material stiffness of each layer in the pavement structure are required.

The stiffness, or elastic modulus, of a pavement material can be obtained in two basic ways. The first uses laboratory testing of material samples. By preparing the sample to simulate field conditions and applying a repetitive load, the elastic modulus of the material is determined (Barksdale and Hicks 1973). Second, the elastic modulus can be obtained by testing the material inplace by using nondestructive techniques. Nondestructive test methods (Lytton 1989) are gaining popularity because they are rapid and relatively inexpensive. The results are also believed to be more representative than laboratory results because the pavement materials are tested in a truly undisturbed state.

Nondestructive deflection testing has become an integral part of the structural evaluation of pavements during the last few decades. From the many static, vibratory, impulse, and vehicular devices (Smith and Lytton 1984), the falling weight deflectometer (FWD) has evolved as one of the most used devices for pavement evaluation (Hoffman 1983, Lytton et al. 1987, Yang 1988). By dropping a mass from a predetermined height onto a specially designed baseplate resting on the pavement surface, the pavement is subjected to an impulse similar to that applied by a moving wheel load (Sorensen and Hayven 1982). The versicle deflection of the pavement is measured through a series of velocity transducers (geophones) at various distances from the baseplate.

Interpretation of the measured deflection data is extremely complex. The response of the pavement structure depends not only on the type and rate of loading but also the stress state, temperature, the suction of the various materials, and the stratigraphy of the pavement section (Rwenbangira et al. 1987). A popular method to analyze deflection data is through elastostatic methods using multilayered elastic principles as first presented by Burmister (1948). The pavement is modelled as a multilayered elastic system founded on a semi-infinite subgrade. It is assumed that all materials are linear elastic, homogeneous, isotropic, and infinite in the horizontal extent (Yoder and Witczak 1975, Yang 1972). The mathematical models were developed to determine pavement responses. Typically, the deflection, stress, and strain induced by a known load are calculated.

The analysis of measured pavement deflections is an inverse process. Instead of predicting the pavement response, it is measured and the pavement properties are "backcalculated." Using iterative programs (Irwin 1983, Bush and Alexander 1985), nomographs (Hoffman and Thompson 1981), or pattern-search techniques (Uzan et al. 1989), the stiffness of each layer in the pavement structure can be determined from the measured load and deflections.

PROBLEM STATEMENT

Although static backcalculation procedures are sophisticated and well developed, several concerns and problems arise in their application. In modelling the pavement during an analysis, the subgrade is usually defined as uniformly stiff. The subgrade thickness is assumed to be infinitely thick, or in some procedures, a rigid layer is placed at an arbitrary depth. The actual subgrade on which the tested pavement structure is founded varies considerably from this model. It is not infinitely thick, and, whether the subgrade is sedimentary or residual in nature, its stiffness normally changes with depth. This change in stiffness can be due to material differences, the stress history, or an apparent increase in stiffness due to the stress dependant behavior of most soils. Furthermore, in many geographic areas rigid layers are encountered within the influence sphere of the falling weight.

As reported by several researchers, the existence of a rigid layer or bedrock at shallow depths has a profound effect on the analysis of deflection data (Uddin et. al. 1986, Briggs and Nazarian 1989). Presently, the majority of backcalculation procedures ignores the existence of a rigid layer and models the subgrade as an infinite halfspace. As a result, the stiffness of the subgrade is overpredicted. This can lead to unconservative pavement designs since the thickness is dependent on the stiffness of the supporting subgrade.

The only way to determine the depth to rigid layers in pavements has been through coring, boring, penetration, or seismic tests. Pavements cover such a large area that it is impractical to use penetration devices and seismic techniques to determine the depth to stiff layers at every point tested with deflection devices. Ideally the depth to a rigid layer should be inferred from the measured deflection information.

It is hypothesized that problems associated with analyzing pavements on subgrades with underlying rigid layers also will arise in the analyses of data on pavements with subgrades increasing in stiffness with depth. The most accurate way to analyze deflections on such a pavement structure is through the use of a finite element model. This allows for the change in material stiffness in the vertical and horizontal extent. Although a nonlinear elastic backcalculation procedure is used in this study, it is not a practical option for everyday deflection analysis. It is time consuming and requires considerable computational power and sophisticated material characterization. A simplified and faster approach which accounts for subgrades stiffening in depth is required for routine use.

RESEARCH OBJECTIVES

The overall objective is to develop a procedure to incorporate depth to rigid layers, or apparent rigid layers, which can be used to determine the design values for use with the new Texas Flexible Pavement Design Procedure (Uzan, et. al. 1990). Secondary objectives of this research include:

- To confirm that the depth to a rigid layer influences the backcalculation of layer moduli and to investigate its influence on predicted pavement responses associated with pavement design.
- To develop a methodology to estimate subgrade changes with depth from surface deflection data.
- To verify this technique on pavement sections by comparing it to the results from other subgrade mapping techniques.
- To study the changing stiffness of clay and sandy subgrades with depth and to use this information to explain why a rigid layer can be used to represent the increasing subgrade stiffness with depth.
- To verify the procedure.
- To evaluate the effective rigid layer technique on an instrumented pavement section and to compare the predicted deflections in the pavement with those measured.

RESEARCH ORGANIZATION

This research has been documented in eight chapters. The second chapter summarizes the existing knowledge and current methods of analyzing nondestructive deflection data. It examines the use of nondestructive testing in the mechanistic-empirical design of flexible pavements. Existing literature on the nonlinear elastic behavior of pavement materials is reviewed, and the fundamental difference in behavior between fine grained and granular soils under typical pavement stresses are discussed. Finally the existing methods to account for changes in subgrade stiffness with depth during deflection analyses are outlined.

Chapter III describes the materials and methods used in this study. Details concerning the ten in-service and two instrumented pavement sections used are documented. The procedure used to collect nondestructive deflection data is listed, and the laboratory results are shown. On five pavement sections, the actual subgrade stratigraphy was determined using seismic refraction analysis and a penetration device. These procedures and the results of the tests are documented. The chapter also includes the procedure and results of two multi-depth deflection tests conducted on the instrumented pavement sections.

In Chapter IV the influence of assumed subgrade thickness on pavement evaluation and design is investigated. It is confirmed that rigid layers do influence the backcalculation of layer moduli. A method to determine the depth to an apparent rigid from surface deflections is developed. This method is based on Bousinesq's equation and is related to a three layer linear elastic system through an extensive regression analysis. The procedure is validated by comparing the predicted rigid layer depths from surface deflections on five pavement sections to that obtained through penetration testing and seismic refraction analysis.

In Chapter V the methodology developed in Chapter IV is extended to pavement systems with the subgrade stiffness increasing with depth. A nonlinear elastic backcalculation technique is used to illustrate the change in apparent stiffness with depth on a sandy and clay subgrade. The chapter illustrates how a three layer linear elastic system with a rigid layer can be used to model the increasing stiffness with depth. Finally this chapter deals with additional improvements made to an existing backcalculation program to account for subgrade stiffness changes with depth.

To evaluate the new procedure, it is compared to existing backcalculation models. Monthly collected deflection data on ten in-service pavement sections are analyzed and the results are compared in terms to results based on available laboratory data. Measured surface and in-depth deflections from two instrumented pavement sections are also analyzed for this purpose. The detailed results from this evaluation are documented in Research Report 1123 (Scullion et al. 1990). The main findings, and a discussion of the results are presented in Chapter VI.

Chapter VII contains conclusions and recommendations for further research developed as a result of this study. Chapter VIII, listing the pertinent references, is followed by a three appendices. The first, Appendix A, contains a copy of the laboratory data for the ten inservice pavement sections. Appendix B includes additional subgrade information obtained from drilling logs and the Texas county soil surveys. Appendix C contains copies of the appropriate soil survey maps.

CHAPTER II
LITERATURE REVIEW

Nondestructive deflection testing has become an integral part of the analysis and design of flexible pavements. This chapter briefly describes deflection testing of pavements with emphasis on the Falling Weight Deflectometer, the device used throughout this study. Current deflection analysis techniques are examined. The use of deflection testing in the overall design process is illustrated and discussed. Existing literature on the nonlinear elastic behavior of pavements is reviewed, and the influence of changes in the subgrade conditions with depth on deflection analysis are addressed.

NONDESTRUCTIVE DEFLECTION TESTING OF PAVEMENTS

A nondestructive test is one from which the necessary information can be obtained to define the physical properties of a sample without destroying it (Yang 1972). In pavement evaluation this requires a large mechanical device to duplicate vehicle loads without destroying the pavement. By measuring the pavement responses induced by this load, the structural integrity or stress-strain properties of the pavement structure can be determined.

Nondestructive deflection testing of pavements has gained in acceptance and popularity since the first Benkelman Beam was developed at the WASHO Road Test (1954). It has become popular because it is rapid, relatively inexpensive, and the pavement materials are tested in a truly undisturbed state. According to Hoffman and Thompson (1981) several testing devices and methods of data interpretation developed through the years due to the need:

- to increase the rate of testing;
- to improve the accuracy of measurements;
- to simulate the traffic loads more realistically in terms of magnitude, shape, and time of loading;
- to simplify testing and data analysis; and
- to reduce the cost of testing and analyzing the deflection data.

Four distinct types of measuring devices were developed. The first group includes static devices such as the plate bearing test (ASTM D 1196-64). The long loading time used in these tests make them unsuitable for defining pavement responses under a moving wheel load. The second group includes the vehicular devices, such as the Benkelman Beam, La Croix Deflectograph, the California Traveling Deflectometer, and others. A common characteristic of these devices is the relative horizontal motion between the load and the testing point during the time of testing. The vehicle velocity of these tests is generally less than 3 mph, resulting in loading times much greater than typically found with moving wheel loads (Hudson et al. 1987).

A third group of nondestructive deflection testing devices are the vibrators. These devices, like the Dynaflect, the Road Rater, and the Cox Device, first apply a static preload to the pavement. Counter rotating masses or an electrohydraulic system then generates a steady-state harmonic vibration in the pavement. The large preloads required to keep such a device in contact with the pavement surface have been found to stiffen the pavement system (Hoffman and Thompson 1981).

The Dynatest, KUAB, and Phoenix Falling Weight Deflectometers (FWDs) are included in the fourth group called the impulse devices. They produce a transient load to the pavement by dropping a load from a predetermined height onto a baseplate sitting on the pavement surface. By changing the drop height or weight of the load, the magnitude of the impulse can be adjusted (Smith and Lytton 1984).

From all the deflection testing equipment developed and used, the FWD has evolved as the favorite and most suitable device for pavement evaluation. In an extensive study, Lytton et al. (1987) evaluated fifteen existing deflection devices. Several agencies were asked to evaluated these devices in terms of cost, accuracy, reliability, rate of testing, etc. Based on utility theory, these subjective ratings were evaluated and the FWD was ranked highest for use in both project and network level pavement evaluation.

The FWD is also popular because of its technical suitability. Hoffman and Thompson (1981) reported that among the different devices and methods analyzed, it appears that the FWD best simulates pavement response under a moving truck load. This view is supported by Sebaaly (1987) who stated:

> The FWD appears to be suitable for the nondestructive testing of pavements because it simulates the shape and temporal nature of moving wheel loading reasonably closely. In addition, the hazards of resonance associated with periodic loading devices such as the Dynaflect and the Road Rater are less acute with the transient loading of the FWD.

Based on measured responses of an instrumented pavement section, Ullitz (1973, 1987) found that the pavement's stress and strain conditions during an FWD test are very similar to the conditions under a heavy vehicle load. The Dynatest FWD used in this study will be described in greater detail in the Materials and Method section.

THE ANALYSIS OF DEFLECTION DATA

The analysis of deflection data, like the deflection measuring devices, has gone through continuous improvements during the last 20 years. Most techniques developed fall into two categories: deflection parameters and backcalculation of layer moduli.

The deflection basin parameters are used directly to evaluate a pavement's structural integrity. These parameters are derived either from the magnitude of the measured deflections, or the shape of the deflection bowl. The most commonly used is the maximum deflection. Table 1 shows some typical deflection basin parameters as adapted from a summary by Horak (1988). These parameters are not a generic property of the pavement system, and at best, they can be empirically related to pavement strength. In the Virginia overlay design procedure (Vaswani 1971) for example, the parameter spreadability is used to calculate the effective thickness of a pavement. These deflection basin parameters are often related to pavement performance. Deflection parameters are used in the overlay design procedures of Louisiana (Kinchen and Temple 1980), Kentucky (Southgate et al. 1978), and Utah (Peterson 1976), to name a few. These empirical relationships are only valid for the environment and type of pavement structures for which they were developed. Furthermore the basin parameters are device dependant. A

Table 1. Deflection Basin Parameters.

Deflection Parameter	Formula	Measuring Device	Reference
Area	$A = \frac{6(\delta_0+2\delta_{12}+2\delta_{24}+\delta_{36})}{\delta_0}$	FWD	Hoffman 1981
Base Curvature Index	$BCI = \delta_{60} - \delta_{48}$ or $BCI = \delta_{24} - \delta_{36}$	Dynaflect FWD	Peterson 1972
Base Damage Index	$BDI = \delta_{12} - \delta_{24}$	RR & FWD	
Bending Index	$BI = \delta_0/a$	BB	Hveem 1954
Deflection Ratio	$DR = \delta_r/\delta_0$	FWD	Claessen 1976
Maximum Deflection	δ_0	BB Dynaflect	Shrivner 1968
Radius of Curvature	$R = \frac{r^2}{(2\ \delta_0\ (\delta_0/\delta_r - 1))}$ *	CM & BB	Dehlen 1962
Radius of Influence	$RI = x/\delta_0$	BB	Ford 1962
Shape Factors	$F_1 = (\delta_0 - \delta_{24})/\delta_{12}$ $F_2 = (\delta_{12} - \delta_{36})/\delta_{24}$	FWD	Hoffman 1981
Slope of Deflection	$SD = \tan^{-1}[(\delta_0 - \delta_r)/r]$	BB	Kung 1967
Spreadability	$S = \frac{25(\delta_0+\delta_{12}+\delta_{24}+\delta_{36})}{\delta_0}$	Dynaflect RR FWD	Vaswani 1971
Surface Curvature Index	$SCI = \delta_0 - \delta_{12}$	BB RR Dynaflect FWD	Shrivner 1968
Tangent Slope	$TS = (\delta_0 - d_x)/x$	FWD	Stock 1984

δ_r	Surface Deflection	BB	Benkelman Beam
r	Distance from the Load (inch)	RR	Road Rater
a	1/4 of Deflection Basin Length	FWD	Falling Weight Deflectometer
x	Distance from Point of Maximum Deflection to Tangent Point	CM	Curvaturemeter
d	Deflection at the Tangent Point	*	r = 127mm

relationship developed using one deflection device may not be applicable for use on deflection data obtained using a different device.

The second type of analysis technique is the backcalculation of layer moduli. It allows for the evaluation of individual layers and provides information to identify the causes of distress in a pavement system. Because the elastic modulus of pavement materials is a fundamental material property, it can be used to evaluate the performance of a pavement structure. The influence of environmental forces and the effect of changing wheel loads can also be investigated.

Several methods to backcalculate the layer moduli from FWD deflections are in use. Lytton et al. (1987) described several approaches which are described in the following.

The Equivalent Thickness Approach

The deflection analysis techniques using the equivalent thickness approach utilize a method developed by Odemark (1949). According to Odemark, a system composed of layers with different moduli can be transformed into an equivalent system having only one layer. This transform, as illustrated in Figure 1, is based on the following equation:

$$h_{eff} = c \sum_{i=1}^{i=n-1} \left\{ h_i \sqrt[3]{\frac{E_i}{E_0}} \right\} \qquad (2.1)$$

where:

- h_{eff} = The equivalent thickness;
- h_i = The thickness of layer i;
- E_i = Young's modulus for layer i;
- E_0 = The modulus of the layer converted to;
- c = Constant of between 0.8 and 0.9.

The power of Odemark's transform lies in its ability to reduce multilayered systems to single layer systems. On a single layer system, Boussinesq's equations for an infinite halfspace can be used. The

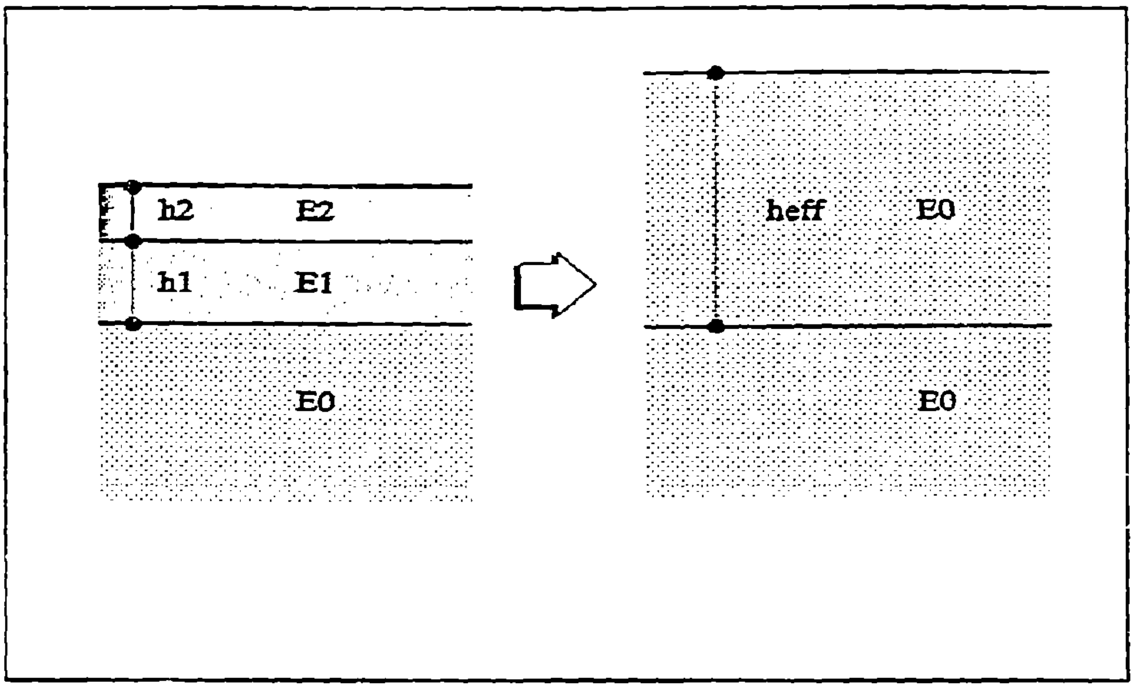

Figure 1. Odemark's Transform as Used in the Equivalent Thickness Approach.

concept of equivalent thickness has been used in conjunction with Bousinesq's equations in the backcalculation program ELMOD (Ullitz and Stubstad 1985). It was also used in a deflection analysis technique developed by Lytton and Michalak (1979). Although several researchers (Kuo 1979, Hung et al. 1982) have found that the method of equivalent thickness has limitations, it is widely used and popular because of its simplicity.

The Layered Elastic Approach

The load deflection relationship of layered systems was first numerically solved for a two layered system by Burmister in 1943. Axum and Fox (1951) extended the theory to a three layer system. In 1961 Shiffman published the solutions for multilayered systems. Since this time many computer programs like BISAR[1] and CHEVRON[2] have been developed. These programs have also recently been converted to run on microcomputers. They use closed form solutions to calculate deflections, stresses, and strains at any position in a multilayered system as shown in Figure 2. In this model the following assumptions pertain:

- all layers consist of homogeneous, isotropic, linear elastic materials that can be described by two properties, Young's modulus of elasticity E, and Poisson's ratio μ;
- all layers are infinite in horizontal extent;
- all layers except the bottom layer are of finite thickness;
- all materials are weightless;
- no surface shearing forces exist; and
- the interface conditions can be assumed as rough (assuming full friction) or smooth (assuming no friction).

Several researchers have reported that the layered elastic approach does a relatively good job of modeling flexible pavements. For example, Hicks (1970) could predict surface deflections, and stresses and strains that develop in the base and subgrade with reasonably good accuracy using a layered elastic model. In their San Diego study, Hicks and Finn (1970) reported reasonably good comparisons on one section between measured responses and those predicted. Other sections however had ratios of predicted over measured responses ranging from 0.4 to 1.4 for deflection and 0.2 to 2.3 for surface strain. Thrower and Lister (1972) reported good agreement on stiff pavements but a poor agreement on softer structures in terms of stresses and strains. Klomp and Niesman (1967) also reported good comparisons in terms of strain induced in the upper layers.

---

[1] BISAR is a layered elastic program developed by the Shell Oil Company for the numeric evaluation of stresses and strains in a multilayered elastic system due to surface loads.

[2] CHEVRON is a layered elastic program developed by the Chevron Research Company.

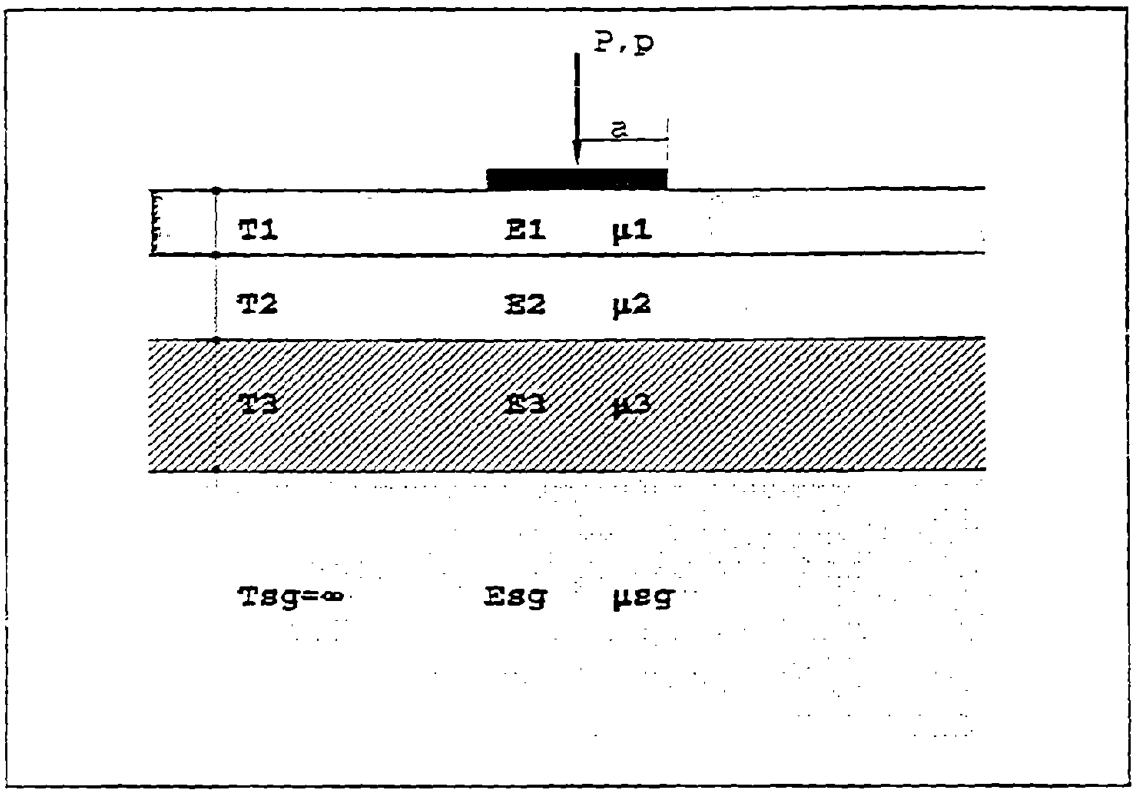

Figure 2. A Generalized Multilayered Elastic Pavement Model.

The mathematical models used in the layered elastic programs were developed to calculate pavement responses under surface loads with known pavement properties. However, in the analysis of deflection data, the load and pavement response (i.e., deflections) are measured, and the pavement properties are the unknown. To use these programs in a reverse fashion, several techniques have been developed. The most common is an iterative technique. A set of layer properties are assumed and the pavement deflections are calculated. Through an iterative process the layered elastic programs are used repetitively. After each trial the predicted surface deflections are evaluated and the layer moduli are adjusted. This procedure is repeated until the calculated surface deflections match the measured deflections for a known load. The iterative process is normally guided by a computer program with a set objective to minimize the difference between the measured and predicted deflections. A list of iterative layered elastic backcalculation programs are given in Table 2.

The iterative techniques are relatively slow and, as a result, expensive. A second approach is to store many generated deflection basins and corresponding layer moduli in a database. When a measured deflection basin is analyzed, the database is screened, and interpolated to find a deflection basin that best represents the measured basin. By eliminating the iterative process, the speed of backcalculation is greatly improved. A database approach has been followed by the developers of COMPDEF (Anderson 1989) and MODULUS (Uzan et al. 1988). The program COMPDEF uses a matrix of precalculated solutions for composite pavement structures where rigid pavement layers were overlain with asphalt concrete. Through interpolation techniques and the matrix of solutions stored in a the database, this program provides layer moduli fast and accurately.

MODULUS generates a database for a specific cross section being analyzed and employs a pattern-search technique and LaGrange interpolation scheme (Ralston and Rabinowitz 1978) to backcalculate layer moduli. Lytton and Michalak (1979) first used a pattern search technique for deflection analysis in the program SEARCH. Using the Hooke and Jeeves' optimization algorithm (1962), the program finds the optimum solution for an objective function. In MODULUS the objective is to minimize the difference between the measured and calculated deflection bowls. First, a deflection bowl data base is generated using an elastic layered program. Then deflections for the pattern search are obtained using the three point LaGrange interpolation scheme. These deflections are compared to the measured deflections on the pavement surface. The principal advantage of this approach is that once a data base has been generated, a series of deflection measurements can be analyzed accurately with little additional execution time.

Nomographs are a third, but less popular, method used to obtain layer moduli. They are developed by generating deflection basins using the layered elastic programs. From these deflection basins, basin parameters, such as the maximum deflection or the basin area, are calculated. These parameters are then graphically related to their

Table 2. Iterative Layered Elastic Backcalculation Programs in Use.

Program Name	Number of Layers	Layer Elastic Program Used	Stress Sensitive Subgrade	Reference
BISDEF	4	BISAR	No	Bush 1980
CHEVDEF	4	CHEVRON	No	Bush 1980
ELSDEF	4	ELSYM5[1]	No	Jordahl 1985
EVERCALC	5	CHEVRON	No	Mahoney 1989
FPEDD1	5	ELSYM5	No	Uddin 1989
FPOD	4	ELSYM5	No	Treibig 1975
IMD	4	CHEVRON	No	Husain 1985
ISSEM4	4	ELSYM5	Yes	Stubstad 1988
MODCOMP2	8	CHEVRON	Yes	Irwin 1983
OAF	4	ELSYM5	Yes	Majidzadeh 1981
WESDEF	4	WESLEA[2]	No	Van Cauwelaert 1989

corresponding layer moduli. This approach has been utilized by Treibig (1977) and Wiseman (1977). More recently nomographs were used by Khosla and Ali (1989). Their nomographs to evaluate deflection data are based on calculations using the VESYS[3] structural subsystem.

Although the multilayered elastic systems are widely used and accepted, they are, at best, a rather poor approximation of the actual pavement system. Most pavement materials are not linear elastic. Many experience elastic deformations for some range of loading, and then viscous, plastic, and visco-elastic deformations occur with increased stress levels. The rate of these deformations is stress dependant, i.e., they are nonlinear. Their material properties often change with time, temperature and moisture levels. Furthermore the materials properties are not isotropic nor uniform but the material is often

---

1 ELSYM5 (Ahlborn 1972) is a layered elastic program that solves the same problem formulation as BISAR.

2 WESLEA is a layered elastic program developed by the US Army Engineer Waterways Experiment Station.

3 VESYS is a visco-elastic adaption of Burmister's layered elastic theory developed and fostered under FHWA sponsorship (Kenis 1977).

particular in nature. The pavement layers are also not infinite in horizontal extent.

The Finite Element Approach

Finite element techniques have been applied to pavement systems for many years (Wilson 1965, Barksdale 1969). The finite element methods allow for the nonlinear elastic modelling of pavement materials. Each element in the pavement system is assigned an independent anisotropic material property thus modelling the pavement more realistically than the purely linear elastic layered model. For granular and fine-grained materials, stress dependent material models and failure criteria are used to define the structural properties of each element in the grid. The structural stiffness properties of each element are obtained using energy principles, approximate displacement functions, and the usual elastic stress, strain, and displacements functions (Zienkiewicz et al. 1967). The analysis of each load deformation problem is based on an iterative process. The solving of a finite element problem is therefore much slower than the close-form solutions of the multilayered elastic approach, and they require more powerful computers.

The size of the computer and the large amount of computer time required to solve finite element problems limits their use in the analysis of deflection data. Iterative techniques, which are popular with the layered elastic approach are not practical for use with Finite Element programs. Backcalculation procedures using the finite element approach have generally made use of nomographs and regression equations. Hoffman and Thompson (1981) used ILLIPAVE (1982) to develop equations and nomographs for the interpretation of measured deflection basins on three pavement types:

- a conventional flexible pavement on a granular base course;
- an asphalt concrete surface on a stabilized base course; and
- a full depth asphalt structure.

They based their equations on two deflection parameters, the maximum deflection and the normalized cross sectional area of the deflection bowl. The equations were developed for a 9000 pounds FWD impulse load on a 12 inch diameter loading plate.

Although the procedure incorporates the nonlinear characteristics of the base and subgrade materials, it suffers a disadvantage of purpose; it was developed for three pavement types on typical Illinois soils. As a result the use of the procedure is limited to similar pavements on corresponding soils. Because the equations were developed using only one type of base course, their application are also restricted. Furthermore, the properties obtained from this method can not be used in mechanistic pavement design procedures that are based on layered elastic principles. The backcalculation procedure should in principle be compatible with model used during pavement design (Lytton 1989).

The Dynamic Analysis Approach

When a deflection test with the FWD is conducted, both the load and geophone sensors record a continuous signal over a duration of 100 milliseconds. Due to the changing velocity of the surface and body waves in different materials, a trace similar to that shown in Figure 3 can be obtained. From this trace, the maximum deflection and load are extracted for the static deflection analysis techniques discussed above. It is therefore assumed that both the load and peak deflections occur at the same instant in time. By ignoring the time trace, the inertial effects, such as "radiative damping" and resonance, are disregarded.

The elastodynamic analysis approach uses the whole time-force and time-deflection trace. By analyzing both the impulse and response signals by frequency, a frequency dependent transfer function at each geophone can be obtained (Lytton 1989). These functions are used to determine the complex modulus and the material damping factor of each material in the pavement system. Several programs that use the dynamic approach exist. These include PUNCH (Kausel and Peek 1982), UTFWIBM (Roesset 1987), and SCALPOT (Magnuson 1988). Although a dynamic analysis can model the dynamic effects more accurately than the static models, these techniques are complex and use large amounts of

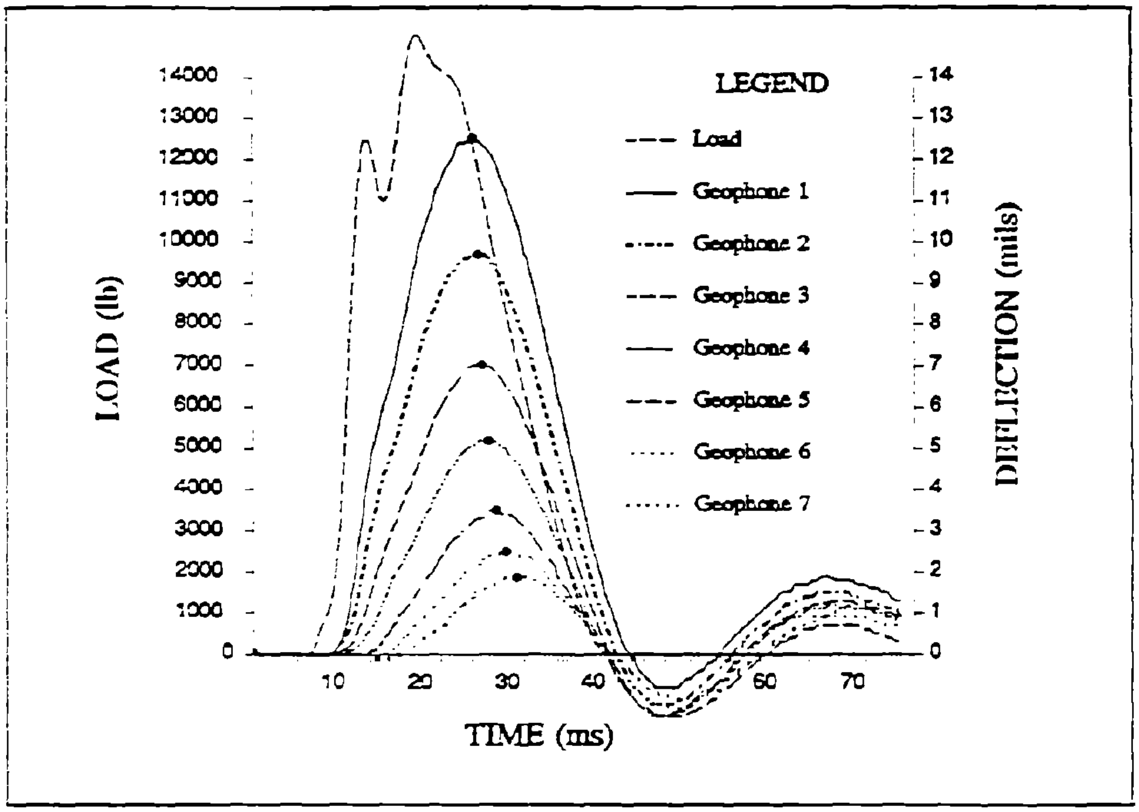

Figure 3. A Typical FWD Load and Deflection Trace.

computational time. Furthermore, the obtained material para-meters are rarely used in pavement design. Presently all mechanistic pavement design procedures are based on elastostatic principles (Thompson 1989a).

THE USE OF NONDESTRUCTIVE DEFLECTION TESTING IN THE MECHANISTIC-EMPIRICAL DESIGN OF FLEXIBLE PAVEMENTS

Pavement design has traditionally used nomographs and other simplified approaches. These relationships were often based on previous experience and engineering judgement. As computer power has increased and the understanding of pavement behavior has improved, mechanistic-empirical design procedures have been introduced. These design procedures are based on the assumption that a pavement structure can be modelled using basic mechanics of materials approaches. The most commonly used is the multilayered elastic system previously discussed and shown in Figure 2. Using the elastic model, stresses, strains, and deflections due to traffic loads and/or the environment can be calculated at any point in the pavement structure for a given set of material parameters. To account for many factors not included in the modeling process, these responses are then related to pavement performance through an empirical transfer function.

The primary benefits from using a mechanistic-empirical design procedure (AASHTO 1986) are:

- improved reliability of pavement design;
- the ability to predict specific types of distresses for different pavement structures; and
- the ability to extrapolate from limited field and laboratory results without full scale tests.

In a layered elastic design the elastic modulus of each pavement layer is required. This material parameter can be obtained in two basic ways: the first is using laboratory testing of soil samples (Thompson 1989b, Barksdale and Hicks 1973). By preparing the sample to simulate field conditions and applying a repetitive load, the elastic modulus of the material is determined. Second the elastic modulus can be obtained by testing the materials insitu using nondestructive techniques (Lytton et al. 1990). Because the material is tested in a truly undisturbed state, the results are more representative than laboratory results. As previously stated the FWD closely simulates a moving wheel load. Because the loads are similar in both time and magnitude, the measured deflections are similar to that expected under a heavy vehicle. As explained by Ullitz (1987):

> If the deflection basin is measured under a FWD test and the theory of elasticity is then used to determine those moduli of the individual layers that would produce the same deflection basin, then the resulting layer moduli will be representative of the pavement materials under heavy traffic loading.

In using mechanistic design procedures for pavement design, it is important to utilize a close-loop approach (Thompson 1989a). Materials testing and evaluation concepts, structural modelling, climatic models etc. used in the design and development of the transfer functions should also be used in the deflection analysis. This important principle is substantiated by Lytton (1989):

> The most common property found by NDT is the elastic stiffness of each layer. The method chosen (elastic modulus or the properties of the nonlinear stress-strain curve) should be compatible with the method that is used to make design calculations (multilayered or finite-element methods). For consistency, the same method should be used to predict remaining life, to monitor the change of layer properties with time, and for use in specification testing.

In terms of the existing deflection analysis techniques, this has several implications. If a layered elastic layered program is to be used in analyzing pavements during design, then a layered elastic or equivalent technique should be used to analyze the deflection data. All assumptions made during backcalculation should be consistent with the pavement model used in rehabilitation design. This includes assumed layer and subgrade thicknesses and material behavior assumptions (i.e., linear elastic or stress sensitive).

In a mechanistic-empirical design process, as shown in the flow diagrams in Figures 4 and 5, deflection testing is used to provide design information. For initial designs, it can be used to provide the stiffness of the subgrade. This is obtained by collecting and analyzing deflection data from existing pavements in close proximity to the new design location with the same soil type. In addition to the subgrade modulus, the stiffness of the base course can also be acquired from existing pavement structures. Due to the stress sensitive behavior of granular base material, the tested pavement should preferably consist of approximately the same thicknesses as the new design.

For rehabilitation designs, deflection testing is even more useful. The structural properties of the subgrade and all pavement layers of the pavement to be rehabilitated are obtained from deflection analysis. The determined insitu layer moduli can be used to help determine the type of rehabilitation and can be used as direct input to the mechanistic analysis of a rehabilitation design.

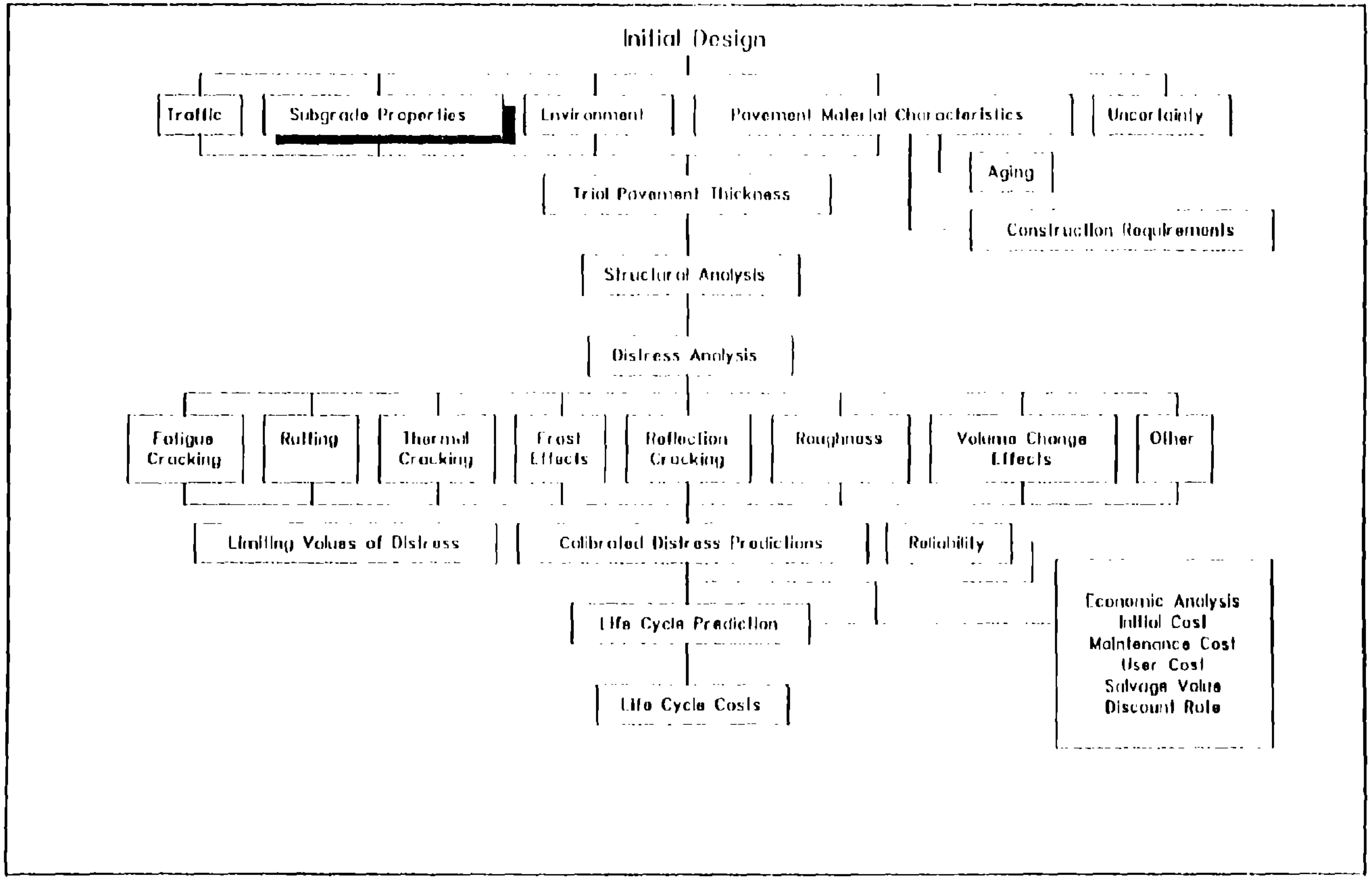

Figure 4. The Place of Deflection Testing in the Mechanistic-Empirical Design of Flexible Pavements (Adapted from AASHTO 1986).

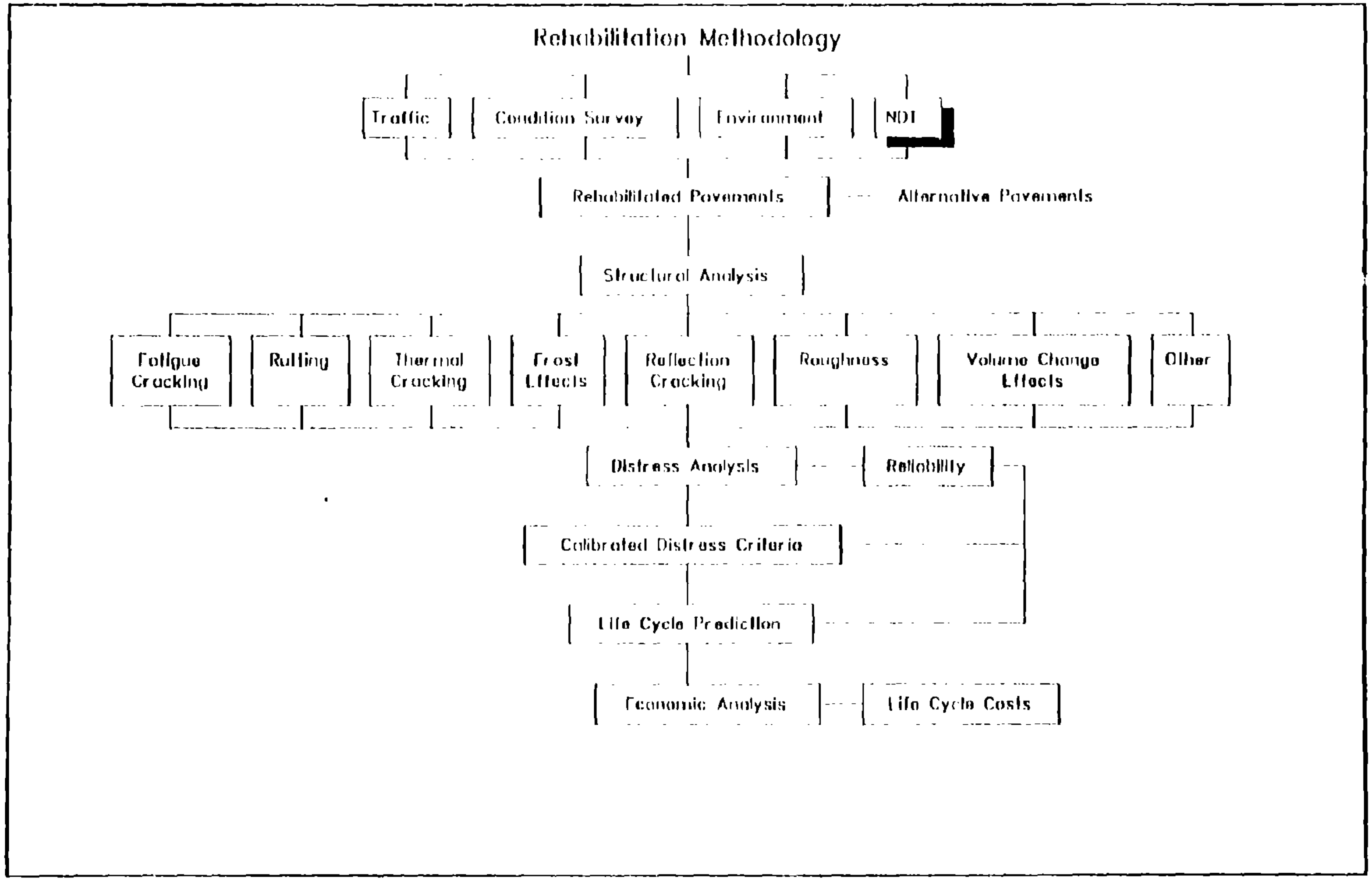

Figure 5. The Place of Deflection Testing in the Mechanistic-Empirical Rehabilitation Design of Flexible Pavements (Adapted from AASHTO 1986).

THE NONLINEARITY OF PAVEMENT MATERIALS

In the analysis of FWD deflection data, it is often assumed that the response of pavement materials is independent of the prevailing stress state. Presently, most analysis techniques use a linear elastic pavement model. In this model a constant stiffness is assumed throughout each pavement layer. Results from repeated load testing of subgrades and bases have shown that the stiffness of these materials are dependant on their state of stress (Barksdale and Hicks 1973).

Several researchers (Elliott and Thornton 1988) have used the concept of resilient modulus to describe the behavior of pavement materials subjected to repeated loads. In the resilient modulus test (AASHTO T-274), a representative sample of a soil or granular material is placed in a triaxial device and subjected to the repetitive loads and stresses expected in a pavement system. The typical response of a pavement material during one load, unload cycle is shown in Figure 6. From the measured responses the resilient modulus is defined as:

$$M_R = \frac{\sigma_d}{\epsilon_R} \tag{2.2}$$

where:

M_R = The Resilient Modulus;

σ_d = The Repeated Deviatoric Stress;

ϵ_R = The Recoverable Axial Strain.

Both the plastic and elastic strain under the deviatoric stress are measured. These responses are stress sensitive in most pavement materials. Unbound granular materials generally exhibit a stress-stiffening behavior under loading while fine-grained soils are generally stress-softening. An analysis of the resilient modulus at various stress levels can be used to develop equations depicting a soil's stress dependant behavior.

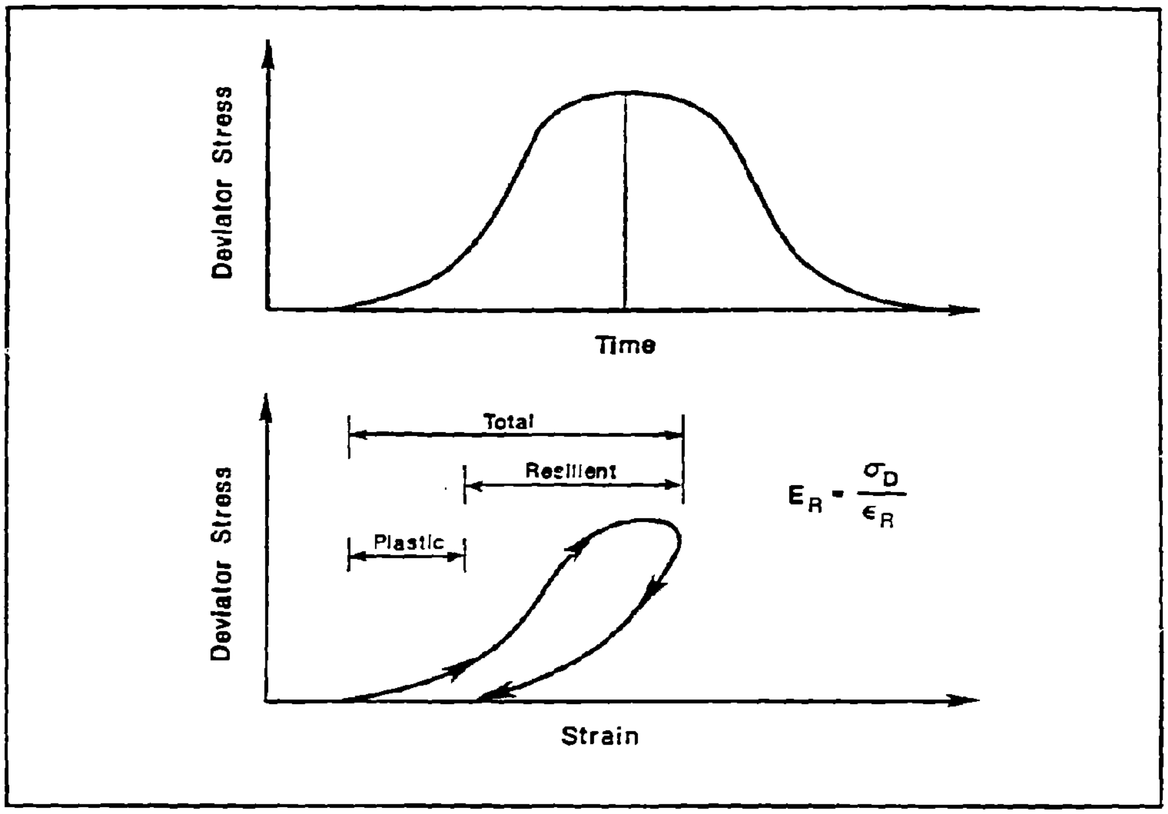

Figure 6. A Typical Stress Strain Response in the Resilient Modulus Test.

Granular Materials

The resilient modulus, and to a lesser degree the Poisson's ratio, of granular soils are influenced by the prevailing stress state. Numerous studies (Barksdale 1971, Ishibashi et al. 1984, Knutson et al. 1976, Pell and Brown 1972, Witczak and Uzan 1988) have shown that the resilient modulus of granular material, sands, and crushed stone increases with an increase in confining stress. To describe the nonlinear stress-strain characteristics of granular materials, several relationships have been suggested and implemented. The classic model, in which the resilient modulus is purely a function of the bulk stress, is most popular (Hicks and Monismith 1971, Shook et al. 1982):

$$E_R = (k_1\ p_a)\left[\frac{\theta}{p_a}\right]^{k_2} \tag{2.3}$$

where:

E_R = Resilient modulus of the granular material;

θ = The bulk stress or first stress invariant $(\sigma_1 + \sigma_2 + \sigma_3)$;

k_i = Constants;

p_a = Atmospheric pressure used in the equation to make the coefficients independent of the units used;

σ_i = Principal stresses as shown in Figure 7.

In 1981, May and Witczak suggested that the resilient modulus of a granular material should also be a function of the shear strain induced by loading. This view was supported by Uzan (1985) who demonstrated that equation 2.3 cannot adequately describe the nonlinear behavior of granular soils. To describe the nonlinear behavior found in repeated load triaxial tests, he proposed the following equation (Witczak and Uzan 1988):

$$M_R = (k_1\ p_a)\left[\frac{\theta}{p_a}\right]^{k_2}\left[\frac{\sigma_d}{p_a}\right]^{k_3} \tag{2.4}$$

where:

σ_d = The deviatoric stress $(\sigma_1 - \sigma_3)$

For the general case, the deviatoric stress can be replaced with the octahedral shear stress, τ_{oct}:

$$M_R = (k_1\ p_a)\left[\frac{\theta}{p_a}\right]^{k_2}\left[\frac{\tau_{oct}}{p_a}\right]^{k_3} \tag{2.5}$$

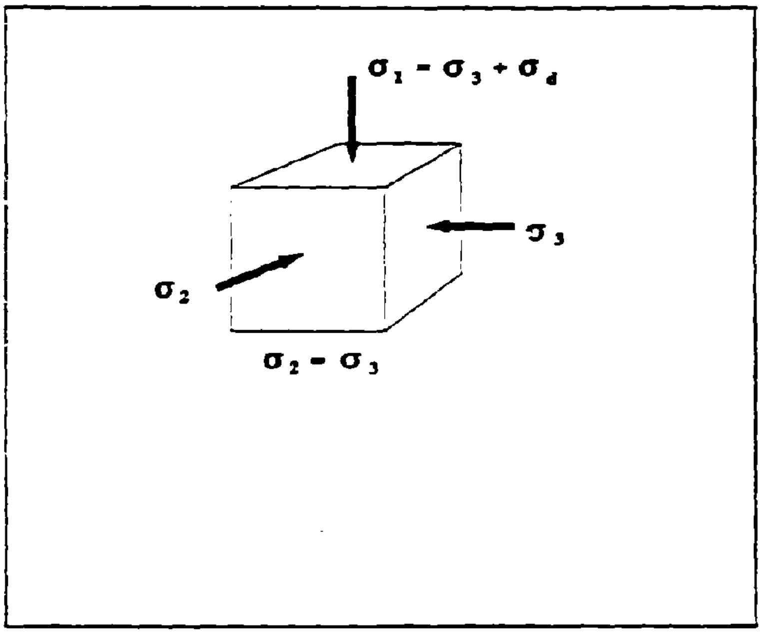

Figure 7. An Illustration of the Principle Stresses Acting on a Soil Element.

where:

$$\tau_{oct}^2 = \frac{1}{9}\left[(\sigma_1-\sigma_2)^2 + (\sigma_2-\sigma_3)^2 + (\sigma_3-\sigma_1)^2\right] \tag{2.6}$$

and for use on triaxial tests where $\sigma_2=\sigma_3$:

$$\tau_{oct} = \frac{\sqrt{2}}{3}\,\sigma_d \tag{2.7}$$

Fine Grained Materials

The resilient modulus of fine-grained soils generally decreases with an increase in deviatoric stress. Unlike the granular materials, their stiffness is not very sensitive to changes in the confining stress. Two basic stress dependant behavior models have been utilized. The first, the arithmetic model (Thompson and Robnett 1976), is shown in Figure 8. The resilient modulus rapidly decreases with an increase in

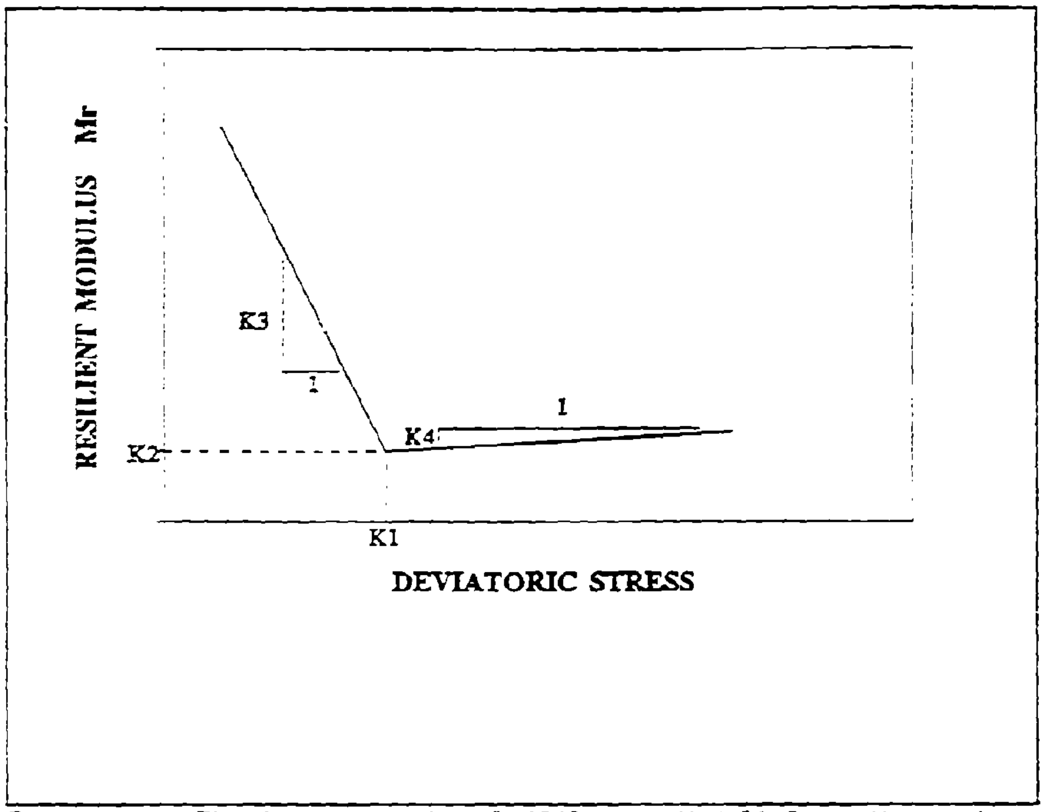

Figure 8. The Arithmetic Model (Bilinear Model) Describing the Nonlinear Resilient Modulus of a Fine Grained Soil.

deviatoric stress until a certain value. Then the soil stiffness gradually increases, stays constant, or shows a slight decrease in stiffness as the deviatoric stress is further increased. The shape of the curve can be described by the following bilinear equation:

$$M_R = K_2 + K_3[K_1 - \sigma_d] \quad for\ K_1 > \sigma_d \tag{2.8}$$

$$M_R = K_2 + K_4[\sigma_d - K_1] \quad for\ K_1 < \sigma_d$$

where:

M_R = Resilient modulus of the fine grained soil;

σ_d = The deviatoric stress $(\sigma_1 - \sigma_3)$.

The second model often used to describe the behavior of cohesive soils is the semi-log model:

$$M_R = k_1(\sigma_d)^{k_3} \tag{2.9}$$

Uzan and Scullion (1990) pointed out that equation 2.4 can be used as a universal model for both granular and fine grained soils. For a constant modulus, or linear elastic material, both k_2 and k_3 are set to zero. By setting only k_3 to zero, equation 2.4 is downgraded to the bulk stress model (equation 2.3). By using only the k_3 coefficient and setting k_2 to zero, equation 2.4 is simplified to the semi-log model of equation 2.9, in which the stiffness is purely a function of the deviatoric stress. As mentioned by Lytton (1989), current research indicates both empirically (Uzan 1985, 1988) and theoretically (Lade and Nelson 1987) that the modulus of most materials depends upon both the mean principal stress and the deviatoric stress and acts as both stress stiffening and softening depending on the relative level of stress. Figure 9 shows the results of a resilient modulus test conducted on a sandy material. Clearly the resilient modulus is a function of the applied deviatoric stress and to an even greater extent the confining stress. Figure 10 shows the results of a resilient modulus test conducted on a fine grained soil. The modulus of the clay is mostly affected by changes in the deviatoric stress. Equation 2.5 can be used to accurately describe the nonlinear behavior of both these materials. Table 3 summarizes typical coefficients for the universal model (equation 2.5), as found in the literature.

DEALING WITH VERTICALLY CHANGING SUBGRADES IN THE ANALYSIS OF DEFLECTION DATA

Although most analyses techniques model the subgrade underlying the pavement as a uniformly stiff and infinitely thick material, the reality is more complex. Rigid layers, or bedrock, are often encountered at shallow depths. The actual subgrade might consist of various layers of material or one material increasing in stiffness with depth. This increase in stiffness can be a result of the stress history or the

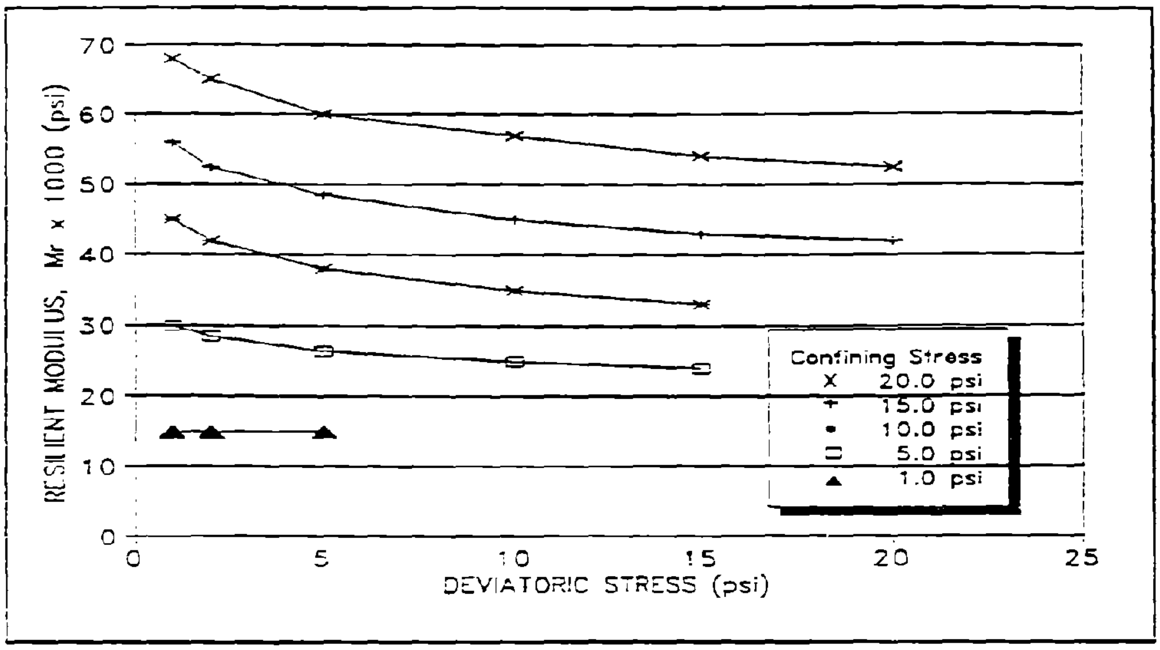

Figure 9. Influence of the Confining and Deviatoric Stress on the Resilient Modulus of a Typical Sandy Subgrade (Sneddon 1988).

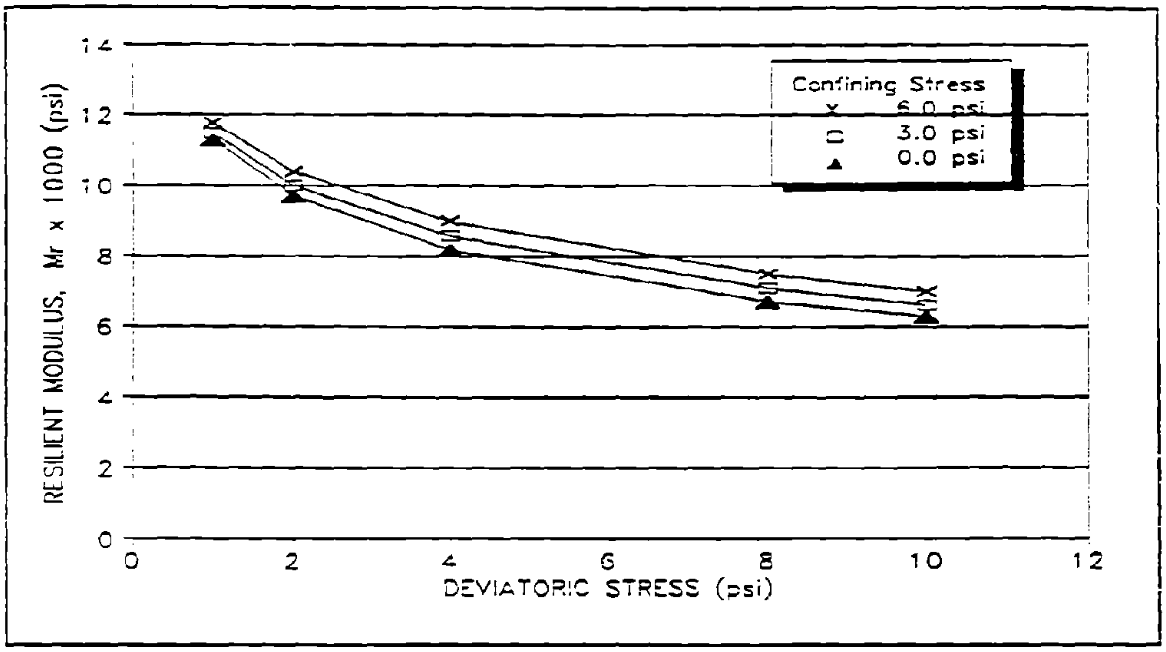

Figure 10. Influence of the Confining and Deviatoric Stress on the Resilient Modulus of a Typical Clay (Sneddon 1988).

Table 3. Typical Coefficients Used in the Universal Stiffness Model (Eq. 2.5).

Material Description	K_1	K_2	K_3	Reference
BASE COURSE				
Dense Graded Limestone	856	0.80	-	Witczak and Uzan 1988
Dense Graded Limestone	462	0.95	0.30	Witczak and Uzan 1988
Crushed Limestone	1153	1.17	-	Crockford et al. 1990
Crusher Run Limestone	1607	0.90	0.50	Witczak and Uzan 1988
Crushed Slag	830	0.90	-	Witczak and Uzan 1988
			0.59	
SUBBASE			-	
Bank Run Gravel	624	0.65	0.30	Witczak and Uzan 1988
Sand and Aggregate	1014	0.50	-	Witczak and Uzan 1988
Blend	1027	0.60	0.50	Uzan and Scullion
Crushed Limestone	2190	0.60		1990
Crushed Limestone				Uzan and Scullion
			-	1990
SUBGRADE	1103	0.75	0.20	
Dry Sand	1577	0.58	-	
Wet Sand	510	0.00	0.10	Crockford et al. 1990
Clay	546	0.00	-	Crockford et al. 1990
Clay			0.20	Uzan and Scullion
			-	1990
			0.20	Uzan and Scullion
				1990
			-	
			0.53	
			-	
			0.35	
			-	
			0.30	
			-	
			0.30	

prevailing stress state. In a normally consolidated sedimentary soil the void ratio and moisture content often decrease with depth, and therefore the stiffness increases. The prevailing stress state during loading also changes with depth. This is the result of the load distribution capabilities of the pavement structure and the weight of the materials. The load related stresses, as illustrated in Figure 11, decreases with depth while the confining stress increases due to the

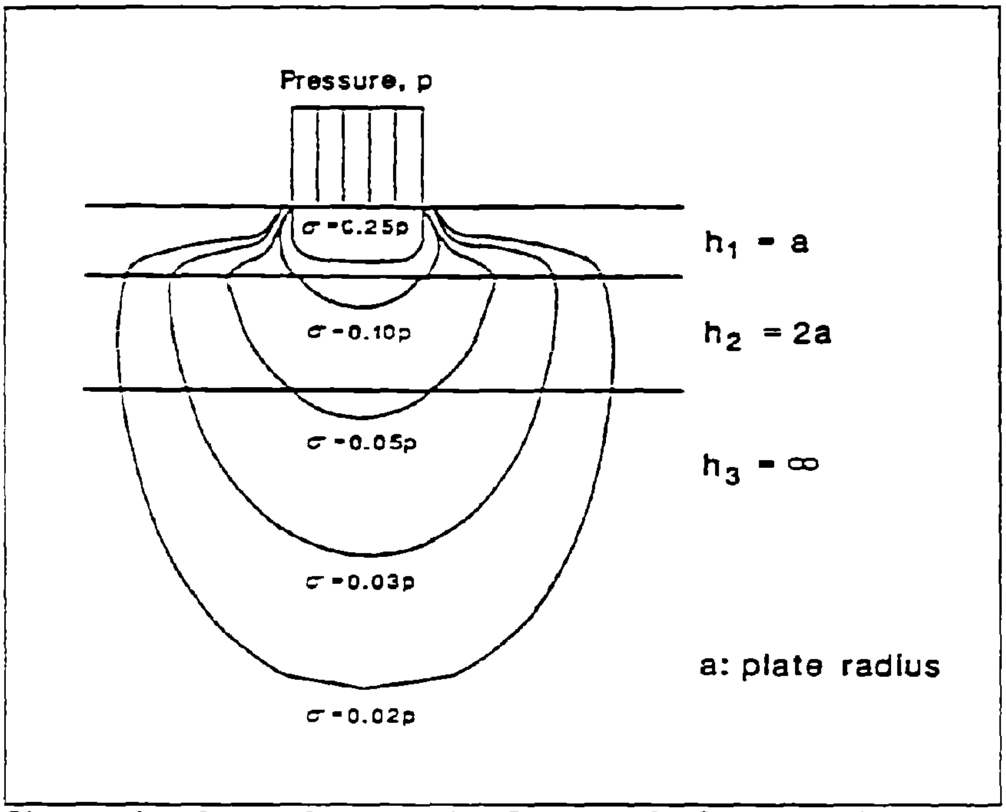

Figure 11. Stress Distribution Due to a Surface Load (Richter 1987).

increasing overburden pressure. As a result the "effective stiffness"of most soils increases with depth. The geostatic stresses are a function of the weight of each material. At any position the vertical overburden pressure can be determined through (Rodriguez et al. 1988):

$$\sigma_v = \sum_{i=1}^{n} (\gamma_i \, h_i) \qquad (2.10)$$

where:

σ_v	=	The vertical overburden pressure;
τ_i	=	The unit weight of layer i;
h_i	=	The thickness of layer i;
n	=	The number of layers.

The horizontal component of the overburden pressure can be calculated from the coefficient of earth pressure at rest, K_o and the vertical overburden pressure, σ_v (Lambe and Whitmann 1969):

$$\sigma_h = K_0\, \sigma_v = K_0 \sum_{i=1}^{n} (\gamma_i\, h_i) \tag{2.11}$$

where:

K_o = 1 - sin ϕ for cohesionless soils and gravels;

K_o = 1 - 0.95 sin ϕ for cohesive soils;

ϕ = Angle of internal friction.

For normal consolidated materials this would result in K_os in the range of 0.4 to 0.6. Because most pavement materials, especially the base course and the top of the subgrade, have been subjected to compaction and frequent loading, Irwin (1983) suggests that the coefficient K_0 should be more in the range of 0.8 to 2.0.

Backcalculation and Rigid Layers Below the Subgrade

Many researchers (Chou 1989, Uddin et al. 1986, Lytton et al. 1990, Yang 1988) have shown that the existence of a rigid layer underlying the subgrade, influences the analyses of deflection data. As stated by Uddin et al. (1986):

> Ignorance of rigid bottom considerations may lead to substantial errors in the predicted moduli of a pavement-subgrade system. The subgrade modulus may be significantly over-predicted if a semi-infinite subgrade is falsely assumed, when actual bedrock exists at a shallow depth.

In a theoretical analysis completed by Briggs and Nazarian (1989), it was found that if a rigid layer was ignored completely in an analysis, or assumed to be twice its actual depth, the backcalculated moduli for the base and subgrade would in no way resemble their actual values. They concluded that a pavement's remaining life would be drastically overestimated, leading to unconservative designs if the depth to a rigid layer is ignored, or overestimated.

The majority of backcalculation procedures incorporate a layered elastic program. A rigid base can be incorporated into this model by assigning a high Young's modulus to the bottom layer; however the depth of this layer is often not known. Several techniques to incorporate rigid layers into the analysis of deflection data have been suggested and implemented. The USCE (Bush 1980) recommends using a twenty foot depth to a rigid layer in all backcalculations. Hudson et al. (1987) recommends using the measured depth to a rigid layer when analyzing FWD deflection data. This approach is not practical because usually the depth to a rigid layer is not only unknown, but also highly variable. To establish the depth is costly, time consuming and often difficult because it can be bedrock, an overconsolidated clay, or a material acting like a stiff layer.

Uddin et al. (1986) suggests a procedure of assigning a thickness to the subgrade. This subgrade thickness is a function of the frequency of loading and the velocity of the compression waves in the subgrade. The ELMOD program (Ullitz 1985) permits the optional inclusion of a rigid layer in the backcalculation model. The depth to a rigid layer is inferred from the measured deflection data. Chou (1989) agreed that rigid layers should be included in the analysis of deflection data. He suggests that the depth to a rigid layer can be estimated by performing several backcalculations assuming various rigid layer depths. The rigid layer depth that minimizes the deflection matching error[1] can be associated with the actual rigid layer depth.

Backcalculation and Subgrades Stiffening with Depth

Although researchers acknowledge that subgrades are stress sensitive, this is ignored, or only partially addressed, in most existing backcalculation procedures. To account for increasing stiffness in a layered elastic program, a model consisting of many layers is required. Each of these layers can be assigned a different stiffness. In the program MODCOMP2 (Irwin 1983), a maximum of eight layers can be used to model a pavement. Each material's resilient modulus can be characterized

---

[1] Chou defined the deflection matching error as the cumulative relative difference between the measured and calculated deflection at all FWD sensors.

by a nonlinear model. Based on these relationships, a stress-compatible modulus for each layer can be backcalculated.

The only accurate way to account for changes in subgrade stiffness horizontally as well as vertically is through the use of finite element techniques. Presently there is no automated nonlinear elastic backcalculation system using this approach. Lytton et al. (1990) suggested that the pattern search technique used in the program MODULUS (Uzan et al. 1988) might be linked to a finite element program such as ILLIPAVE (1982) to model nonlinear bases and subgrades. The disadvantage of such a procedure is the considerable time and computer capacity required to perform the calculations. In using deflection testing for design purposes the engineer has to deal with a great amount of deflection data and computational speed is of great importance. Furthermore computer capacity is limited because minicomputers are normally used for field application. A layered elastic approach, where the increasing subgrade stiffness with depth is represented by a rigid layer at some finite depth, would be the most practical and effective method of dealing with this problem.

SUMMARY OF THE LITERATURE REVIEW

1. Through the years, many nondestructive deflection devices have been developed. Such devices can be divided into four distinct types: the static devices, the vehicular devices, the vibrators, and the impulse devices. Among the last group is a nondestructive deflection test device called the Falling Weight Deflectometer. This device has been reported to be one of the best devices to simulate pavement response under a moving wheel load.
2. Different techniques to analyze surface deflection data have been developed. Most techniques fall into two categories: deflection parameters and the backcalculation of layer moduli. Several methods to backcalculate the layer moduli are in use such as the equivalent thickness method, the layered elastic method, the finite element method, and the dynamic analysis method. Among these methods the multilayered elastic approach has proven to provide satisfactory results in determining stresses, strains, and deformations in

pavement systems.

3. In the mechanistic-empirical design of flexible pavements the analysis of deflection data can be used to provide material properties for new or rehabilitation designs. In using nondestructive testing with a mechanistic pavement design procedure, it is important to use a close loop approach. The method used for deflection analysis (layered elastic or nonlinear elastic) should be compatible with the design model.
4. Although the layered elastic pavement model assumes materials to be linear elastic, the stiffness of most pavement materials is actually stress dependant. The resilient modulus of granular materials and fine grained soils behaves fundamentally different, and several models to describe their stress-strain characteristics have been developed. In general the stiffness of the fine grained material are dominated by the deviatoric stress, while the stiffness of the granular soils is also influence by the confining stresses.
5. Several researchers have shown that the existence of rigid layers below the subgrade influences the deflection analysis. Presently the majority of backcalculation procedures ignores the existence of a rigid layer and model the subgrade as infinitely thick, resulting in inaccurate results. Several techniques to incorporate rigid layers into the analysis of deflection data have been suggested, but a method to obtain the depth to a stiff layer from deflection data is badly needed.
6. Although researchers acknowledge that subgrades are stress sensitive, this is ignored, or only partially addressed, in most backcalculation procedures. Presently there are no automated nonlinear elastic backcalculation methods. This will require the repetitive use of a finite element program demanding considerable computational time and computer capacity.

CHAPTER III

MATERIALS AND METHODS

Subgrades with increasing stiffness with depth, and rigid layers at shallow depths, influence not only deflection data but also their analysis. The layered elastic backcalculation procedures are popular and widely used but do not account for these changes in the material properties. To develop, verify, and evaluate a method to account for theses changes in the analysis of deflection data, an extensive study was undertaken. Ten test pavement sections, shown in Figure 12, were used for this purpose. Deflection data were collected over a period of one year with a Dynatest 8000 FWD. On these sections, the subgrade stratigraphy was determined by coring. Samples were taken from the pavement layers for laboratory testing. On five of the sections the depth to a rigid layer was determined using penetration and seismic techniques. The layout and location of the test sections, the materials, and the various tests conducted are described in this section.

LAYOUT AND LOCATION OF TEST PAVEMENT SECTIONS

The ten test pavement sections used in this study were selected from a group of 22 inservice pavement structures originally set out in a study for the National Cooperative Highway Research Program (Lytton et al. 1990). Five pavement structures were selected in District 8, near Abilene, Texas. In this area, stiff layers are often encountered at shallow depths. Another five pavement structures were selected from District 21, near Brownsville. Texas. The subgrades in this region are thick, and shallow rigid layers are a less frequent occurrence. Table 4 summarizes the location and pavement structure of the selected test sites.

At each test section, ten positions, ten feet apart, were marked in the outside wheelpath. These ten positions, as shown in Figure 13, were used for the position of the monthly deflection testing. Cores of the asphalt layer at each site were taken from position 05. A testpit was also dug in the middle of each section to obtain base and subgrade samples for laboratory testing. To classify the subgrade, a hole was

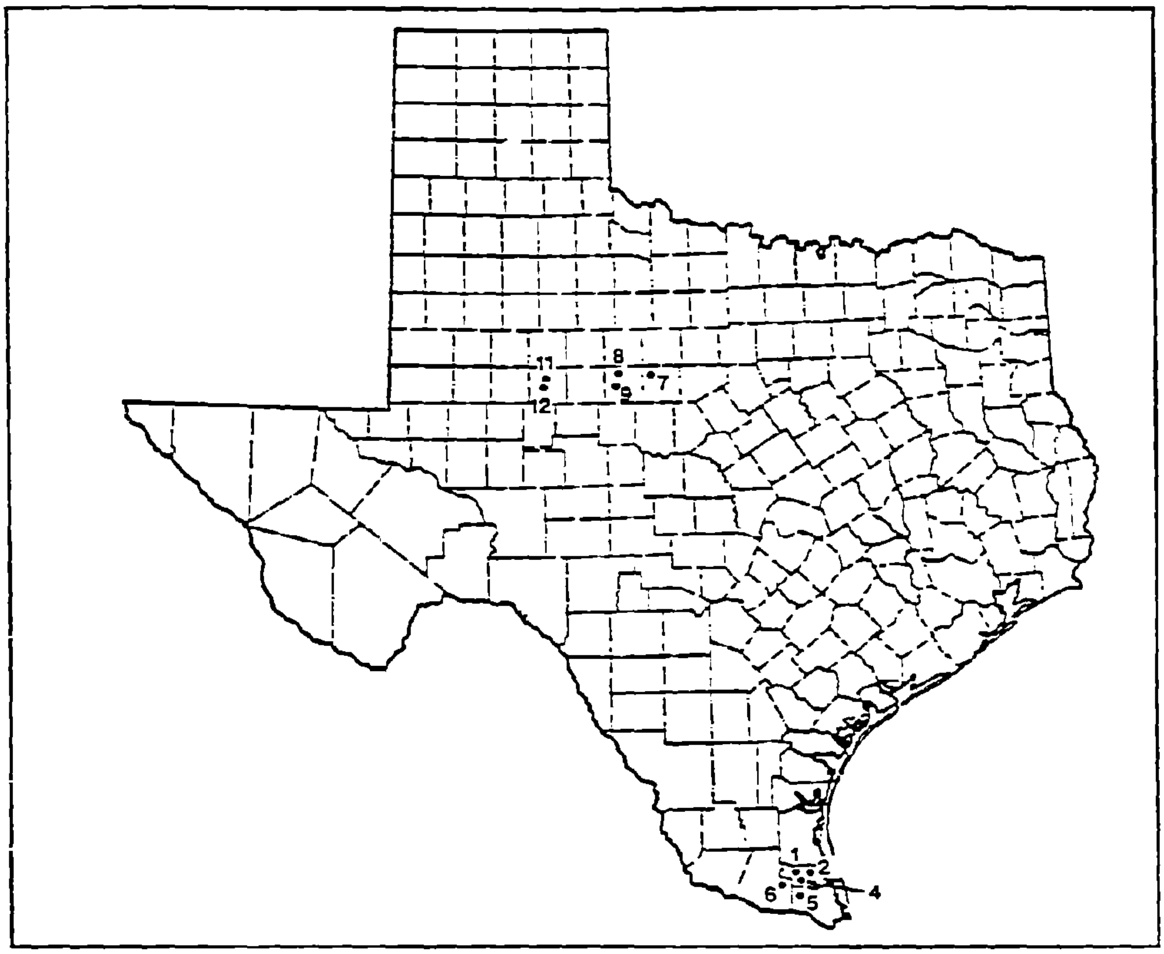

Figure 12. Location of the Test Pavement Sections.

drilled to a depth of twelve feet or until the water table was reached. On the sections where penetration tests were done, the subgrade was penetrated at positions 00, 05, and 09.

Table 4. The Location and Pavement Structure of the 10 Test Sites.

Site	District	County	Route	Pavement Structure and Subgrade*
1	21	Willacy	US 77 MP 4.1	2.25 Asphalt Concrete " Asphalt Treated Base 4.25 Flex Base " Sand Subgrade 6.0"
2	21	Willacy	SH 186 MP 33.2	1.0" Surface Layer 8.8" Calacie Flex Base Sand Subgrade
4	21	Willacy	FM 1425 MP 5	4.0" Asphalt Concrete Lime Treated Calacie 5.0" Clay Subgrade
5	21	Hidalgo	FM 1425 MP 3	3.0" Asphalt Concrete Asphalt Concrete 3.0" Calacie Flex Base 6.0" Dark Sandy Clay
6	21	Hidalgo	FM 491 MP 6.1	1.2" Surface Layer Calacie Flex Base 7.8" Clay Subgrade
7	8	Callahan	IH 20 MP 293	10.0 Asphalt Concrete " Limestone Base 11.0 Clay Subgrade "
8	8	Taylor	IH 20 MP 273.6	8.0" Asphalt Concrete Limestone Base 13.0 Clay Subgrade "
9	8	Taylor	FM 1235 MP 21	1.0" Seal Coat Limestone Base 8.0" Clay Subgrade
11	8	Mitchell	IH 20 MP 216	5.0" Asphalt Concrete Limestone Base 18.0 Sand Subgrade "
12	8	Mitchell	FM 1983 MP 1.0	1.0" Asphalt Concrete Limestone Base 8.0" Sand Subgrade

* Additional Subgrade Information are given in Appendix B

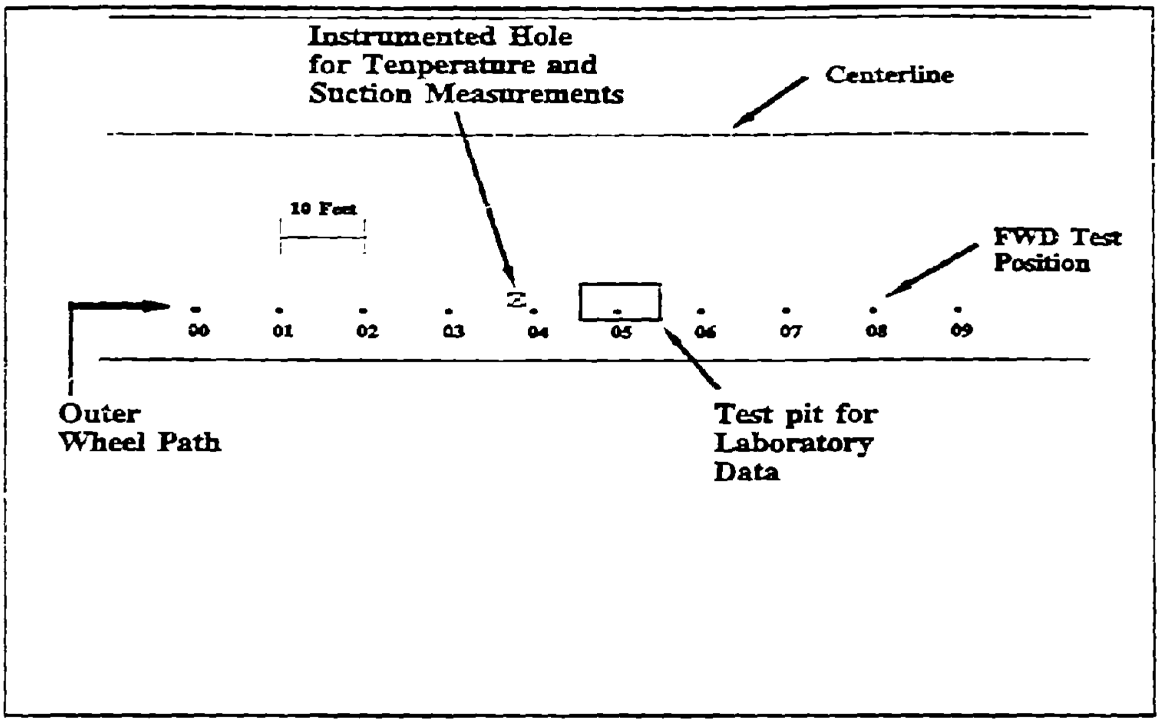

Figure 13. The Layout of a Typical Test Section.

SURFACE DEFLECTION TESTING

Equipment Used

The Dynatest Model 8000 FWD[1] has evolved as one of the most popular deflection testing devices in the United States. It was selected for use in this study because of its popularity and recent selection as testing device for the LTPP program of SHRP[2] (Richter and Rauhut 1989).

The Model 8000 FWD is a trailer mounted testing system towed by, and operated from, a standard automobile. A mass is hydraulically raised to

---

1 The Dynatest Model 8000 Falling Weight Deflectometer is manufactured by Dynatest Consulting Inc. in Ojai, California.

2 The Long Term Pavement Performance Study is one of the four major areas of the five year $150 million Strategic Highway Research Program.

a specified level, released on an electronic signal, and dropped onto a specially designed base plate resting on the pavement surface. This base plate is 11.8 inches in diameter and can tilt up to six degrees to conform to unlevel testing surfaces. It is also padded with a rubberized membrane to help distribute the load. A schematic of the FWD mass system is shown in Figure 14a. A load pulse, approximately in the shape of a half-sine wave form, is created. This load pulse, as shown in Figure 14b, has a duration of approximately 25 to 30 milliseconds. The magnitude of this load can be changed by changing the drop height or the weight of the mass.

A strain gauge load transducer, or load cell, measures the magnitude of the impact load to an accuracy of better than 2% ± 0.07 kN (Hudson et al. 1987). Up to seven geophones, or velocity transducers, measure the deflection induced by the load. One of these geophones is placed at the center of the base plate while the others can be placed at distances of the operators choice. The maximum possible distance from base plate to geophone is 7.4 feet. The absolute accuracy of the velocity transducers is better than 2% ± 2 microns (0.08 mils). The typical relative accuracy is 0.5% ± 1 micron (0.04 mil). The accuracy of the load cell and velocity transducers is within the ASTM-D4694[3] specifications.

Data from the velocity transducers and the load cell are passed through a processing system and stored on an on-board IBM compatible microcomputer. This computer monitors and controls the whole testing procedure. This includes lowering the loading plate and deflection sensors, raising and releasing the weight, recording the results, and raising the loading plate and geophones at the completion of the test.

Testing Procedure

FWD deflection testing was conducted at all test sections over a period of one year. Monthly, a series of deflection tests were conducted in the morning and the afternoon at every site. During these

[3] Annual Book of ASTM Standards. Vol 04.03. - Road and Paving Materials.

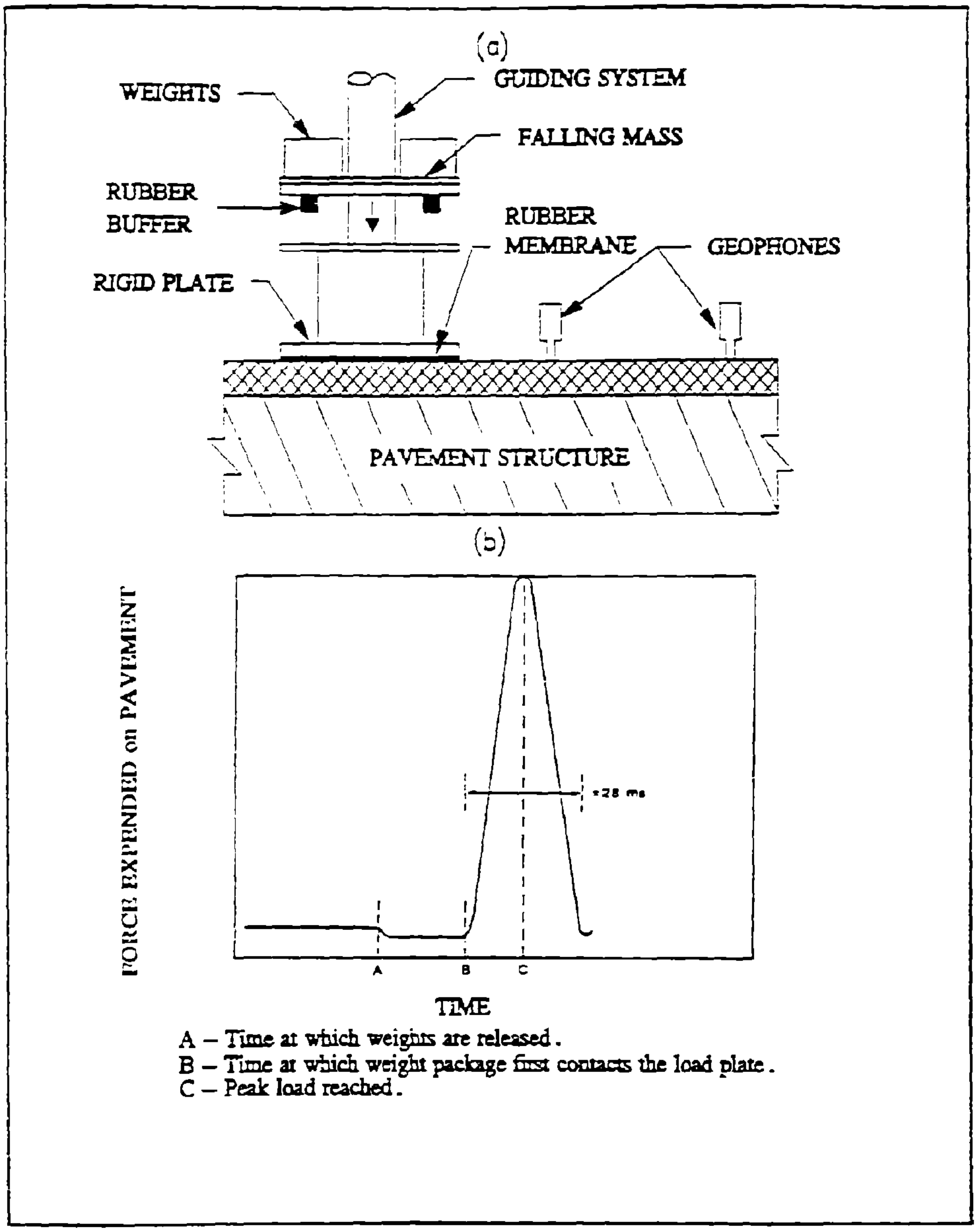

Figure 14. Schematic of the Falling Weight Mass System and a Typical FWD Load.

tests, the following FWD configuration was used: an 11.8 inch diameter loadplate, the 440 lb. weight set, and deflection sensors placed at radial distances of 0, 12, 24, 36, 48, 60, and 72 inches. The FWD was periodically calibrated as recommended by the manufac-turer to ensure the accuracy of the load cell, the deflection sensors, and the data acquisition system. The general testing procedure at each test site was as follows:

- The FWD operating software was set up to record the load and deflections with the proper gains.
- Starting at position 0, the following drop height sequence was used:
  - 1 seating drop to ensure proper contact,
  - 1 drop with an applied load of 6000 lb. ± 10%,
  - 1 drop with an applied load of 9000 lb. ± 10%,
  - 1 drop with an applied load of 12000 lb. ± 10%,
  - 1 drop with an applied load of 16000 lb. ± 10%.
- The drop sequence was repeated and recorded at all 10 positions.
- The pavement temperature was recorded from thermocouples placed in the asphalt and the base.
- The air temperature was recorded.
- The data was saved on floppy diskette for later analysis.

LABORATORY TESTING

Selected samples obtained from the asphalt concrete, the base course, and the subgrade were subjected to standard ASTM and AASHTO test procedures (Scullion et al. 1990, Kashyapa and Lytton 1988). This testing was required to determine the basic constitutive relationship between stress and deformation of the test site materials. For the asphaltic concrete the indirect tension test was chosen, while a repeated load triaxial test was selected for characterization of the base course and subgrade.

To model the behavior of base cources and subgrades, under a cyclic load such as expected under traffic, a repeated load triaxial device was used. In this test a cyclic load can be applied to a test sample while the confining pressure is controlled. The test has two major limitations. The deviatoric stress can only be applied along the principal axis of the specimen, and two of the three principal stresses are equal. The triaxial device can therefore only reproduce a stress state directly under a wheel load or the FWD base plate. As reported by McVay et al. (1985), even at this position a moving wheel load might induce a rotation of the principal axis. Furthermore, the confining stresses expected under a vehicle or FWD load changes in a cyclic nature, while the standard test only applies a constant confining stress. Allen and Thompson (1984) found that the improvements in testing the sample using cyclic confining stresses were not significant enough to be required. To characterize the test site materials, the following procedures were followed.

Asphalt Concrete

On each test site, four inch diameter cores were taken through the asphalt concrete at approximately position 05. On the thicker pavement structures, these cores were retrieved, and sawn to produce two samples (i.e., top and bottom section) for testing. Cores from the thinner asphalt sections were left intact. From these samples, an indirect tensile test was run at two frequencies, 10 and 20 Hz, and at four different temperatures, 0, 32, 77, and 100 degrees Fahrenheit. These temperatures were selected to provide a representative range of pavement temperatures.

Because an impulse load like the FWD excites a wide range of frequencies, it is not possible to identify a single frequency to simulate during the laboratory testing. By assuming that the FWD load is a harmonic wave, the frequency can be approximated as between 17 and 20 Hz. From the time history and auto power spectra for the FWD, it was found that the predominant frequency excited by the FWD was in the order of 20 to 21 Hz (Hudson et al. 1987). The results of these tensile tests are listed in Tables A1 through A10 in Appendix A.

Granular Base

Samples from the granular base material were also obtained from all test sections. This material, obtained from a test pit at approximately position 05, was bagged and brought to the laboratory. Before disturbing the material in the test pit, the moisture content and density were obtained using a nuclear density device (AAHTO T238-79). In the laboratory, six inch diameter specimens, twelve inches long, were remolded at approximately the measured field moisture content, and field density. These cylindrical specimens were tested in a repeated load triaxial test according to AASHTO T 274-82. All measurements were made in the 200th cycle. The test sequence used and the confining and deviatoric stresses applied were as specified in the AASHTO test procedure for granular soils. The calculated resilient modulus, and pressures at which the deformations were measured are listed, per test site, in Tables A1 through A10 of Appendix A.

The measured resilient moduli and stress states for each sample were used to develop equations in which the resilient modulus is a function of both the mean principal stress and the octahedral shear. The form of this equation is given in equation 2.4. From a least square curve fitting analysis, the obtained coefficients k_1, k_2, and k_3 are listed in Table 5. The coefficient of determination, r^2, for each set of data is also shown.

Subgrade

Samples of the subgrade material were obtained from thin walled sampling tubes, pushed into the subgrade at the position of the test pit. These samples, extruded from the tubes, were wrapped and brought to the laboratory for testing purposes. In the laboratory, the fine grained samples, as retrieved from the thin walled sampling tube trimmed to a diameter of 2.81 inches and used for resilient modulus testing. The material retrieved from sites with sandy subgrades, were remolded to the field measured moisture content and density obtained using a nuclear density testing device. The specimens 2.81 inches in diameter were subjected to a standard resilient modulus test as described in AASHTO T 274-82. All measurements were made in the 200th cycle. The calculated resilient moduli, for every stress state are listed, per test site, in Tables A1 through A10 of Appendix A.

Table 5. Base Course Coefficients for Equation 2.4.

SITE	MATERIAL	k_1	k_2	k_3	r^2
1	Calacie	779	0.89	-0.47	0.93
2	Calacie	495	0.83	-0.36	0.75
4	Lime Treated Calacie	433	0.62	-0.52	0.95
5	Calacie	128	1.49	-1.53	0.96
6	Calacie	645	0.63	-0.22	0.86
9	Limestone	1282	0.32	-0.06	0.91
11	Limestone	307	0.78	-1.39	0.52
12	Limestone	699	0.60	-0.08	0.84

The measured resilient modulus and stress states for each sample were used to develop equations in which the resilient modulus is a function of both the mean principal stress and the octahedral shear. The results of the curve fitting analysis, are shown in Tables 6 and 7. In Table 6 the coefficients for the universal model (equation 2.4) are listed. For the sites with clayey subgrades the data were also fitted with the bilinear model (equation 2.8). The coefficients and coefficient of determination are shown in these tables.

SUBSURFACE EXPLORATION

The drilling conducted at every test section consisted of a single hole drilled to a depth of 12 feet. To confirm rigid layers recorded on the drilling logs, and to determine the depth of stiff layers deeper than the drilling depth, additional tests were carried out. In District 8, where stiff layers are often encountered at shallow depths, seismic refraction techniques and dynamic penetration methods were used. The equipment used, the testing procedure, and the methods of data interpretation are described in this section.

Table 6. Subgrade Coefficients for Equation 2.4.

SITE	MATERIAL	k_1	k_2	k_3	r^2
1	Sand	340	0.43	-0.84	0.92
2	Sand	148	0.25	-0.48	0.76
4	Clay	82	0.10	-0.86	0.97
5	Sandy Clay	109	0.17	-0.67	0.92
6	Clay	46	0.25	-1.38	0.95
7	Clay	255	0.11	-0.32	0.93
8	Clay	127	0.16	-0.81	0.87
9	Clay	119	0.09	-0.95	0.87
12	Sand	207	0.51	-0.75	0.97

Table 7. Subgrade Coefficients for the Bilinear Model (Equation 2.8). on Sections with Clay Subgrades.

SITE	MATERIAL	k_1	k_2	k_3	k_4	r^2
4	Clay	5.1	4019	2605	-102	0.98
6	Clay	4.6	6426	7144	-519	0.95
7	Clay	6.3	4864	331	-224	0.80
8	Clay	6.1	5406	2582	124	0.90
9	Clay	5.1	5832	5830	170	0.98

Seismic Refraction Analysis

Seismic analyses techniques are well established. Since the 1920s they have been widely used in many geophysical applications. Especially in the area of bedrock mapping, they have become increasingly popular (Peffer and Robelen 1983). The seismic method measures the travel time of seismic shock waves to increasingly distant geophones, placed in a line on the ground surface. Three types of seismic waves are normally observed in engineering seismology. These are the compression (P) wave, the shear (S) wave, and the Rayleigh (R) surface wave. As illustrated in Figure 15a, these waves are refracted and reflected at all interfaces where a significant change in velocity occurs. Similar to the refraction of light rays, Snell's law can be applied. In refraction analysis, the first arrival time of the fastest wave, the compression wave, is recorded at every geophone. From the variation in travel time with distance, the depth and nature of the refracting material can be determined (Richart et al. 1970).

From a typical time-distance plot, as shown in Figure 15b, the depth of any interface can be calculated using the following two equations (Steward and Beaven 1980, Mooney 1977):

$$D_2 = \frac{V_3\ T_{i3}}{2}\ \frac{1}{\sqrt{\left(\frac{V_3}{V_2}\right)^2 - 1}} - D_1 \left[\frac{\sqrt{\left(\frac{V_3}{V_1}\right)^2 - 1}}{\sqrt{\left(\frac{V_3}{V_2}\right)^2 - 1}} - 1\right] \tag{3.1}$$

$$D_1 = \frac{V_2\ T_{i2}}{2}\ \frac{1}{\sqrt{\frac{V_2}{V_1}^2 - 1}} \tag{3.2}$$

where:

D_x = Depth from the surface to the bottom of layer x;

T_{ix} = The intercept time by extending V_x on the time-distance plot;

V_x = The velocity of the P waves in layer x.

These equations are adequate for analyzing structures with close to horizontal interfaces. The layer thickness of non-horizontal structures can be determined by also conducting a reverse seismic profile. This requires taking two profiles in opposite directions along the same line.

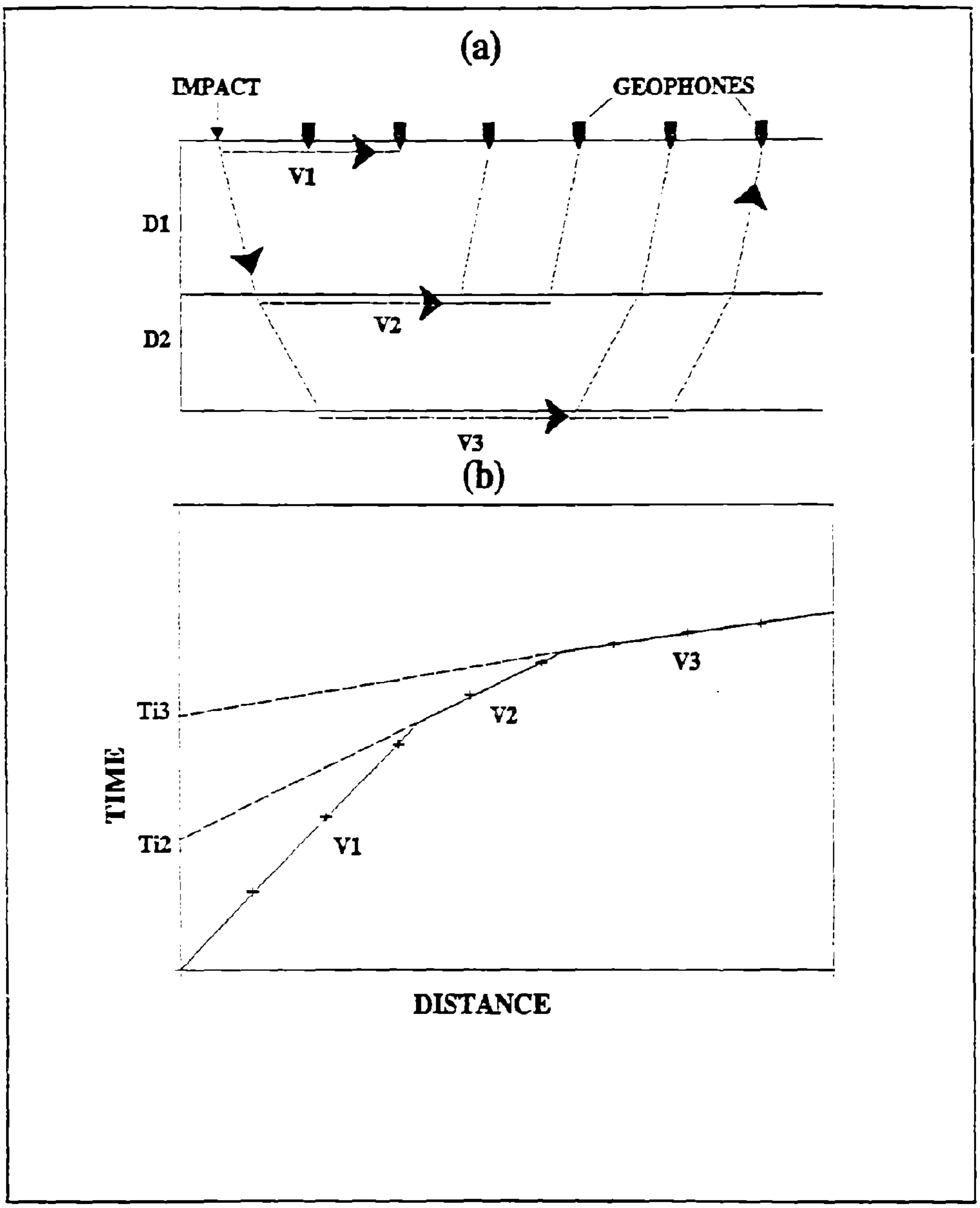

Figure 15. Seismic Refraction of an Idealized Three-Layer System.

Identical travel-time plots in both directions are a sign of horizontal layers. Non-identical time-distance plots are an indication of dipping interfaces. Mooney (1977) published procedures for the interpretation of time-distance plots for multiple dipping structures.

The velocity of the compression waves is an additional source of information obtained from the seismic analysis. From experience it is possible to relate the wave velocity to material type since harder, denser materials have a higher velocity than loose and soft materials. Typically compression wave velocities are in the range of 1000 to 23,000 ft./sec. Table 8, adapted from Jacosky (1950), lists some typical velocities of longitudinal compression waves in different material types.

The seismic refraction technique does have limitations. Steward and Beaven (1980) pointed out the following problems and limitations:

- A thin layer of hard material within a soft material may not cause any refractions, and might not be detected;
- If two layers with distinct engineering characteristics have similar seismic velocity, they will be identified as one layer;
- If a first refracting layer is relatively thin, and is underlain by a second refractor, the first layer might go undetected; and
- The theory of refraction assumes that the seismic velocity increases with depth. "Reverse" structures cannot be analyzed.

Equipment and Test Procedure

The equipment employed for the seismic survey was a Nimbus Model ES-1210F[4] exploration seismograph with associated cables and geophones. This twelve channel instrument is equipped with signal enhancement and filtering capabilities. Background noise can be greatly reduced by recording several impacts and superimposing the recorded signals. This

[4] The Model ES-1210F is a product of EG&G Geometrics, Sunnyvale, CA.

Table 8. Typical Compression Wave Velocities by Material.

Material	Velocity	
	Ft./sec.	M/sec.
Weathered Surface Material	1000 - 2000	305 - 610
Gravel, Rubble, or Sand (dry)	1500 - 3000	470 - 900
Sand (wet)	2500 - 6000	610 - 1800
Clay	3000 - 9000	900 - 2750
Water (depend on temperature and salt content)	4700 - 5500	1450 - 1700
Sandstone	6000 - 13000	1800 - 4000
Shale	9000 - 14000	2750 - 4300
Chalk	6000 - 13000	1800 - 4000
Limestone	7000 - 20000	2100 - 6100
Granite	15000 - 19000	4500 - 5800
Metamorphic Rocks	10000 - 23000	3050 - 7000

is done by stacking the filtered signals in the seismograph's digital memory. This model is also equipped with a writing oscillograph, that can print the recorded signals at the completion of the test.

As an energy source, an 8 pounds sledgehammer was used to strike a striker plate. This plate ensured that the energy was coupled to the ground and that a reliable triggering of the hammer switch was obtained. The geophone-spread cable was placed over a distance of 120 feet. Figure 16 shows the spacing of the geophones. On all sites seismic profiles were recorded in both directions to determine the dipping of any stiff layers underlying the subgrade. The results of the refraction analysis are shown in Table 9.

Minicone Penetration Device

Penetration devices have long been used in deep subsurface investigations and geotechnical analysis. Recently, this technique has also been applied to shallow subgrade soil investigations (Khedr et al. 1985). A penetration device is a rod with a larger diameter conical tip that is forced vertically into the ground. This penetration can be at a constant rate or by impact. The resistance to penetration is normally related to material properties or empirical material qualities. It is

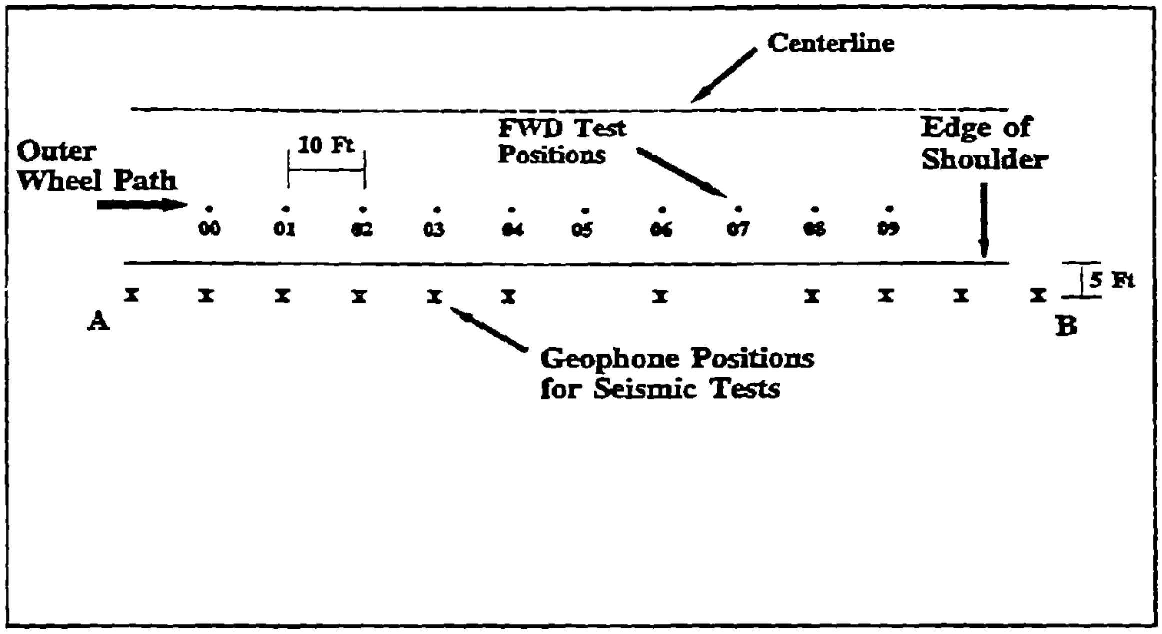

Figure 16. The Typical Layout of the Seismic Test.

Table 9. Results of the Refraction Analysis.

SITE	LAYER DEPTH (Position 00)	LAYER DEPTH (Position 09)	COMPRESSION WAVE VELOCITY
7	0 to 7.6 ft. 7.6 to 14.0 ft. 14 0 +	0 to 9.9 ft. 9.9 to 25.2 ft. 25.2 +	1100 ft/sec 5500 ft/sec 12400 ft/sec
8	0 to 16.8 ft. 16.8 +	0 to 17.0 ft. 17.0 +	1200 ft/sec 7800 ft/sec
11	0 to 13.5 ft. 13.5 +	0 to 13.5 ft. 13.5 ÷	1300 ft/sec 3400 ft/sec
12	0 to 7.6 ft. 7.6 +	0 to 12.1 ft. 12.1 +	1200 ft/sec 3100 ft/sec

well suited as a logging tool for delineation of stratigraphy (Douglas and Olsen 1981).

The Minicone[5], the penetration device used in this study, is a smaller version of the standard penetration cone. The device is operated from a standard pick-up truck and can penetrate the earth to a depth of 40 feet. Using the truck's hydraulic system, the cone is pushed into the subgrade at a constant rate. The penetration rod is equipped with an electric cone, the diameter of a pencil. This cone measures both the tip and sleeve resistance against penetration. The data are continuously recorded against depth and saved by a portable microcomputer. A schematic of the minicone is shown in Figure 17.

The primary objective of using the Minicone in this study was to determine the depth to a stiff layer. This condition was defined as the point at which the Minicone refused further penetration. As shown later, this assumption provided a good comparison with the rigid layer interfaces determined through seismic refraction. In addition to defining the point of refusal, the measured tip and sleeve resistance were used to classify the subgrade material. This material identification was based on the measured tip and sleeve resistance and a soil behavior type classification chart shown in Figure 18 (Douglas and Olsen 1981, Robertson and Campanella 1983). The friction ratio, fr, is defined as:

$$fr = \frac{f_c}{q_c} \tag{3.3}$$

where:

f_c = Measured cone tip resistance;

q_c = Measured cone sleeve resistance.

At each test site in District 8, the subgrade was penetrated at the beginning, middle, and end of the section. First a percussion drill

[5] The Minicone has been developed by Fugro-McClelland Marine Geosciences Inc., Houston, Texas.

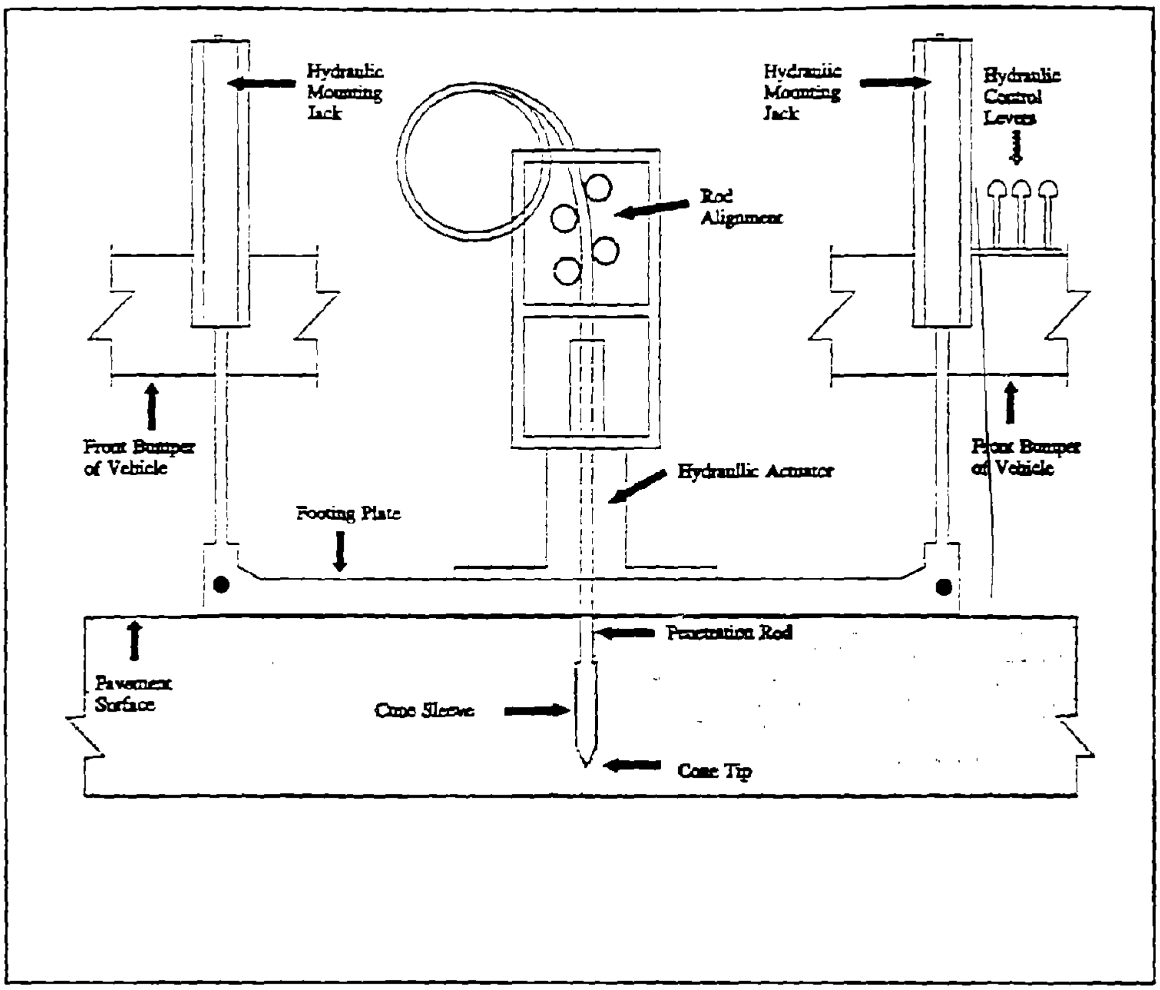

Figure 17. A Schematic of the Minicone Penetration Device.

was used to drill a 1.5 inch diameter hole through the surface and base in the outer wheelpath. Next the Minicone, mounted on the front buffer of a pick-up, was vertically aligned with the drilled hole. The tip of the cone was lowered to the bottom of the hole and then pushed into the subgrade using the pick-up's hydraulic system. The electric cone measured the tip and sleeve resistance until refusal. The depth at which the subgrade refused further penetration is listed in Table 10. As listed the penetrations conducted at position 09 of site 9 and 11 were unsuccessful due to mechanical problems.

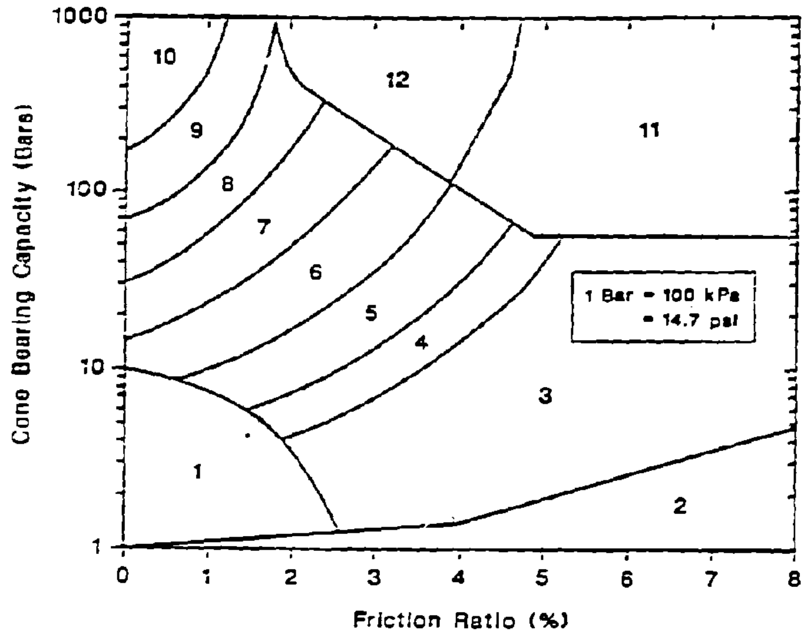

Zone	Soil Behavior Type
1	Sensitive Fine Grained
2	Organic Material
3	Clay
4	Silty Clay to Clay
5	Clayey Silt to Silty Clay
6	Sandy Silt to Silty Clay
7	Silty Sand to Sandy Silt
8	Sand to Silty Sand
9	Sand
10	Gravely Sand to Sand
11	Very Stiff Fine Grained
12	Sand to Clayey Sand

Figure 18. A Simplified Soil Behavior Chart for an Electronic Friction Cone (adapted from Robertson and Campanella 1983).

Table 10. Depth at which the Subgrade Refused Further Penetration by the Minicone.

SITE	POSITION	TEST SUCCESSFUL	DEPTH
7	00	Yes	7.6 ft
	06	Yes	9.0 ft
8	06	Yes	20.0 ft
	09	Yes	19.3 ft
9	00	Yes	12.6 ft
	06	Yes	12.5 ft
	09	No	--
11	00	Yes	17.0 ft
	09	No	--
12	00	Yes	8.7 ft
	09	Yes	12.0 ft

CHAPTER IV
ADDRESSING RIGID LAYERS BELOW THE SUBGRADE IN LAYERED ELASTIC BACKCALCULATION

This chapter discusses the analysis of deflection data on sections where the subgrade is underlain with rigid layers or bedrock. In the mechanistic analysis of nondestructive deflection data, a multilayered, linear elastic pavement model is often used. In this model, the assumed subgrade thickness influences the backcalculation of layer properties and, as a result, the predicted pavement performance. This chapter illustrates the influence of the assumed rigid layer depth on the analysis of deflection data and confirms its influence on pavement design. A procedure to estimate the effective depth to a rigid layer from deflection measurements is developed for a multilayered elastic system. The procedure is used to predict the effective depth to a rigid layer on several of the test sections. This depth is compared to information from drilling logs and laboratory tests, as well as the results obtained from the penetration tests and seismic refraction techniques.

INTRODUCTION

An inherent assumption of layered elastic theory, often used to model a multilayered pavement system, is that the subgrade is infinitely thick (Burmister 1943). However most subgrade have a profile that varies with depth. Whether the soil is sedimentary or residual in nature, or even a man-made deposit like a fill, it is usually underlain by a stiff material or a rigid layer (Lambe and Whitman 1969). The depth to this stiffer material varies considerably, and it is expensive to determine.

In a layered elastic system an underlying rigid layer is normally modeled by assigning a high Young's modulus to the material below the depth at which the rigid layer occurs. The surface deflections predicted by layered elastic programs are highly influenced by the depth assigned to a rigid layer as shown in Figure 19. It can therefore be expected that a deflection analysis to determine layer moduli based on layered elastic theory will be influenced by the subgrade thickness

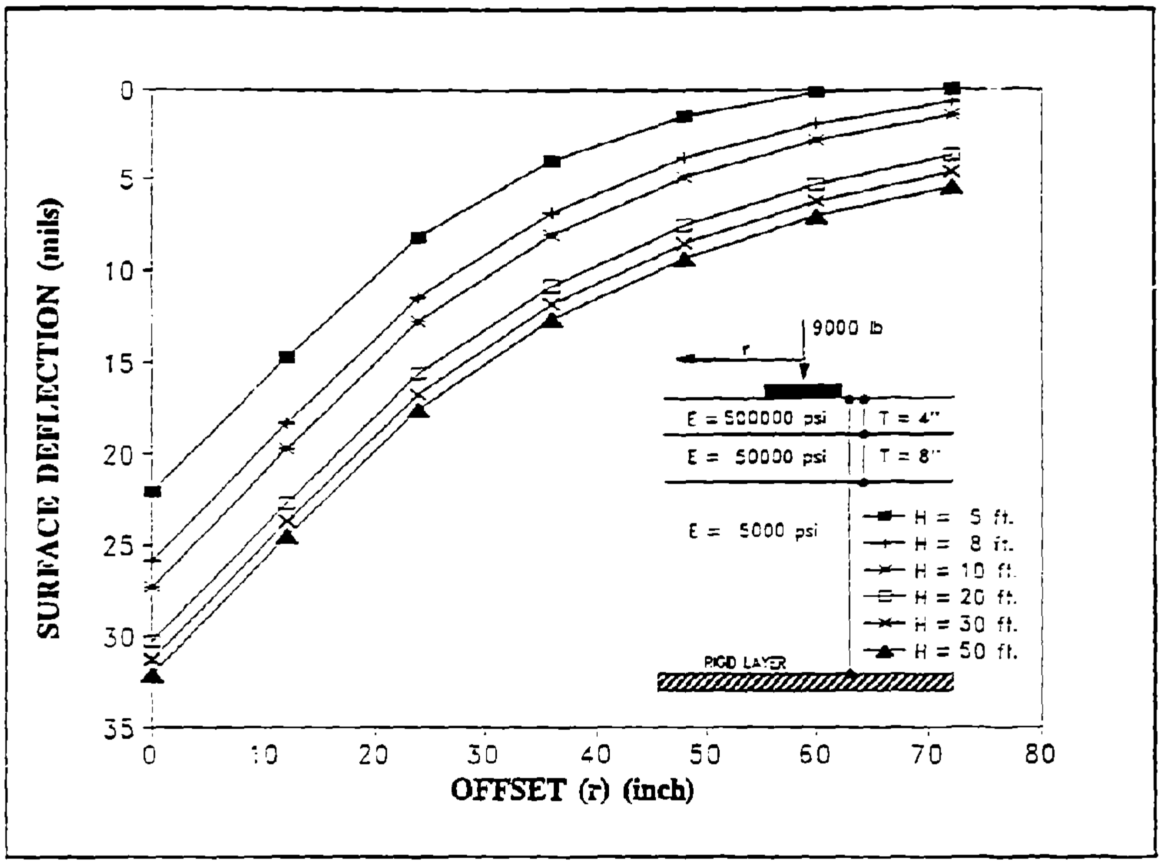

Figure 19. Influence of a Rigid Layer on the Theoretically Calculated Surface Deflections under an FWD Load.

assumed during the analysis. The influence on the backcalculated moduli in itself is not the issue but rather how the eventual pavement design is affected. The deflection data on two of the test sections are analyzed to illustrate the influence of subgrade thickness assumptions on pavement evaluation and design.

INFLUENCE OF ASSUMED SUBGRADE THICKNESS ON PAVEMENT EVALUATION AND DESIGN

Influence on Deflection Analysis

In the mechanistic analysis of nondestructive deflection data, the thickness of each pavement layer is usually known, while the subgrade thickness is normally assumed to be infinitely thick. Some procedures suggest using an arbitrary subgrade thickness such as 20 feet (Bush

1980), while others recommend the use of the actual subgrade thickness (Uddin et al. 1986). The assumed subgrade thickness does however influence the backcalculation results (Yang 1989, Briggs and Nazarian 1989).

On two test sections, sites 7 and 11, deflection measurements were obtained using an FWD at four different load levels. At each of the ten test positions per site, eight deflection bowls were measured. Using the backcalculation program MODULUS 3.0 (Uzan et al. 1988), the deflection bowls were analyzed assuming several subgrade thicknesses. On these pavement sections the actual measured depth to a stiff layer was in the order of 10 feet for site 7, and 14 feet for site 11. The influence of the assumed subgrade thickness during deflection analysis on the backcalculated moduli is shown in Figures 20 and 21.

In both pavement structures the backcalculated subgrade moduli become stiffer as the assumed depth to the rigid layer becomes larger during the analysis. In order to match the same deflection bowl the modulus of the granular base decreases, as the subgrade modulus and assumed depth to the rigid layer increases. The stiffness of the asphalt surface is least affected by the assumed subgrade thickness. As later discussed in Chapter VI, the best backcalculation results are obtained when the actual depth to the rigid layer is used in the analysis. This will be substantiated by the laboratory results; although, a perfect agreement between the laboratory results and the backcalculated moduli should not be expected.

Influence on Pavement Design

Although each set of backcalculated moduli and assumed subgrade thickness matches the same deflection data, they ultimately lead to different designs. The backcalculated moduli as shown in Figures 20 and 21 were used to design a rehabilitation project and a new design. The influence of the assumed rigid layer depth on pavement design is illustrated in terms of predicted pavement performance. The rut depth, and cracked surface area after 1 million repetitions of a standard

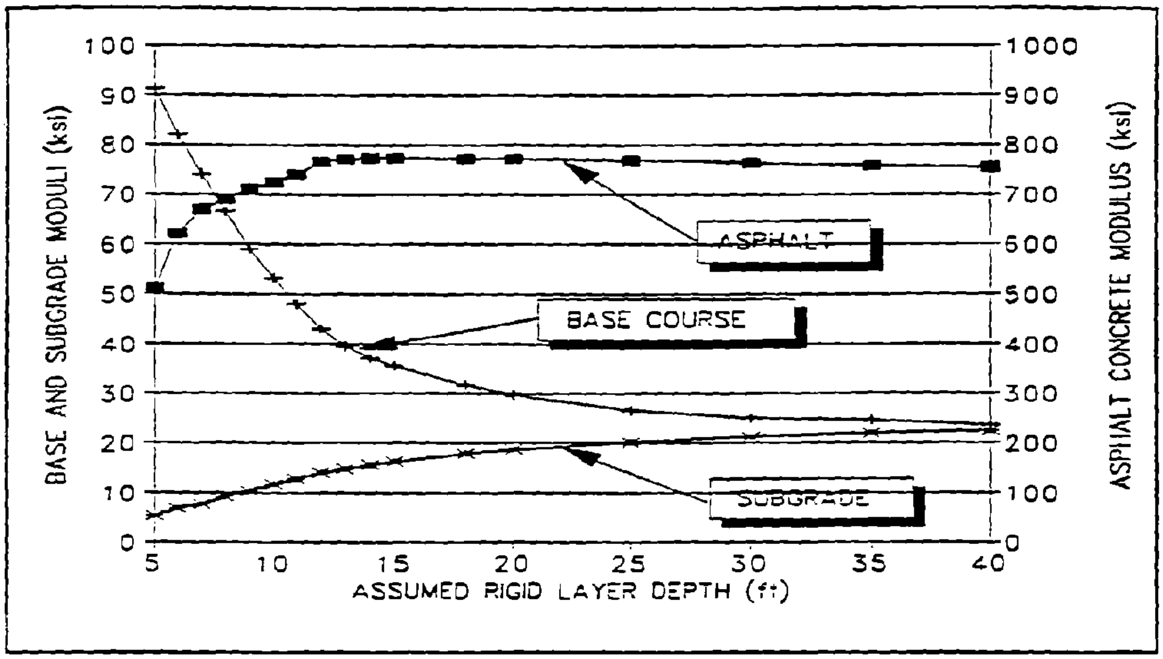

Figure 20. Influence of the Assumed Subgrade Thickness on the Backcalculation of Layer Moduli for Test Site 7.

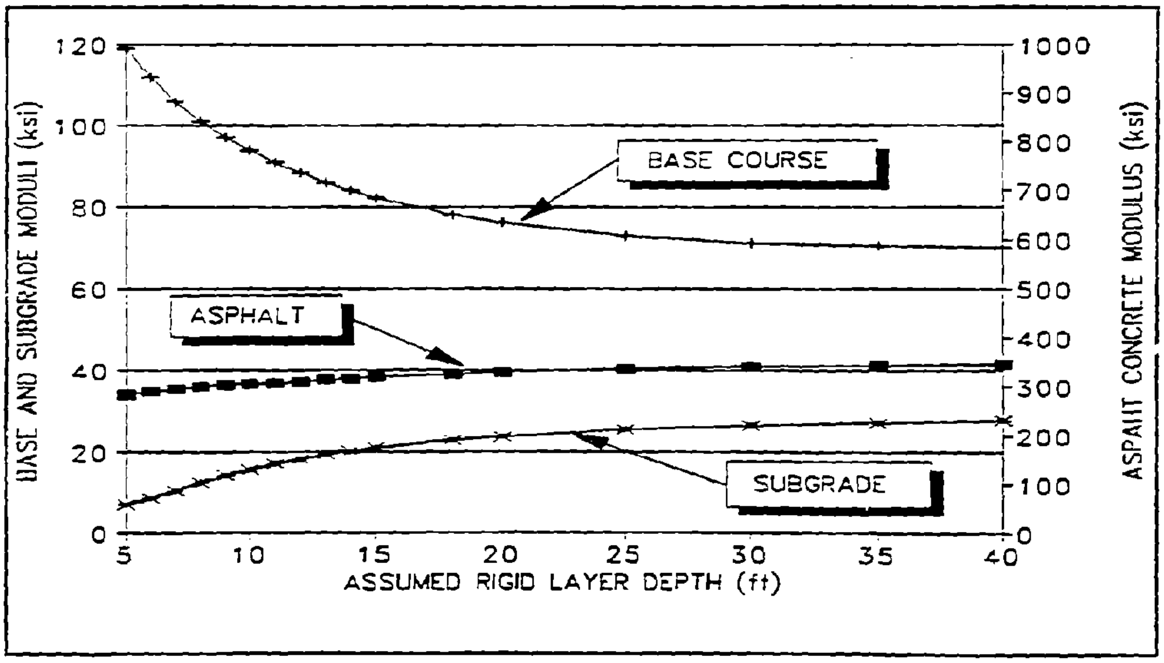

Figure 21. Influence of the Assumed Subgrade Thickness on the Backcalculated Layer Moduli for Test Site 11.

18,000 lb. (80 kN) single axle load are predicted. For this purpose the methodology used in the new Texas State Department of Highways and Public Transportation's mechanistic-empirical design program TFPS (Uzan et al. 1989, Rohde et al. 1989) was used.

In TFPS the cracked surface area is a function of the calculated tensile strain at the bottom of the asphalt layer, the number of load repetitions, and the stiffness of the asphalt layer. The rutting model in TFPS is based on a quasi-linear elastic analysis using an incremental procedure (Uzan and Lytton 1982). The rutting, or permanent deformation, develops in all pavement layers and is a function of each material's stiffness and permanent deformation characteristics.

Influence on a Rehabilitation Project

On a rehabilitation project nondestructive deflection testing is typically used to obtain the pavement properties of the existing surface, base and subgrade. To this pavement structure an asphalt overlay is often added to provide an acceptable pavement service for a given design period. To show the importance of the assumed rigid layer depth during backcalculation, on the eventual design of rehabilitation projects, the following was done: a two inch asphalt overlay was added to the pavement structure backcalculated and shown in Figures 20 and 21. The predicted performance of the "rehabilitated" pavements is shown in Figures 22 and 23.

Figure 22 shows the expected cracking based on an analysis using a range of assumed rigid layer depth in both the backcalculation and performance analysis. The predicted cracking is plotted in terms of percent change in the predicted cracked surface area. The cracking predicted using the actual rigid layer depth during analysis is used as reference. The actual rigid layer for site 7 is 10 feet, and for site 11 is 13 feet. Clearly an overestimate of the depth to a stiff layer results in higher expected cracking. The expected rutting, as shown in Figure 23, is only slightly higher if the stiff layer is placed to deep. These results can be explained by the influence of the assumed rigid layer on the backcalculation results, shown in Figures 20 and 21. When the subgrade thickness is over-predicted, the backcalculated subgrade

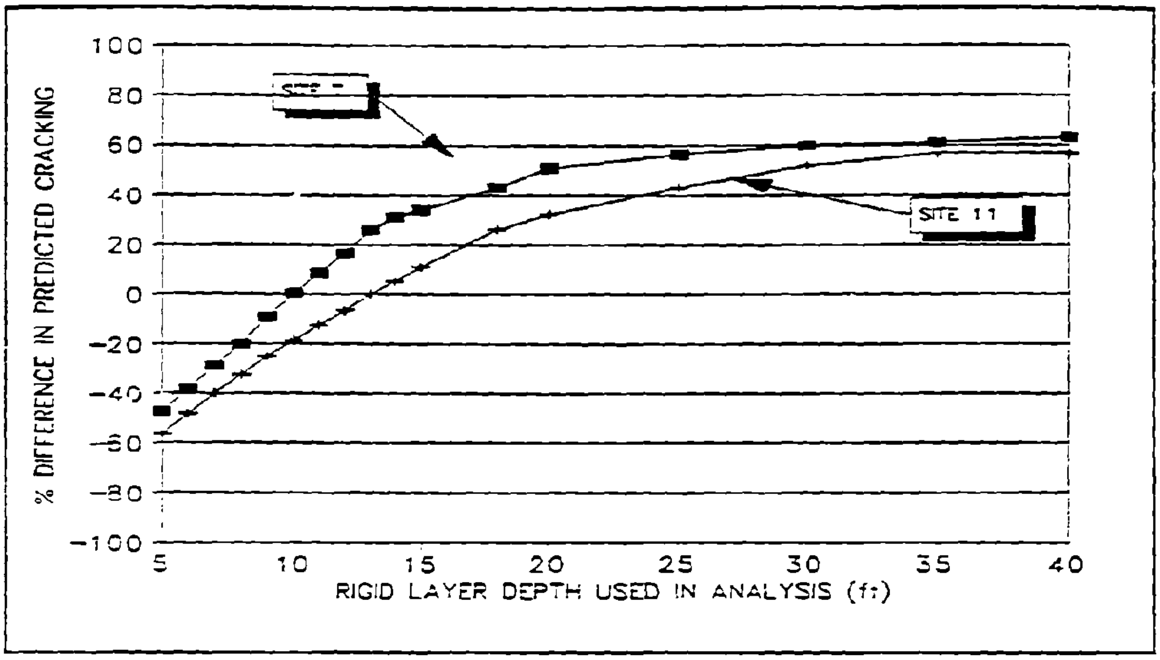

Figure 22. Influence of Assumed Subgrade Thickness on the Expected Cracking of a Rehabilitation Design (Sites 7 and 11).

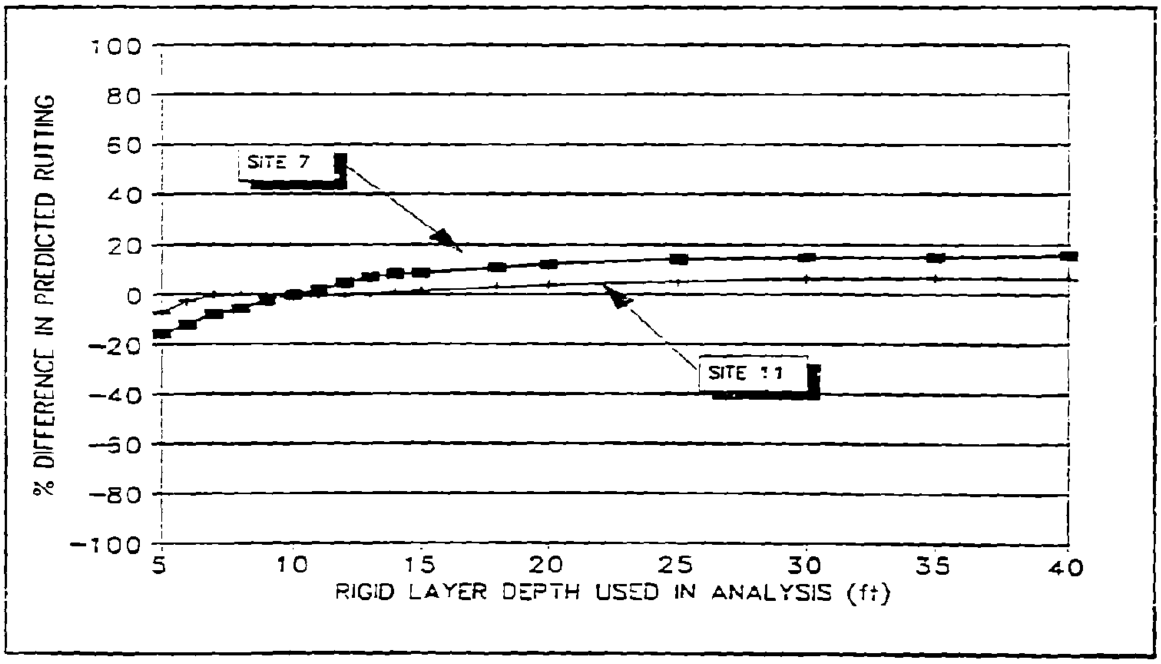

Figure 23. Influence of Assumed Subgrade Thickness on the Expected Rut Depth of a Rehabilitation Design (Sites 7 and 11).

moduli are too high and the base moduli too low. With an overestimate of the rigid layer depth, the reduction in the base modulus is higher than the increase in the subgrade modulus. This results in excessive rut and crack prediction. In general an overestimate of the subgrade thickness during deflection analysis would ultimately result in conservative rehabilitation designs. Estimating the depth to a rigid layer to less than that which actually occurs would generally provide an unconservative rehabilitation design due to an overestimation of the base modulus.

Influence on a New Design

For a new pavement design, backcalculation procedures are often used to obtain only the subgrade modulus. This requires conducting deflection testing on existing pavements founded on the same subgrade. In the design process the thicknesses of all pavement layers are then determined to provide an acceptable pavement service for a given design period. To illustrate the influence of the assumed subgrade thickness during deflection analysis on the design of a new pavement structure, the following analysis was completed: the predicted performance of a five inch asphalt surface, and eight inch granular base on the backcalculated subgrade shown in Figures 20 and 21, was predicted. To determine the stiffness of the base, the USCE procedure (Barker and Brabston 1975) was used. In this procedure the stiffness of the base is a function of the subgrade modulus and the thickness of the base layer. The predicted performance of the new pavements, designed on subgrades similar to that of sites 7 and 11, are shown in Figures 24 and 25.

Unlike the rehabilitation designs, an overestimate of the subgrade thickness leads to unconservative pavement designs for new construction. For example, on the subgrade of site 7, the cracking can be underpredicted by as much as 60 percent if an infinite halfspace was used during backcalculation and design. The expected rutting could be underpredicted by 50 percent if a rigid layer was not considered during the analysis. By overestimating the rigid layer depth the subgrade modulus is overestimated. This in turn leads to an underprediction of the expected cracking and rutting. The same would apply for a rehabilitation design where the existing base is replaced or reworked.

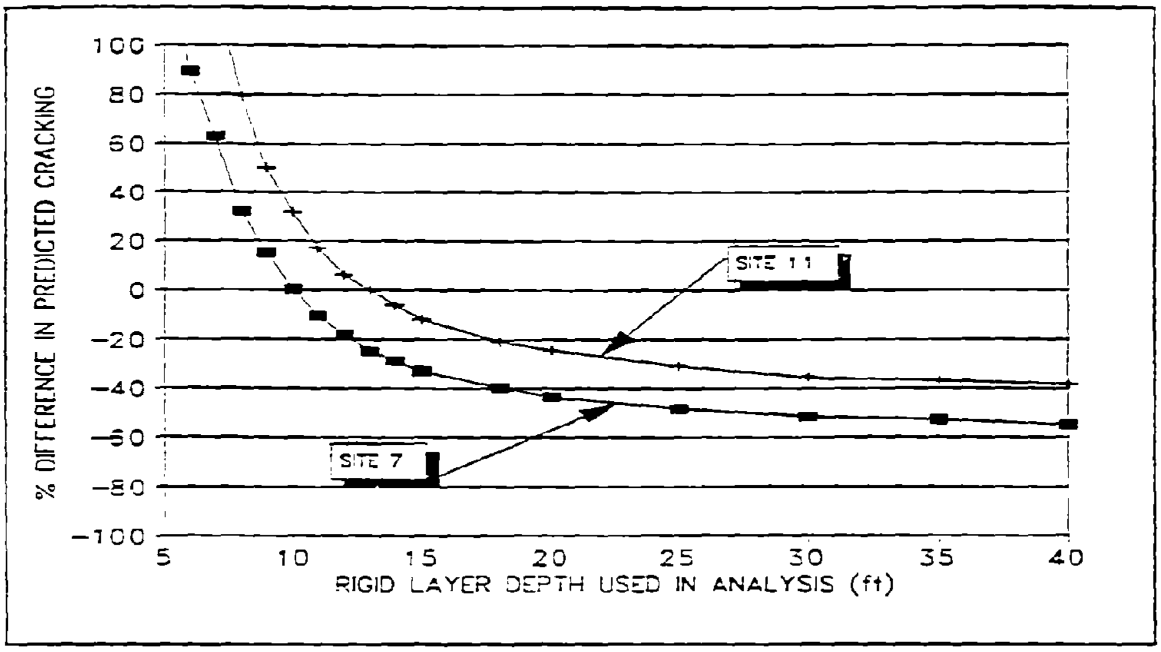

Figure 24. Influence of Assumed Subgrade Thickness on the Expected Cracking of a New Design near Sites 7 and 11.

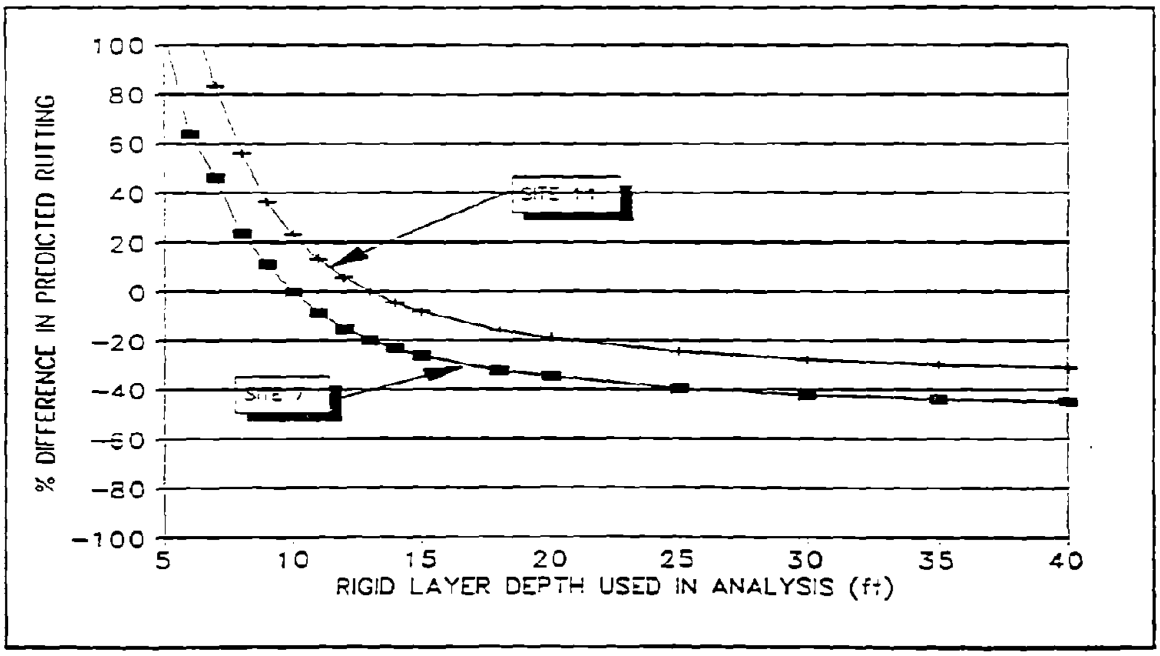

Figure 25. Influence of Assumed Subgrade Thickness on the Expected Rut Depth of a New Design near Sites 7 and 11.

Because only the backcalculated subgrade modulus is used in the performance prediction, the design would be unconservative. If the depth to a rigid layer is estimated to be less than the actual depth, a conservative design would be the result.

It needs to be pointed out that the trend in results is not a function of the backcalculation program used but of the multilayered linear elastic model employed. A similar trend would result from an analysis using BISDEF, CHEVDEF (Bush 1980) or any of the backcalculation procedures using a linear elastic multilayered program.

It has been shown that the assumed rigid layer depth significantly influences the backcalculation process. To determine the consequences of using the correct subgrade modulus, but the wrong rigid layer depth in the design process, the following analysis was conducted. A new pavement design, as described above, was performed using the subgrade modulus associated with the actual rigid layer depth. The cracking and rutting was predicted using one set of layer moduli and changing only the subgrade thickness of the design pavement model. The results are shown in Figures 26 and 27. Clearly the predicted cracking and rutting are not significantly affected by the assumed subgrade thickness if the correct layer moduli are used. It can be concluded that the influence of the assumed rigid layer depth is primarily a backcalculation issue. Once the correct moduli are obtained, the assumed rigid layer depth in itself does not significantly influence the performance predictions.

A METHOD TO ESTIMATE THE DEPTH TO A RIGID LAYER

As apparent from the previous section, the depth to a rigid layer is important for accurate deflection analysis and pavement design. Due to the nature of pavements, this parameter often varies considerably along the length of a pavement section. To establish this depth from penetration tests or other techniques is costly and often not practical. Ideally it should be inferred from the deflection or other nondestructive testing data.

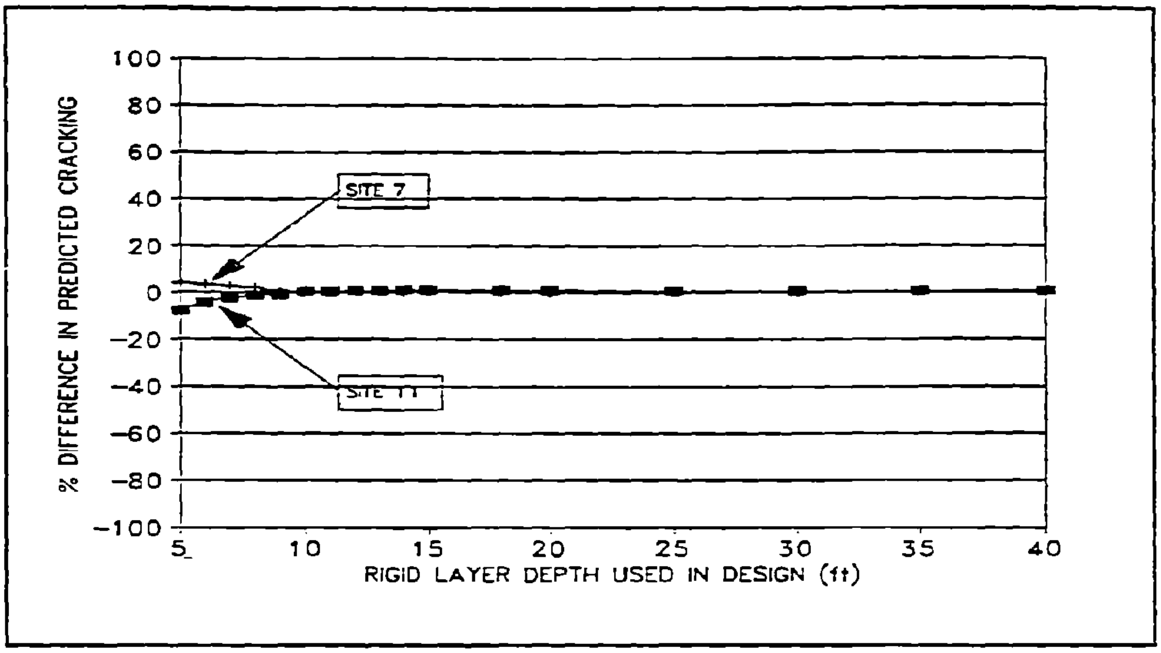

Figure 26. Influence of Assumed Subgrade Thickness During Design on the Expected Cracking of a New Design near Sites 7 and 11.

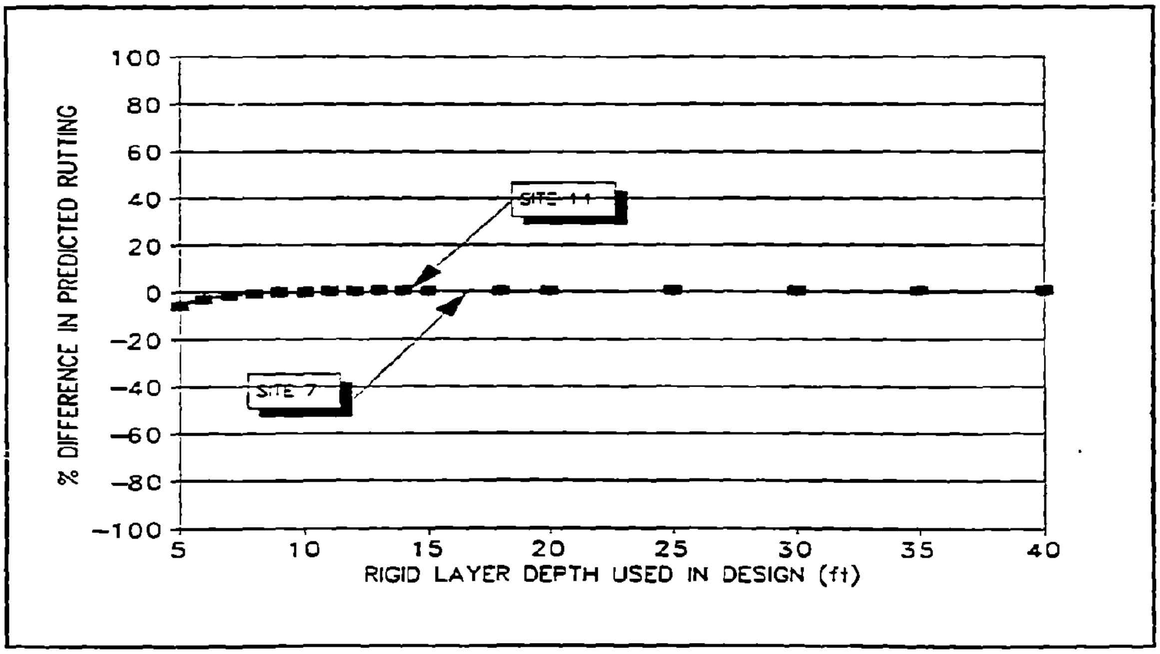

Figure 27. Influence of Assumed Subgrade Thickness During Design on the Expected Rut Depth of a New Design near Sites 7 and 11.

A couple of methods to determine the depth to a rigid layer using FWD deflections were investigated. The first method evaluated was the approach suggested by Chou (1989) and explained in Chapter II. This method consists of analyzing deflection data using different rigid layer depths. For each calculated deflection bowl, the root mean square percent error (RMSE) is calculated using the following equation:

$$RMSE = \sqrt{\frac{1}{n} \sum_{i=1}^{n} \left[\frac{\delta_{ci} - \delta_{mi}}{\delta_{mi}} \right]^2} \tag{4.1}$$

where:

n = The number of geophones;

δ_{mi} = The measured surface deflection at geophone i;

δ_{ci} = The calculated surface deflection at geophone i.

The depth to a rigid layer is determined by finding the rigid layer depth and set of moduli associated with the smallest RMSE.

To evaluate this approach, the FWD deflection data collected on sites 7 through 12 were analyzed. On each of the ten test positions per site, eight FWD tests were conducted. This consisted of two drops per load level. Using the program MODULUS 3.0, the deflection data were analyzed using several subgrade thicknesses. For each deflection bowl analyzed, the RMSE was calculated according to equation 4.1. The results are shown in Figure 28. The error per sensor plotted is the average RMSE for the 80 backcalculated deflection bowls per test section. The actual rigid layer depths for each site determined from seismic and penetration tests are also shown.

The results clearly indicate that the minimum error per sensor does not always correspond with the actual rigid layer depth. On sites 7 and 12 the minimum error occurred when the actual subgrade thickness was used in the deflection analysis. On the other sites the minimum error was obtained using a semi-infinite subgrade during the backcalculation.

A second approach suggested by Per Ullitz and used in the program ELMOD (Ullitz and Stubstad 1985) was adapted for use on multilayered systems. Figure 29 shows a schematic diagram of a typical multilayered system deflected under a FWD load. As the load is applied, it spreads

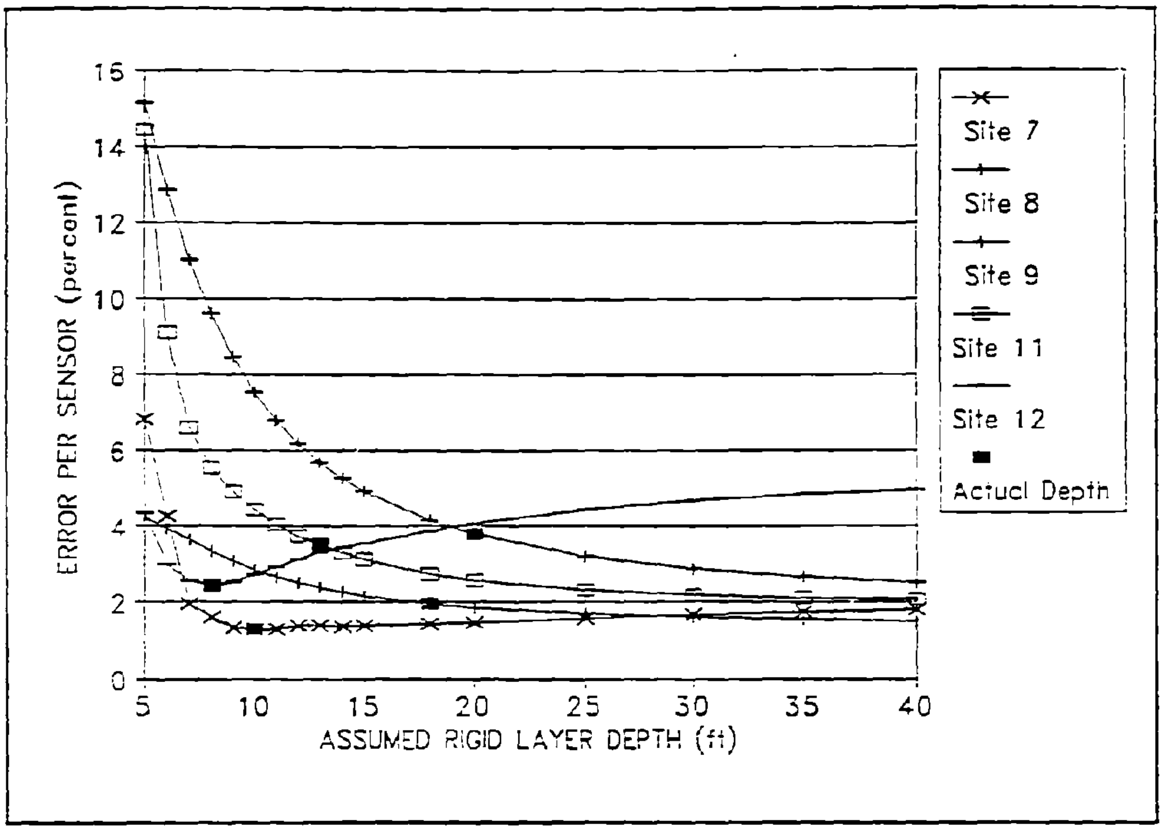

Figure 28. Estimating Rigid Layer Depths by Minimizing the RMSE.

through a portion of the pavement system as represented by the conical zone in the figure. The slope of this stress zone varies from layer to layer and is related to each layer's stiffness. The stiffer the layer, the wider the stress distribution. Because it is assumed that the area above the stress zone is not affected by the load, the measured surface deflection is purely a result of the deformation of the material in the stress zone. The measured surface deflection at any offset is therefore a result of the deflection below a certain depth in the pavement. If a stiff layer occurs at some depth, no surface deflection would occur beyond the offset at which the stress zone and the stiff layer intercepts. The method to predict the apparent depth to a rigid layer is based on the hypothesis that the position of zero surface deflection should be strongly related to the depth in the pavement at which no deflection occurs (i.e., a stiff layer).

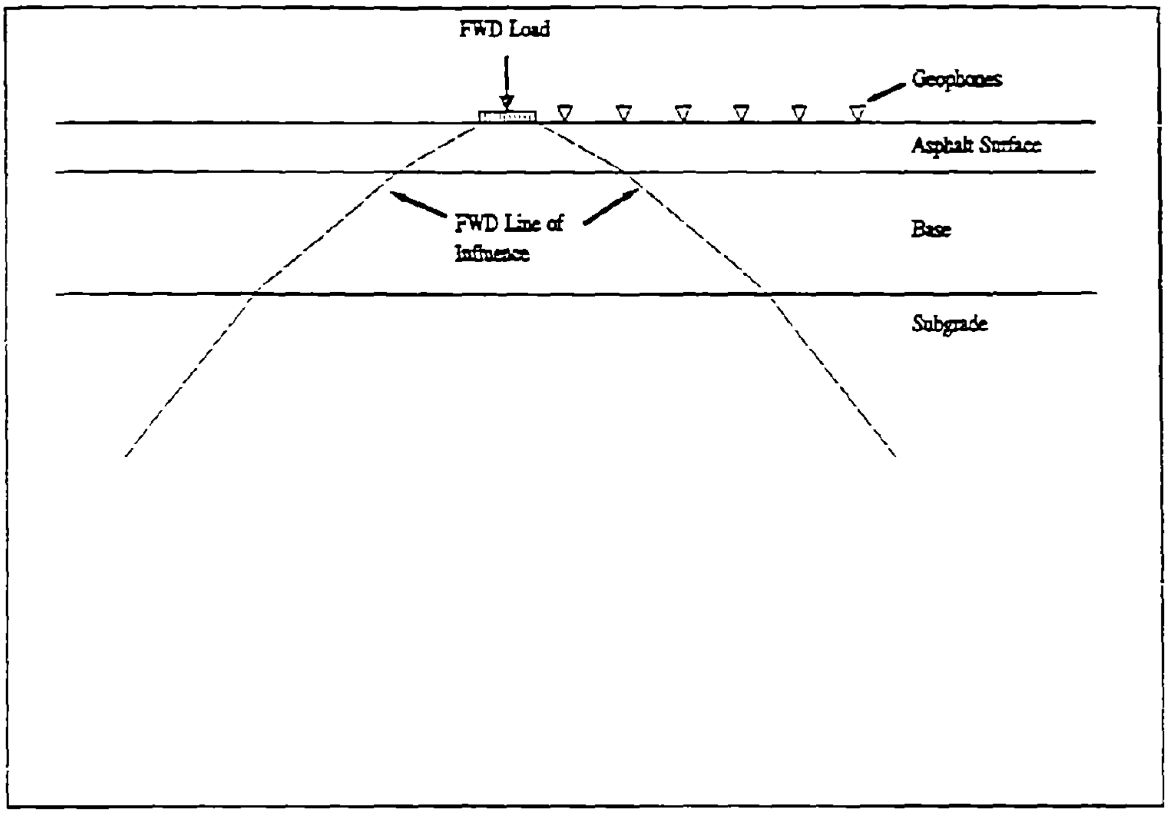

Figure 29. A Schematic of the Stress Distribution Below a FWD Load.

To predict the position of zero surface deflection the concept employed in Boussinesq's equations for deflection from a point load on an infinite halfspace is used:

$$D_r = \frac{P\ (1 - \mu^2)}{\pi\ r\ E_r} \tag{4.2}$$

where:

D_r = Surface deflection at offset r due to load P;
P = Point load;
μ = Poisson's ratio;
r = Horizontal offset from the load;
E_r = Representative Young's modulus of the halfspace.

For any deflection bowl on an infinite halfspace, equation 4.2 can be rewritten as:

$$D_r = k\left[\frac{1}{E_r}\right]\left[\frac{1}{r}\right] \tag{4.3}$$

where:

$$k = \frac{P(1-\mu^2)}{\pi}$$

In Figures 30 through 32 the deflections caused by a surface load on a series of hypothetical pavement structures are plotted against the inverse of the offset (i.e., 1/r). These deflections were predicted using the layered elastic program BISAR. The pavement structure and applied load are also shown.

For a point load P on an infinite halfspace with a constant E_r and μ, there is linear relationship between the deflection, D_r, and the inverse of the horizontal offset r. This relationship for a point load is shown in Figure 30. When the load is not concentrated but distributed over a circular area, the deflections close to the load are affected and cause the curvature as found near point A in Figure 30. Further from the load (position B) the calculated deflections for a point load and a circular load are similar. According to equation 4.3 the slopes of the lines for the point load and for the circular load in the region near position B are inversely related to the modulus of the halfspace E_r. The intercept of this line with the 1/r axis is at the origin, suggesting that the position of zero surface deflection is at an infinite distance from the load.

Pavements without stabilized layers generally consist of layers of stiffer material over layers of softer material. In Figure 31 the calculated deflections for a three layer system is plotted against the inverse of the horizontal offset r. It is generally recognized that the deflections close to a load are heavily influenced by the upper layers. These stiff layers further contribute to the curvature as apparent near

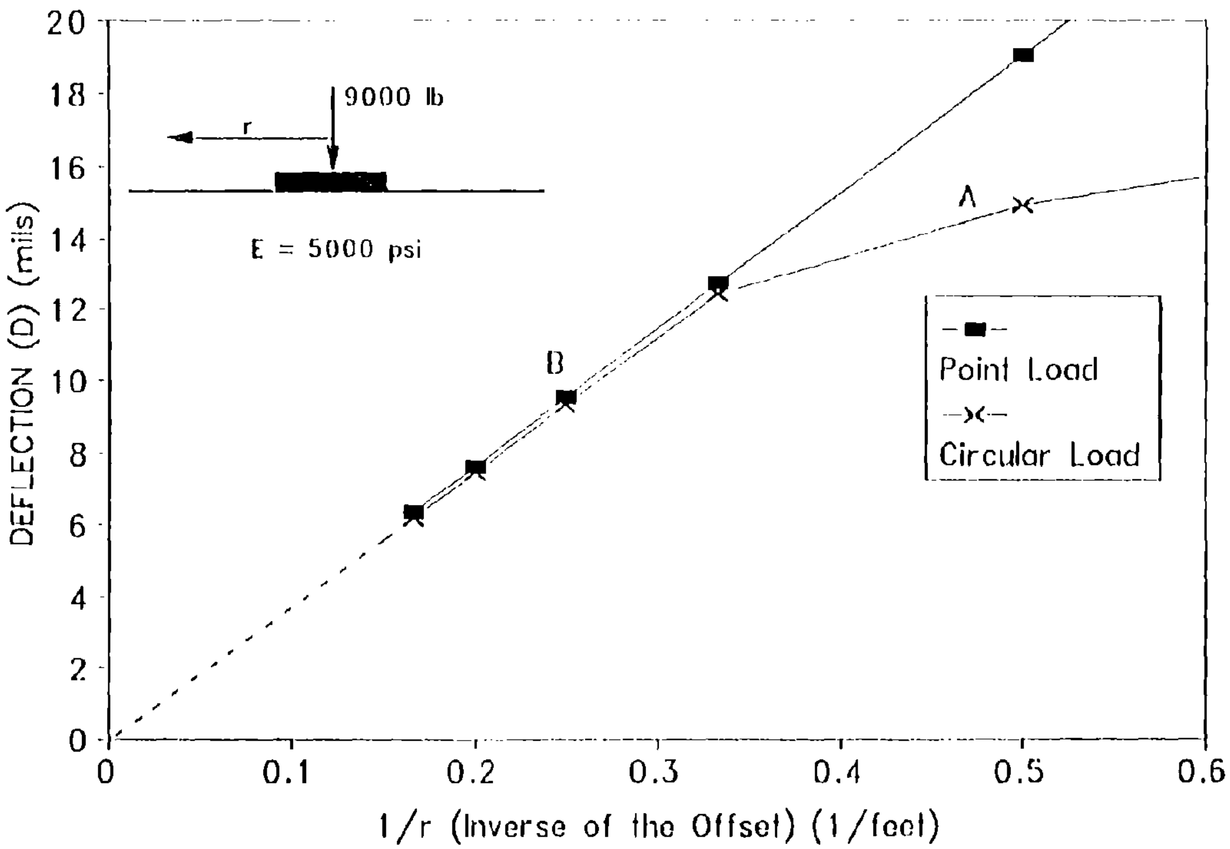

Figure 30. Measured Deflection vs. Inverse of the Offset for a One Layer Case.

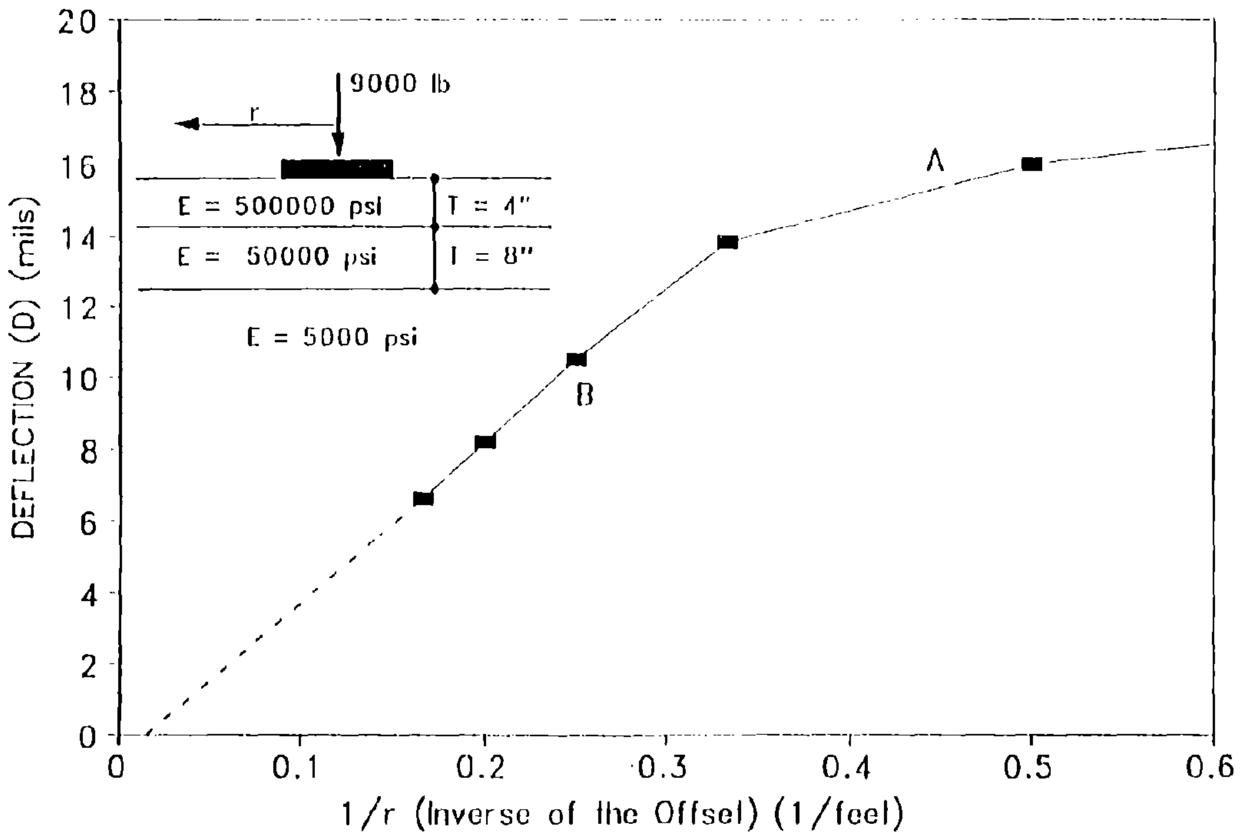

Figure 31. Measured Deflection vs. Inverse of the Offset for a Three Layer System.

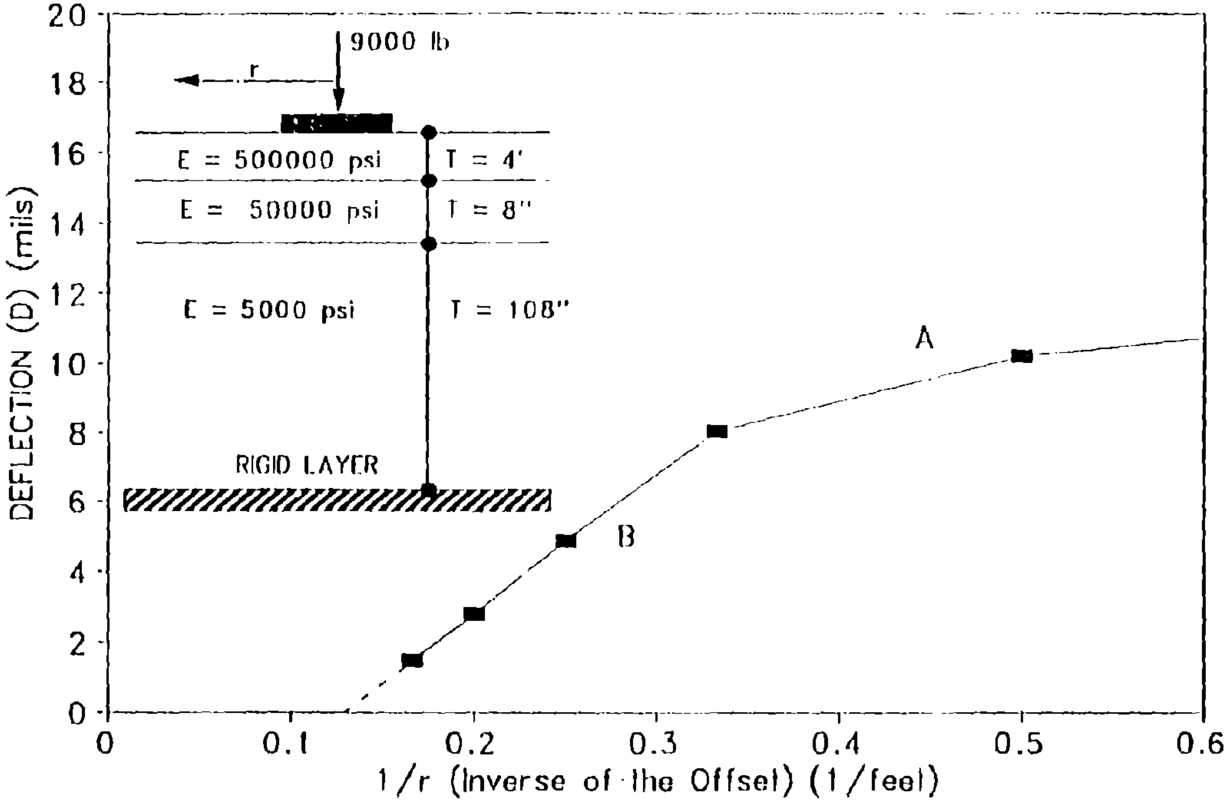

Figure 32. Measured Deflection vs. Inverse of the Offset for a Three Layer System Founded on a Rigid Layer.

position A in Figure 31. The deflections calculated for position B, some distance away from the load, are generally attributed solely to the effects of the subgrade and are similar to the one layer case providing a linear relationship between the deflection D_r and 1/r. However, the slope of this line is steeper than the slope found in Figure 30. This is caused by the stiff upper layers that distributed the surface load over a wider area of the subgrade, reducing the vertical stress and thus decreasing the deflection. The intercept of the line with the 1/r axis is still close to the origin indicating that the position of zero surface deflection is at a large distance from the load.

Figure 32 shows the same three layer case with a rigid bottom at a depth of 10 feet. As discussed, the curvature near point A can be attributed both to the upper stiff layers and because the load is distributed over a circular area. At position B, the linear section of the curve, the deflections originate solely in the subgrade and because the modulus of this layer is constant, the curve has a constant slope. The intercept of this line with the 1/r axis suggests that the position of zero surface deflection ($D_r = 0$) is much closer to the load than found in Figure 31.

In Figure 33, deflections for a number of pavement structures calculated using the multilayered, linear elastic program BISAR have been plotted against the inverse of the offset. The load level, pavement structure, and material properties used are also shown. When the subgrade modulus is changed, the slope of the lines change but the intercept with the 1/r axis remains relatively constant. The deeper the rigid layer, the smaller the intercept. This intercept is also influenced by the stiffness and thickness of the upper layers.

To develop a relationship between the depth to the rigid layer and the 1/r intercept, a regression analysis was completed. Deflection bowls and 1/r intercepts were generated for 1008 pavement structures under a 9,000 lb. (40 kN) load structured to be equivalent to a FWD load. The structures had the following moduli and thicknesses:

$$\frac{E_1}{E_{SG}} = 10,\ 30,\ 100;$$

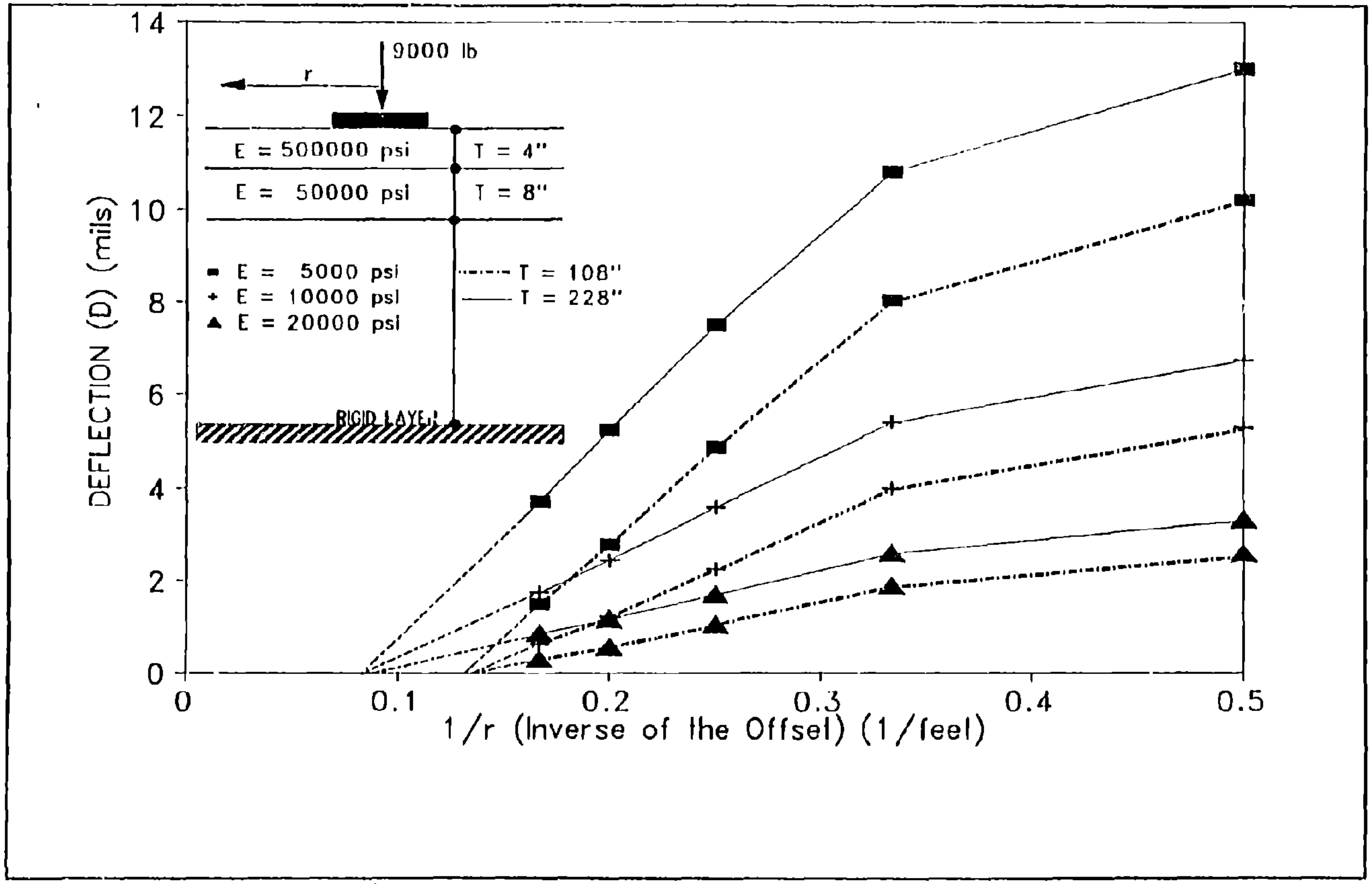

Figure 33. Deflection vs. the Inverse of Offset (1/r) for a Number of Hypothetical Pavement Structures.

$$\frac{E_2}{E_{sg}} = 0.3,\ 1.0,\ 3,\ 10;$$

$$\frac{E_{rigid}}{E_{sg}} = 100;$$

T_1 = 1, 3, 5, and 10 inches (25, 75, 125, 250 mm.);

T_2 = 6, 10, and 15 inches (150, 250, 375 mm.);

B = 5, 10, 15, 20, 25, 30, and 50 feet (1.52, 3.05, 4.57, 6.10, 7.62, 9.14, 15.24 m).

where:

E_i = Young's modulus of layer i;

T_i = Thickness of layer i;

B = Depth to the rigid layer from the pavement surface in feet.

In the analysis the relationship between the rigid layer depth and the 1/r intercept was improved by also accounting for the stiffness and thickness of the upper layers. This was done by using the basin shape factors SCI, BCI, and BDI, as defined in Table 1, Chapter II. The results were further improved by developing four separate equations based on the asphalt layer thicknesses. For pavement with asphalt surface layers less than 2 inches (50 mm.) the following equation was found (r^2 = 0.98):

$$\frac{1}{B} = 0.0362 - 0.3242r_0 + 10.2717r_0^2 - 23.6609r_0^3 - 0.0037BCI \tag{4.4}$$

For pavements with asphalt surfaces between 2 and 4 inches (50 and 100 mm.) the following equation was found (r^2 = 0.98):

$$\frac{1}{B} = 0.0065 + 0.1652r_0 + 5.42898r_0^2 - 11.0026r_0^3 + 0.0004BDI \tag{4.5}$$

For pavements with asphalt surfaces between 4 and 6 inches (100 and 150 mm.) the following equation was found ($r^2 = 0.94$):

$$\frac{1}{B} = 0.0413 + 0.9929r_0 - 0.00125SCI + 0.0063BDI - 0.0778\log(BCI) \qquad (4.6)$$

For pavements with asphalt surfaces greater than 6 inches (150 mm.) the following equation was found ($r^2 = 0.97$):

$$\frac{1}{B} = 0.0409 + 0.5669r_0 - 3.0137r_0^2 + 0.0033BDI - 0.0665\log(BCI) \qquad (4.7)$$

where:

B = Depth to a rigid layer in ft. (1 ft. = 0.304 m);

r_o = 1/r intercept by extrapolating the steepest section of the 1/r vs. deflection curve as shown in Figure 34a. (1/ft. units);

SCI = $D_0 - D_1$ (Surface Curvature Index);

BDI = $D_1 - D_2$ (Base Damage Index);

BCI = $D_2 - D_3$ (Base Curvature Index);

D_i = Surface deflection (inches 10^{-3}) normalized to a 9,000lb. (40kN) load at an offset i in feet. (1 mill = 24.5μm) (1ft. = 0.304m).

The stiffness of a subgrade is seldom linear elastic but rather stress sensitive as discussed in Chapter II. As a result the curves plotted from actual surface deflections are not linear at the outer sensors but have an S-shape as shown in Figure 34a. Because the soils in this region (near position C) are further from the load, they are subjected to less deviatoric stress. Furthermore the confining stresses have increased due to increasing overburden pressure. Being stress sensitive the apparent stiffness of the soil increases. This can be approximated in elastic layered analysis by using successfully stiffer layers with depth. The results of such an analysis are shown in Figure 35. They shows that the slope of deflection vs. 1/r curve reduces at the

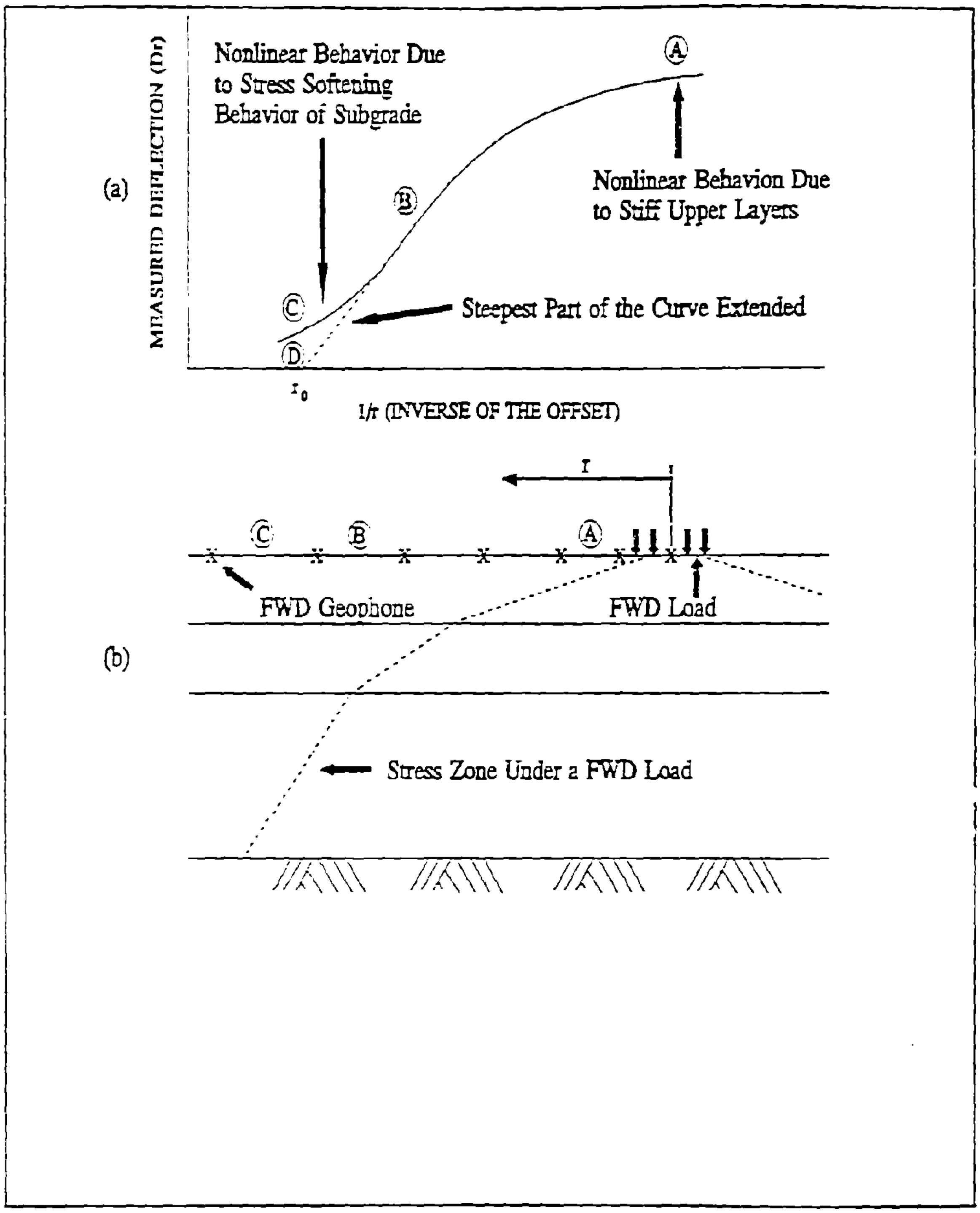

Figure 34. An Illustration of the Method to Determine the Effective Depth to a Rigid Layer.

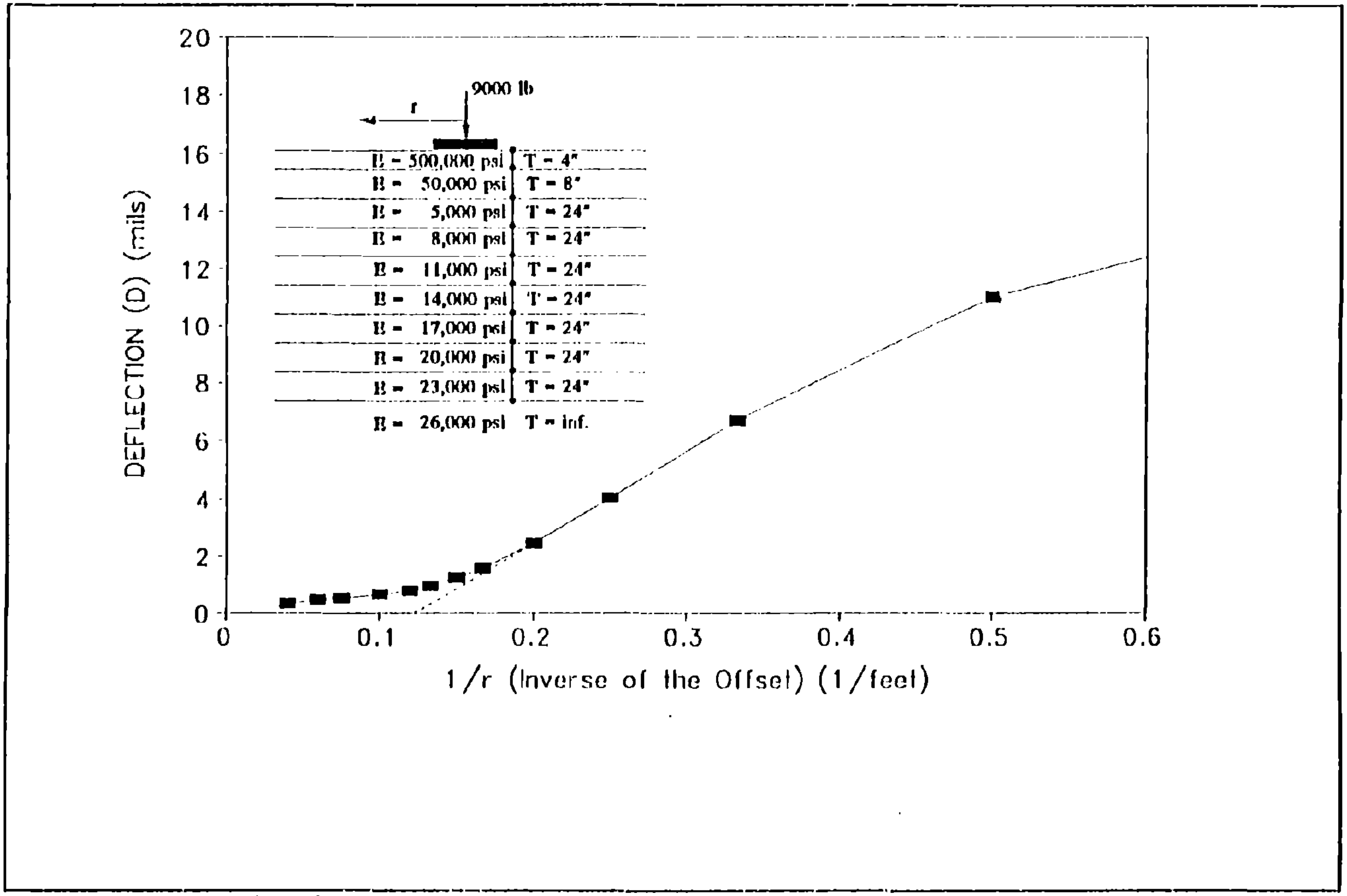

Figure 35. Measured Deflection vs. Inverse of the Offset for a Three Layer System Founded on a Rigid Layer.

outer sensors resulting in the S-shape. It is postulated that the deflections near the point of the steepest slope, identified as point B in Figure 34a, reflect the weakest modulus, normally found near the top of the unmodified subgrade. The 1/r intercept of a line drawn through the point of steepest curvature should be used in the equations 4.4 to 4.7 to predict the depth to a rigid layer.

VERIFICATION OF THE PROCEDURE

To verify that the effective depth to a rigid layer can be inferred from surface deflections using these equations, an extensive field study was conducted on the test sites near Abilene, Texas. On these sections, sites 7 through 12, the stratigraphy of the subgrade was determined by coring to a depth of 12 feet. The information from the drilling logs (Appendix B) was supplemented with penetration tests and a seismic analysis to establish the actual depth to a rigid layer. This information was compared with rigid layer predictions made from surface deflections.

On each of these sections deflection data conducted over a period of one year were used to predict the subgrade thickness. All the FWD deflection tests conducted at the 9000 lb. and 12000 lb. load levels were analyzed using equations 4.4 through 4.7. A summary of the results is shown in Table 11. A frequency distribution for the 360 rigid layer predictions at site 7 and 11 are shown in Figures 36 and 37.

The rigid layer depths determined from the surface deflections were compared to the subgrade stratigraphy obtained through coring, penetration and refraction analysis. The results of this comparison are shown in Figures 38 through 42. The results for site 7 are shown in Figure 38. The drillers log, the seismic refraction analysis, and the penetration test indicate a rigid layer at a depth of approximately ten feet. This depth was also predicted using the surface deflections and equation 4.5. Fifty percent of the 360 predictions estimated the rigid layer at a depth of between 9.7 and 11.7 feet.

The stiff layer encountered at site 8 (Figure 39) was between a depth of 17 feet, as indicated by the refraction analysis, and a depth of 20 feet at which the subgrade refused further penetration by the

Table 11. Predicted Rigid Layer Depth from 360 Deflection Tests per Site.

STATISTICAL DESCRIPTION	SITE 7	SITE 8	SITE 9	SITE 11	SITE 12
Average (ft.)	10.75	15.99	17.41	14.49	9.41
Median (ft.)	10.67	15.14	16.61	12.07	8.67
Standard Dev.	1.38	5.70	4.91	13.56	3.20
Lower Quartile	9.74	12.69	14.65	10.48	7.18
Upper Quartile	11.69	17.56	19.28	13.77	10.66
Interquart. Range	1.95	4.87	4.63	3.29	3.48
Sample Size	360	360	360	360	360

minicone. The effective rigid layer depth predicted from the surface deflections were on the average 16 feet. Vertical inclination of the penetration rod, a change in soil type, or water table could be reasons for the difference in measurements between the refraction analysis and the minicone.

On site 9, the seismic analysis was unsuccessful and it is suspected that a layer with a high compression wave velocity is overlying a material with a lower velocity. According to the drillers log, clay was found to a depth of 12 feet. The high water table, found at a depth of 10.75 feet, might also be the reason for the unsuccessful seismic test. The penetration device failed penetration at a depth of 13 feet, while the predictions from the surface deflections estimated the rigid layer at an effective depth of 17 feet. The stiff layer at the end of the penetration test was not confirmed by the refraction analysis. It is believed that the clay material continues below this stiff but possibly thin layer.

On site 11, the rigid layer estimates from surface deflections are in close agreement with the seismic analysis. As shown in Figure 41 the measured tip resistance during penetration indicates the stiffening of the sandy subgrade with depth. Although the penetration test failed at a depth of 17 feet, it is felt that the predicted rigid layer depth of 13.5 feet is an effective depth, representing the material with increasing stiffness. Unfortunately the drilling operation was discontinued at a

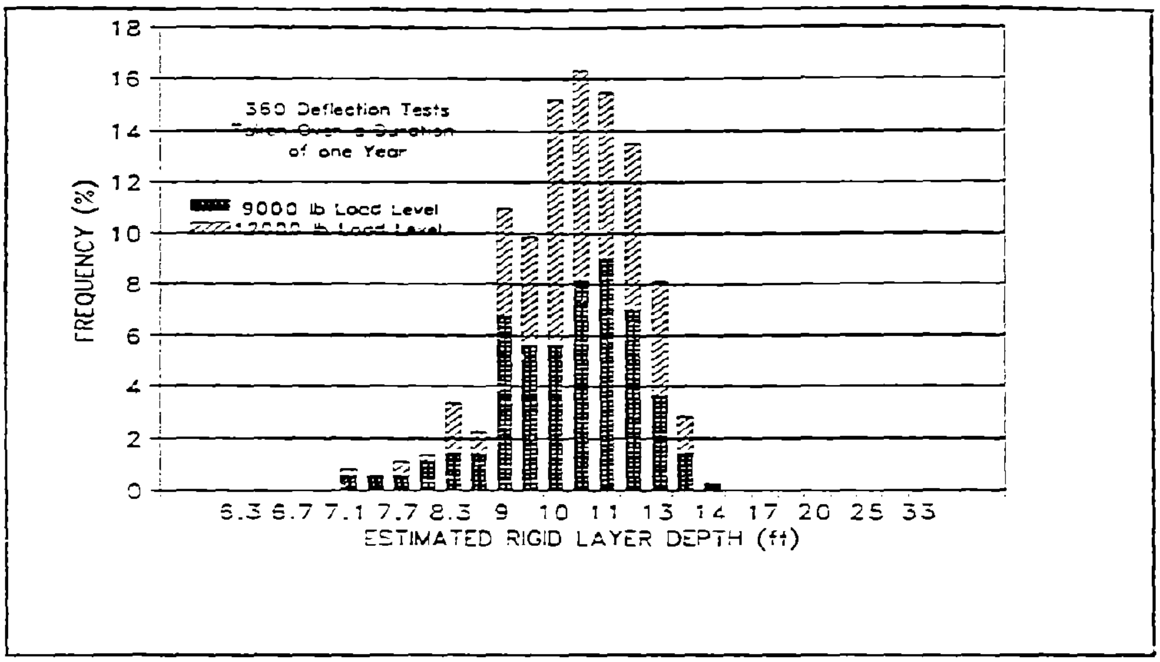

Figure 36. A Frequency Distribution of the Estimated Rigid Layer Depth (Site 7).

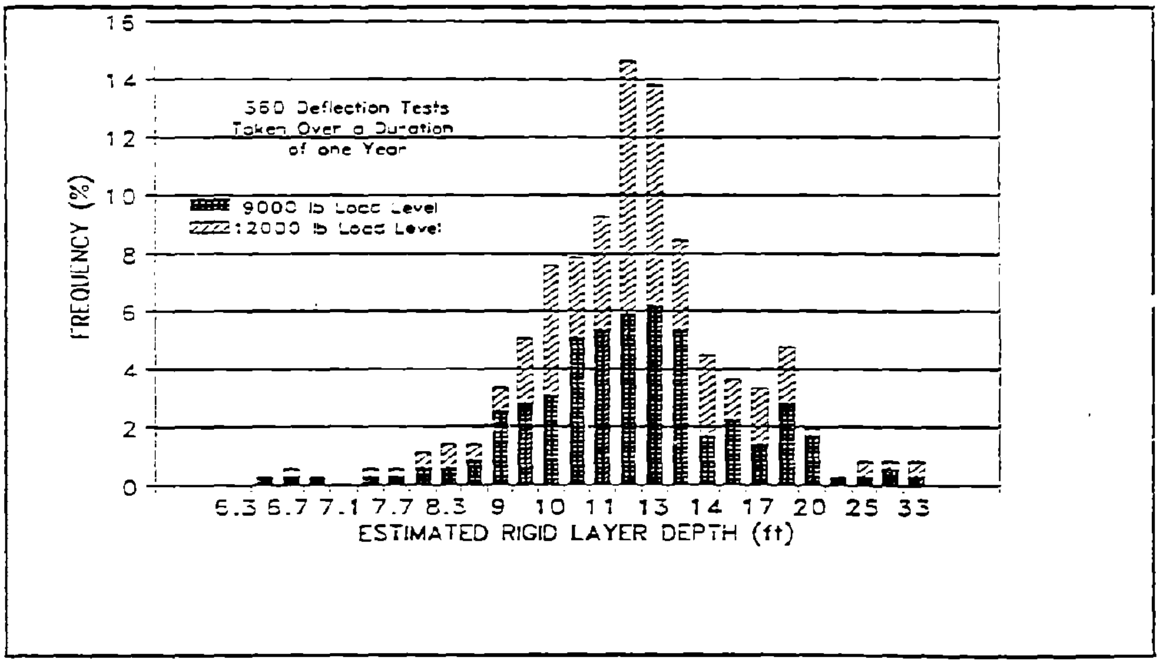

Figure 37. A Frequency Distribution of the Estimated Rigid Layer Depth (Site 11).

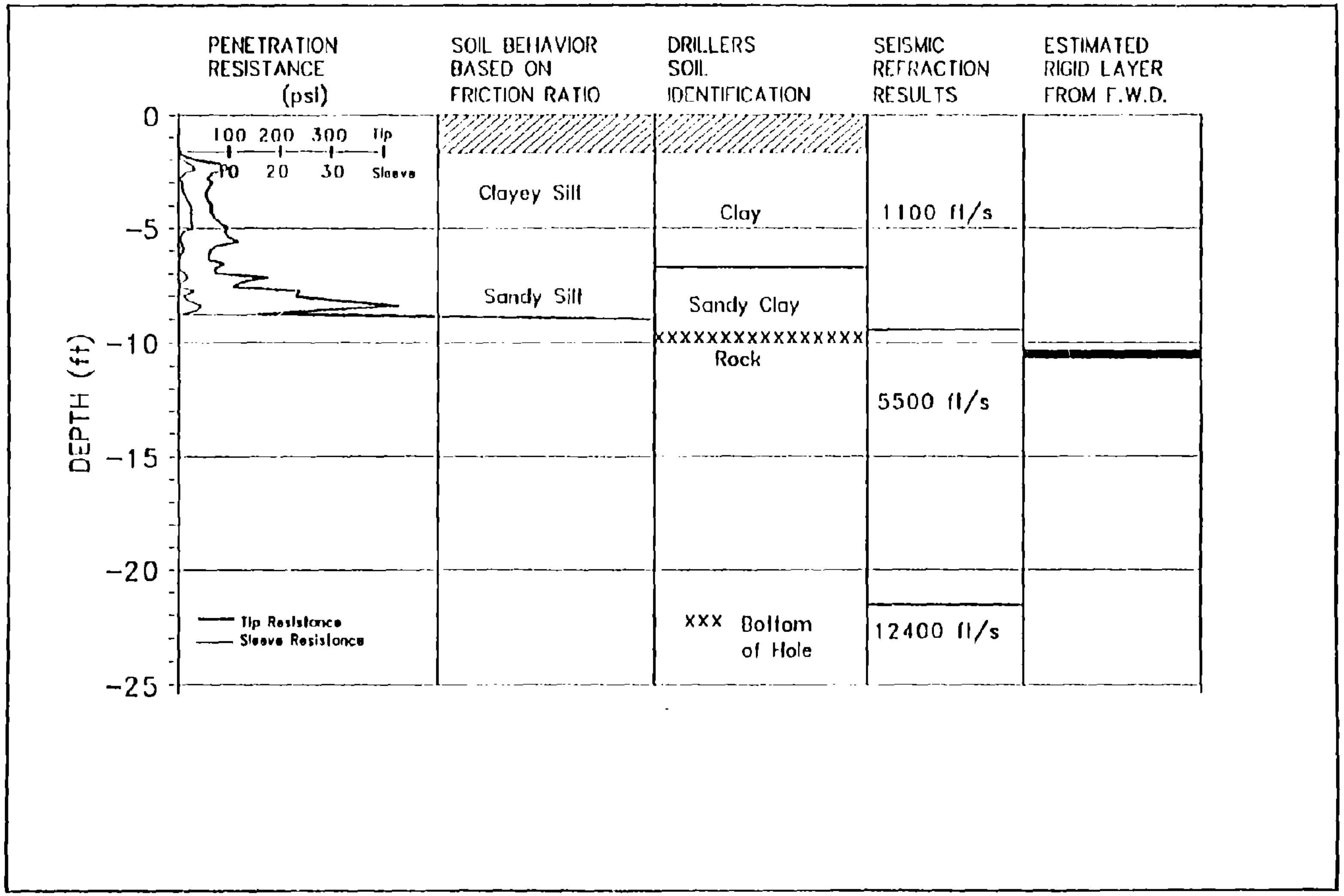

Figure 38. Subgrade Stratigraphy for Site 7.

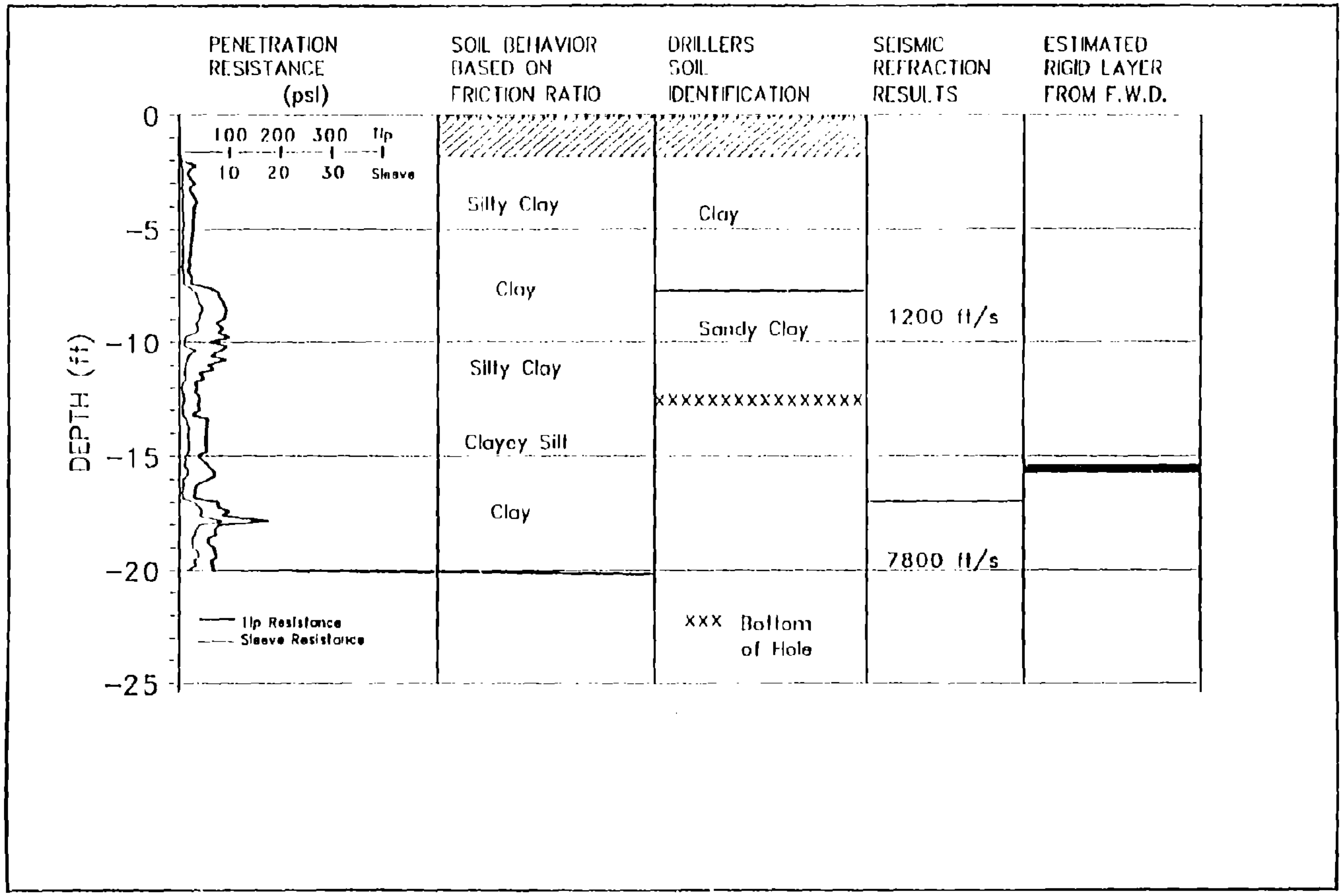

Figure 39. Subgrade Stratigraphy for Site 8.

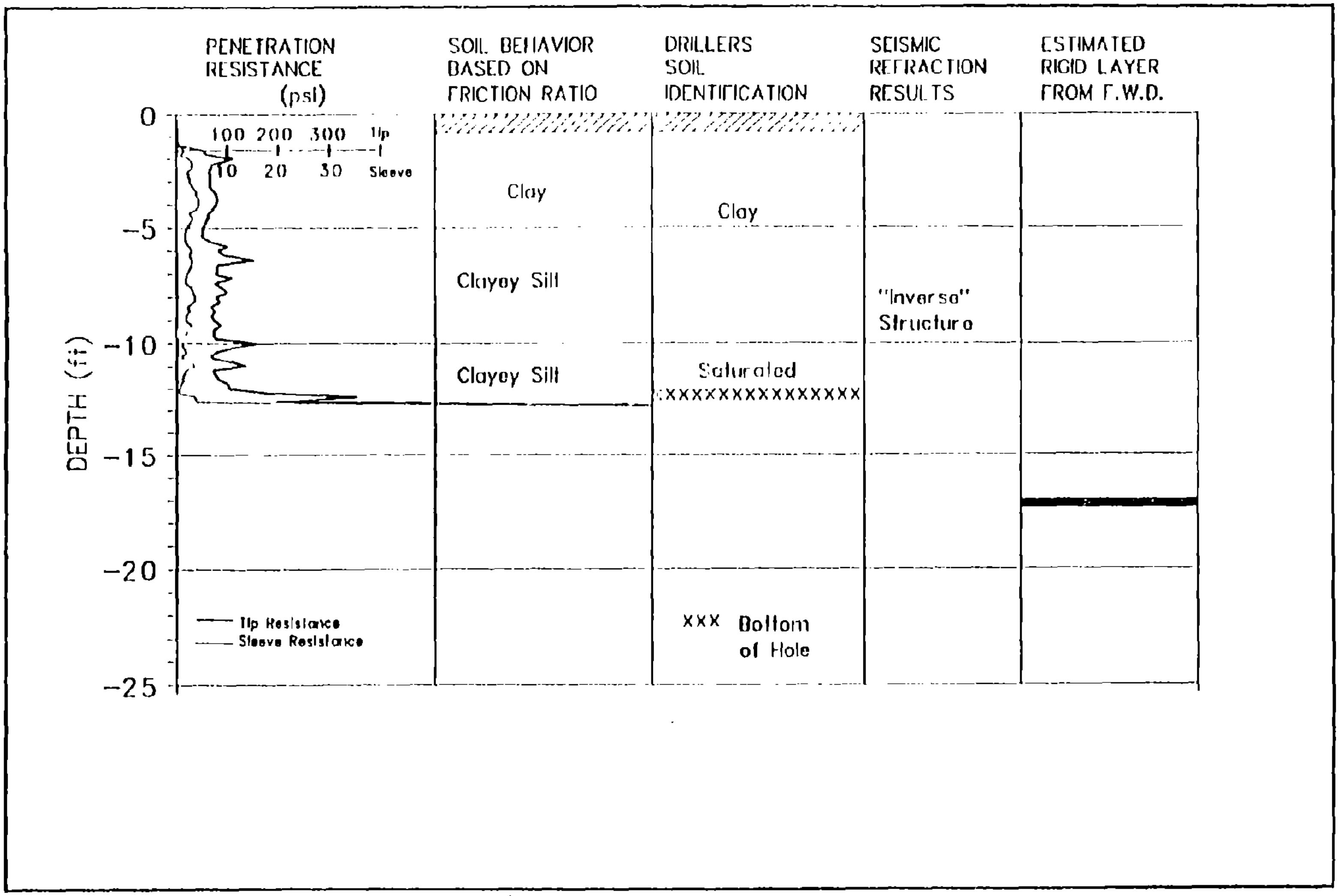

Figure 40. Subgrade Stratigraphy for Site 9.

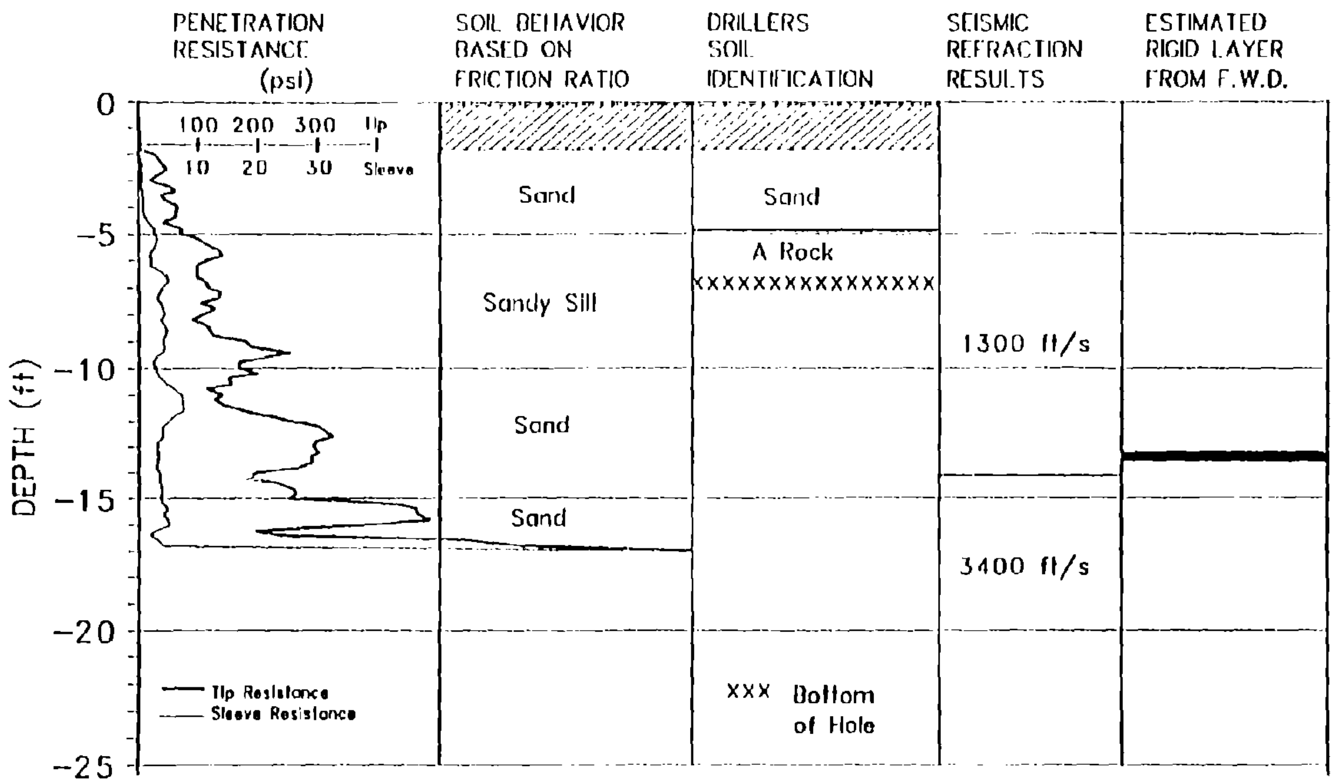

Figure 41. Subgrade Stratigraphy for Site 11.

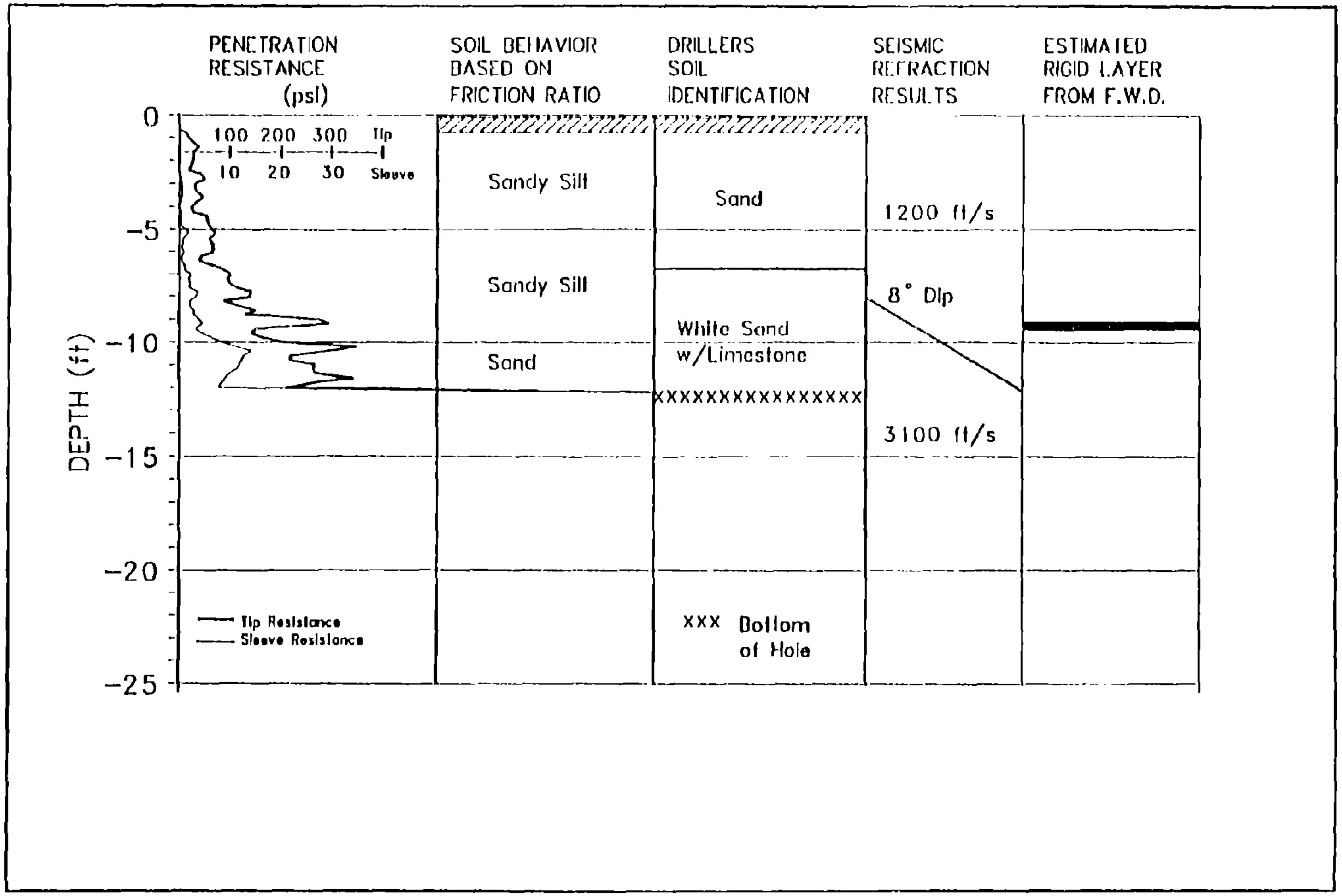

Figure 42. Subgrade Stratigraphy for Site 12.

depth of 7 feet due to a rock. No stiff layer at this depth was indicated by either the minicone or the seismic analysis, suggesting that the rock recorded in the drilling log is an isolated boulder.

On site 12, the seismic refraction analysis indicated a dipping rigid layer. The depth of this layer is 8 feet at position 0, and 12 feet at position 09. This is confirmed by the drillers log and the penetration test conducted at position 09. The rigid layer estimate from the FWD data is 9.4 feet. The big variability in the estimates on this site, as shown in Table 11, can be explained by the slope of the actual rigid layer. Fifty percent of the 360 deflection bowls analyzed predicted the rigid layer at a depth of between 7.2 and 10.7 feet.

CONCLUSION

When analyzing nondestructive deflection data to obtain pavement design parameters, it is important that the backcalculation technique is compatible with the design procedure. Because most of the mechanistic-empirical design procedures currently used incorporate a multilayered linear elastic model, this model is an obvious choice for the analysis of the deflection data. The backcalculated moduli and pavement performance predictions using the layered elastic model are influenced by the depth to a stiff layer. An inaccurate estimate of the subgrade thickness leads to inaccurate designs for rehabilitation and new projects.

A method to determine the depth to a rigid layer was developed. The effective depth to the stiff layer is a function of the shape and magnitude of the measured deflection bowl. This procedure was verified by comparing its results to those obtained from an extensive subsurface investigation. Although the deflection tests were conducted throughout the year, the predicted depth to a stiff layer were consistent with a small standard deviation. On four of the five sites the estimated rigid layer compared favorably with the information from the drilling logs, the penetration results and the refraction analysis. On the fifth site, the estimated rigid layer was deeper than indicated through penetration. A thin but stiff layer is suspected as the reason for this discrepancy.

CHAPTER V

DEALING WITH SUBGRADES STIFFENING WITH DEPTH IN LAYERED ELASTIC BACKCALCULATION

This chapter deals with analyzing deflection data for sections in which the actual or effective stiffness of the subgrade increases with depth. A nonlinear backcalculation approach based on a finite element analysis is used to illustrate how the effective stiffness of many subgrade soils increases with depth. This is due to a decrease in the load related deviatoric stress with increased distance from the load and an increase in confining stress caused by the weight of the materials with depth. Due to the fundamental difference in behavior between fine grained and sandy materials, a set of deflection data collected on each of these types of subgrades is analyzed.

Because the nonlinear analysis of deflection data is too costly, complex, and cumbersome for daily use, a layered elastic approach to deal with changing subgrades is developed. It involves adding a rigid layer to the bottom of a linear elastic subgrade to account for the increasing stiffness with depth. The depth of this layer is determined from the shape of the deflection data as discussed in Chapter IV. Deflection data of a number of pavement sections are analyzed to illustrate that the apparent rigid layer depth as estimated from surface deflections are related to the subgrades' stress sensitivity.

INTRODUCTION

An inherent assumption of most backcalculation procedures is a linear elastic and infinitely thick subgrade. However, most subgrade soils are stress sensitive, and the stiffness of the subgrade is influenced by the prevailing stress state. The stress condition changes vertically and horizontally and so does the stiffness of the subgrade. The stress condition of any soil element depends on its distance from the load and the geostatic overburden pressure as described in Chapter II.

When a backcalculation procedure based on a layered elastic program is used to analyze deflections, it does not consider changes in subgrade stiffness with depth. A uniformly stiff and infinitely thick subgrade is often assumed. As found with the omittance or inaccurate modelling of a rigid layer below the subgrade, this results in inaccurate designs. By ignoring the increasing stiffness of some subgrades with depth during the deflection analysis, the backcalculated subgrade modulus is overestimated, resulting in unconservative new designs. It is hypothesized that a rigid layer below a linear elastic subgrade can be used to model subgrades that stiffen with depth.

To illustrate how the stiffness of sandy and clay subgrades changes with depth, a nonlinear deflection analysis is completed on two pavement sections.

A NONLINEAR ANALYSIS OF DEFLECTION DATA

Finite element techniques have long been used in modelling the nonlinear behavior of pavement materials (Yang 1972). These programs are time consuming and, for backcalculation purposes iterative techniques often used with layered elastic programs, are impracticle. The analysis approach used in this study was first suggested by Lytton (1989) and Uzan et al. (1989) to backcalculate nonlinear elastic material properties. A finite element program is used repeatedly to generate a database of surface deflections. Then, the pattern-search technique used in MODULUS (Uzan et al. 1988) is utilized to obtain stress sensitive parameters defining the nonlinear characteristics of the pavement materials.

The technique to generate a database to backcalculate nonlinear elastic material properties is explained using a hypothetical pavement structure. This pavement consists of an asphalt concrete surface and a granular base founded on a clay subgrade. To backcalculate one nonlinear property per pavement layer, the technique requires running a finite element program 27 times. This consists of combinations of three asphalt moduli (A1, A2, and A3), three sets of base moduli (B1, B2, and B3), and three sets of subgrade moduli (S1, S2, and S3) as illustrated in Figure 43. For this example the asphalt surface layer is assumed linear elastic. The asphalt stiffness used in generating the database

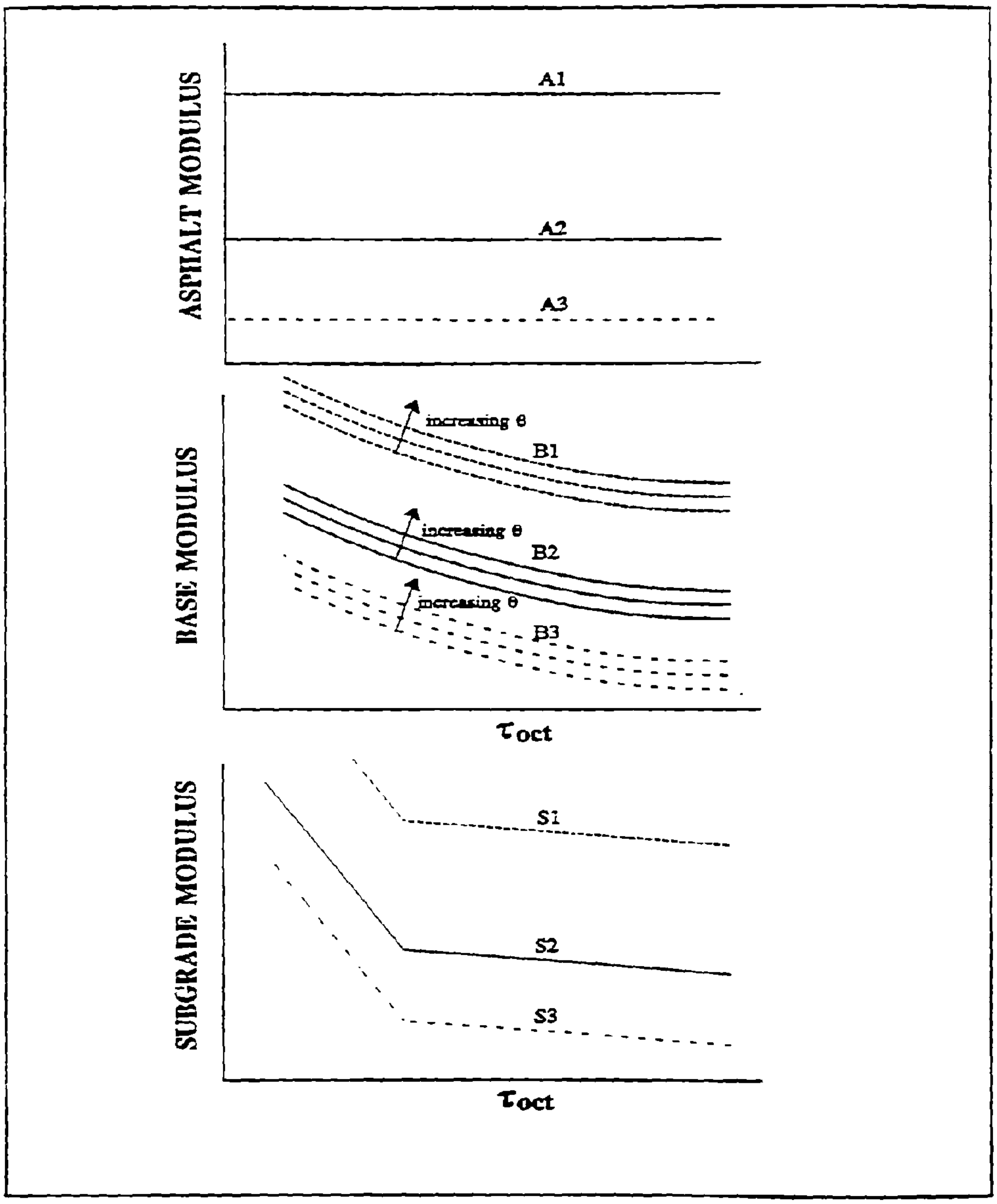

Figure 43. A Schematic Illustrating the Stiffness Models Used to Generate a Database of Solutions for the Nonlinear Backcalculation of Material Properties.

(A1, A2, and A3) are chosen to cover the expected range of possible solutions.

For the granular base the universal model in which the stiffness of the material is a function of both the octahedral shear and the bulk stress is used (Equation 2.5). If available, the resilient modulus test results are used to define the stress-stiffness relationship B2. B1 and B3 are defined varying the k_1 parameter in equation 2.5 such that the models B1, B2, and B3 cover the expected range of possible solutions. For the clay subgrade in this example the bilinear model (equation 2.8) has been selected as the stress-stiffness model. In generating the database, the k_2 parameter in equation 2.8 was varied to produce the three nonlinear subgrade moduli S1, S2, and S3, as shown in Figure 43.

For each of the 27 finite element runs, the surface deflections expected to occur at the FWD sensor positions are calculated and stored in a database. Using the search routine and the three point LaGrange interpolation scheme employed in MODULUS (Uzan et al. 1988), the measured deflections are compared with the calculated deflections in the database. The stiffness parameters associated with a deflection bowl matching the measured deflection bowl are obtained. In the example, the backcalculation results consist of a surface modulus, a backcalculated k_1 for the base and a k_2 for the subgrade. These backcalculated parameters are then used in the finite element program to calculate the stiffness of each element in the finite element mesh. To illustrate how the stiffness in a typical clay and sandy subgrade changes vertically and horizontally, deflection data collected on site 8 (clay subgrade) and site 1 (sandy subgrade) were analyzed.

The finite element computer code used in this analysis was originally developed by Wilson (1963) and was later also incorporated into the ILLI-PAVE (1982) and TTI-PAVE (Crockford et al. 1990) computer programs. The pavement is modelled using a finite number of axisymmetric and constant strain elements. Each element can be characterized differently in the horizontal and vertical directions. To improve the modelling of pavement behavior and to ensure convergence, the principal stresses in the granular and subgrade layers are modified at the end of each iteration so that they do not exceed the strength of the materials as defined by the Mohr-Coulomb failure envelope. This correction, first applied by Raad and Figueroa (1980), is justified by residual stresses that develop during construction and loading, as described by Witczak and Uzan (1988).

To model the two sections analyzed, a finite element model consisting of 420 elements connected at 462 nodal points was used. The boundaries of the finite elements were placed at a radial offset of 15 feet and a depth of 20 feet to reduce the influence of boundary effects. These are adequate based on the criteria suggested by Duncan et al. (1968). The interfaces were assumed to be perfectly rough with full continuity of stresses and displacements across the interfaces. The boundary conditions assumed are shown in Figure 44.

Nonlinear Deflection Analysis of a Flexible Pavement on a Clay Subgrade

Table 12 shows the material properties used to model site 8. The densities and thicknesses were measured in the field. Other properties such as the Poisson's ratio (μ), lateral earth pressure coefficient (K_o), angle of friction (ϕ), and cohesion (c), have been assigned typical values (Yoder & Witzcak 1975). The asphalt surface is assumed linear elastic, while the limestone base is modelled using the universal model with typical coefficients as summarized in Chapter II. The subgrade is modelled using a bilinear model. The coefficients used in this model have been determined from laboratory results as discussed in Chapter III. The bilinear model has been selected to model the subgrade because it describes the laboratory results better than the universal model. The backcalculation results are shown in Table 13, and the calculated stiffness values throughout the structure are presented in Figure 45.

Nonlinear Deflection Analysis of a Flexible Pavement on a Sandy Subgrade

To illustrate the change in stiffness with depth in a sandy subgrade, deflection data collected on site 1 were analyzed. The density, thickness and other material properties used to model this

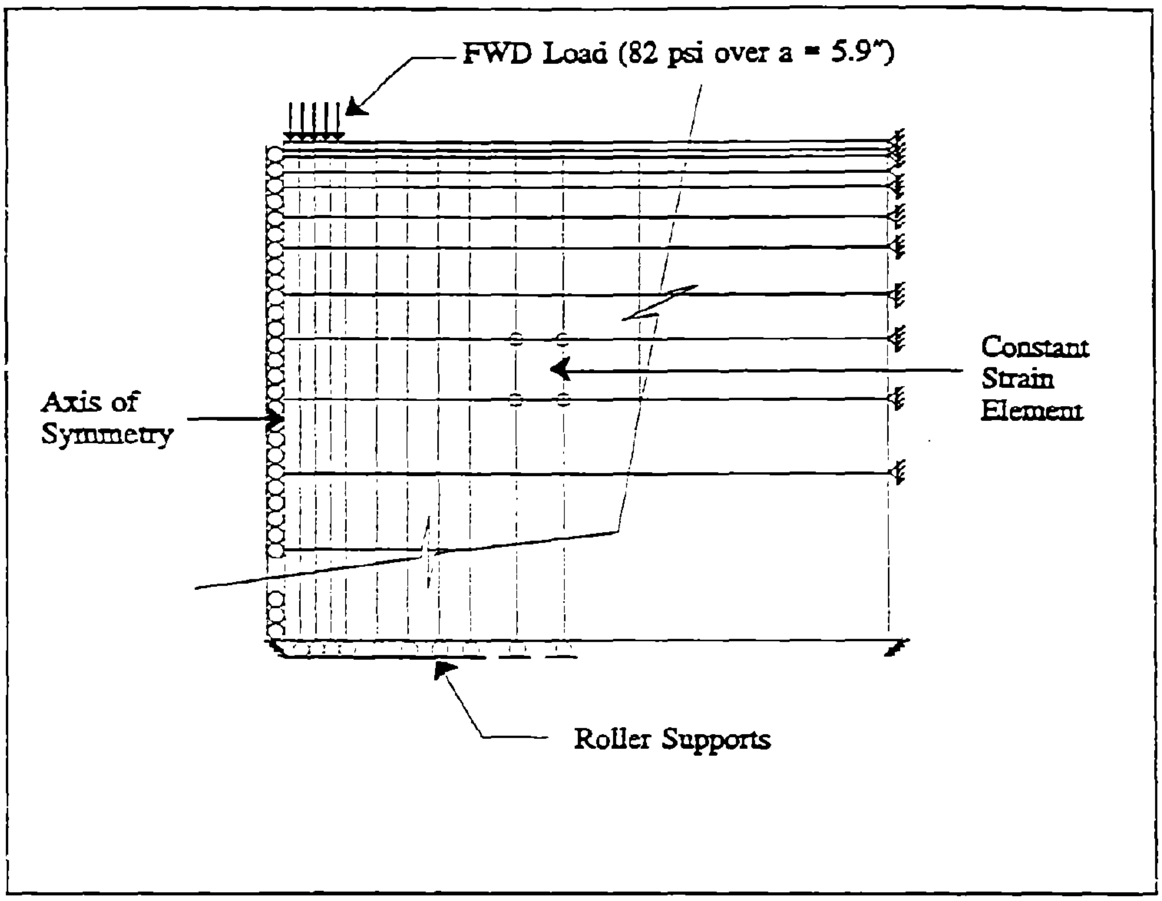

Figure 44. Boundary Conditions of the Finite Element Used to Backcalculate Nonlinear Material Properties.

section are shown in Table 14. The asphalt surface is assumed linear elastic, while the base course is modelled using the universal model with typical coefficients as summarized in Chapter II. The sandy subgrade is modelled using the universal model (equation 2.5) with coefficients as determined in the laboratory. A summary of the backcalculation results is shown in Table 15. Figure 46 illustrates how the stiffness in the pavement structure changes horizontally and vertically.

Table 12. Material Properties Used in the Finite Element Model for Site 8.

Material Properties Used to Model Site 8			
Material Property	**Asphalt**	**Base**	**Clay**
Thickness (inch)	8	13	219
Poison's Ratio	0.35	0.40	0.45
Density (pcf)	150	132	118
Stiffness Model	Linear **	Equation	Equation
K_1	--	2.5	2.8
K_2	--	**	6.1
K_3	--	0.8	**
K_4	--	-0.3	2582
		--	124
Angle of Friction	45		
(ϕ)	1000	38	0
Cohesion (c)	0.7	2	4.5
K_0		0.8	0.8

** Parameter varied in the database and determined through backcalculation

Table 13. The Backcalculation Results for Site 8.

Deflection Results							
Geophone Offset (inches)	0	12	24	36	48	60	72
Measured Deflection (mils)	7.10	5.61	4.02	2.84	2.15	1.65	1.34
Calculated Deflection (mils)	7.14	5.51	4.02	2.91	2.12	1.55	1.16
Used in Backcalculation	✓	✓	✓	✓	✓	-	-
% Difference (RMSE)	-0.56	1.72	0.00	-2.63	1.60	5.96	13.60
Absolute Difference (mils)	0.04	0.10	0.00	0.07	0.03	0.10	0.18
Average Error per Sensor (%)	1.30 (over 5 sensors)						
Avg. Absolute Difference (mils)	0.05 (over 5 sensors)						

Backcalculated Stiffness Models	
$E_{Asphalt}$ (psi)	816,000
E_{Base} (psi) (eq. 2.5)	$4824\ p_a \left(\frac{\theta}{p_a}\right)^{0.8} \left(\frac{\tau_{oct}}{p_a}\right)^{-0.3}$
$E_{Subgrade}$ (psi) (eq. 2.8)	$4055 + 2582(6.1-\sigma_d)$ for $\sigma_d < 6.1$ $4055 + 124(6.1-\sigma_d)$ for $\sigma_d > 6.1$

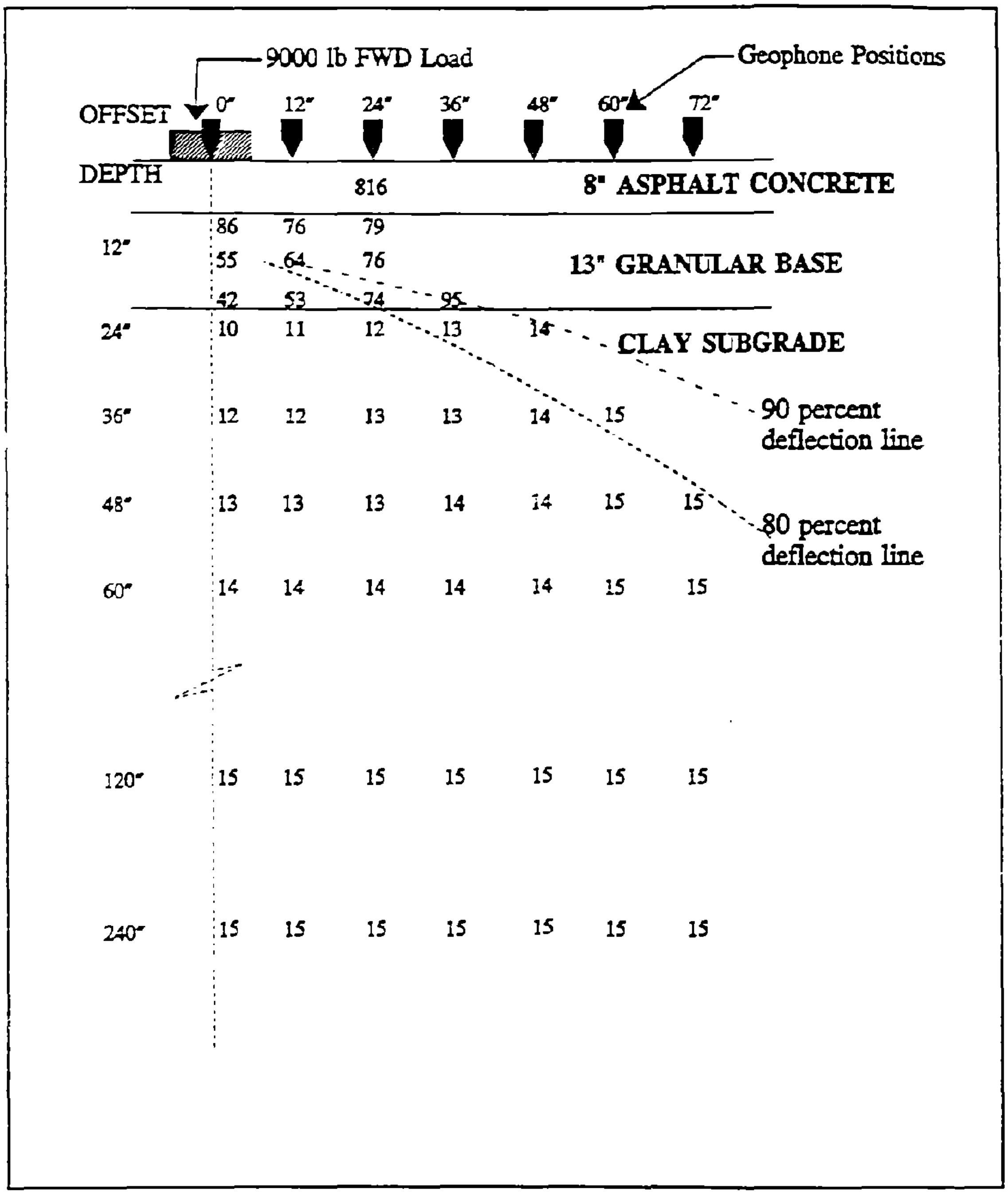

Figure 45. Backcalculated Moduli for Site 8 (Moduli in ksi).

Table 14. Material Properties Used in the Finite Element Model for Site 1.

Material Properties used to Model Site 1			
Material Property	Asphalt	Base	Sand
Thickness (inch)	6.5	6.0	227.5
Poison's Ratio	0.35	0.40	0.45
Density (pcf)	150	132	108
Stiffness Model	Linear **	Equation	Equation
K_1	--	2.5	2.5
K_2	--	**	**
K_3	--	0.8	0.4
		-0.3	-0.8
Angle of Friction	45		
(ϕ)	1000	38	20
Cohesion (c)	0.7	2	4.5
K_o		0.8	0.8
** Parameter varied in the database and determined through backcalculation			

Table 15. The Backcalculation Results for Site 1.

Deflection Results							
Geophone Offset (inches)	0	12	24	36	48	60	72
Measured Deflection (mils)	19.16	13.86	8.12	4.61	2.94	2.16	1.66
Calculated Deflection (mils)	19.31	13.47	8.01	4.71	2.74	1.72	1.10
Used in Backcalculation	✓	✓	✓	✓	✓	-	-
% Difference (RMSE)	-0.79	2.81	1.35	-2.16	5.80	20.22	33.69
Absolute Difference (mils)	0.51	0.39	0.11	0.10	0.20	0.43	0.55
Average Error per Sensor (%)	2.58 (over 5 sensors)						
Avg. Absolute Difference (mils)	0.19 (over 5 sensors)						
Backcalculated Stiffness Models							
$E_{Asphalt}$ (psi)	287,000						
E_{Base} (psi) (eq. 2.8)	$3474\ p_a \left(\frac{\theta}{p_a}\right)^{0.8} \left(\frac{\tau_{oct}}{p_a}\right)^{-0.3}$						
$E_{Subgrade}$ (psi) (eq. 2.8)	$54\ p_a \left(\frac{\theta}{p_a}\right)^{0.45} \left(\frac{\tau_{oct}}{p_a}\right)^{-0.8}$						

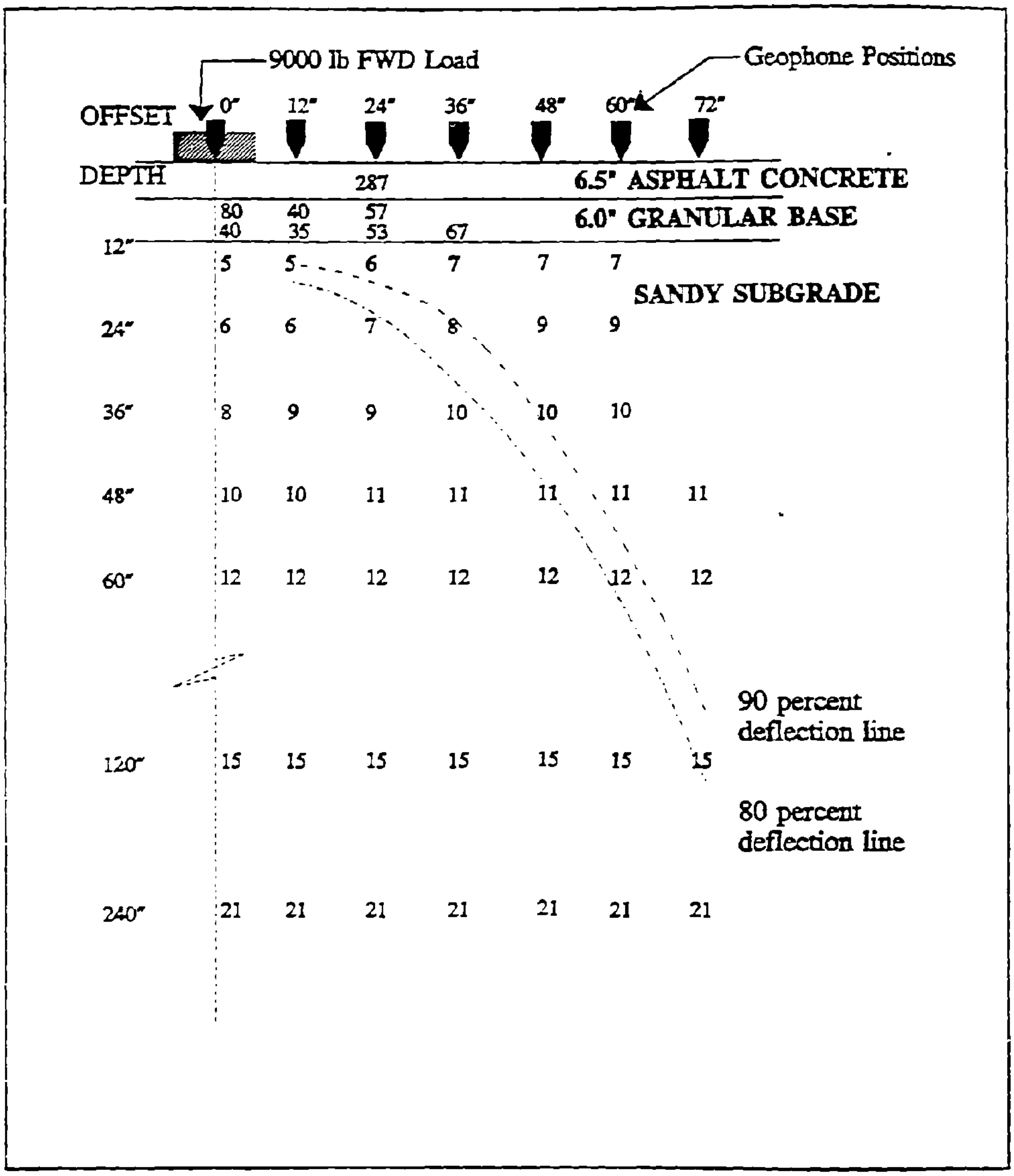

Figure 46. Backcalculated Moduli for Site 1 (Moduli in ksi).

Discussion of the Results

The backcalculated pavement structures shown in Figures 45 and 46 clearly illustrate the crucial difference in nonlinearity between fine grained and sandy subgrade materials. The stiffness of the clay subgrade, shown in Figure 45, is only influenced by the deviatoric stress. At the outer sensors, the subgrade shows no increase in stiffness with depth. Directly beneath the load there is slight increase in stiffness to a depth of eight feet after which no increase occurs. The sandy subgrade, shown in Figure 46, shows a significant increase in stiffness with depth. Below the outer sensors, where little change is expected in terms of the load related deviatoric stress, the subgrade increases from 7,000 psi to 21,000 within 20 feet. This is a result of the increase in bulk stress due to an increase in overburden pressure. This increase in stiffness is even more significant beneath the load due to the high deviatoric stresses found near the top of the subgrade.

The increase in stiffness shown on the sandy subgrade section is believed to be conservative. The stiffness model used for the sandy material was assigned a maximum modulus associated with a deviatoric stress of 1 psi as shown in Figure 47. This maximum modulus is not an actual material property but is the stiffness assigned to material at deviatoric stresses lower than 1 psi. This upper limit in material stiffness is required because no laboratory data are collected at that low stress levels (Thompson and Robnett 1976). The measurable deformation becomes so small that the stiffness determined in the laboratory test is not dependable. Without this criterium the stiffness in the bottom half of the subgrade, where the deviatoric stresses are smaller than 1 psi, would be even larger than shown.

The dotted lines shown on Figures 45 and 46 are used to represent the depth below which the measured surface deflections originate. Ninety percent of the measured surface deflections originated below the

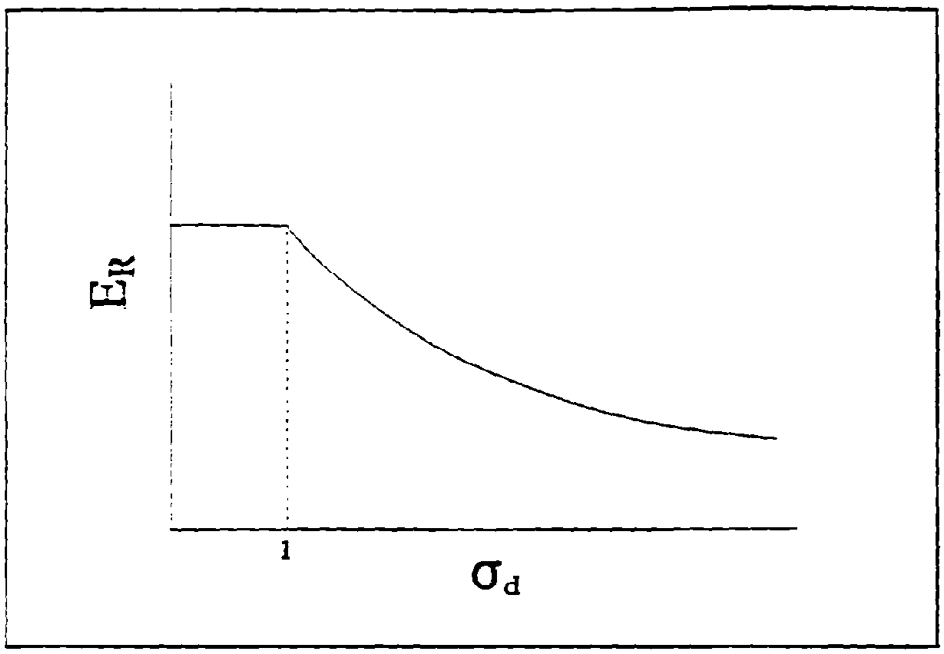

Figure 47. A Schematic Illustrating How the Deviatoric Stress Used to Calculate the Stiffness is Not Allowed to Reduce Below 1 psi.

dotted line. The slope of this line agrees well with the "two-third"[1] rule used by Irwin (1983). He suggested that the measured surface deflections are attributable to compression occurring in layers below a line that can be approximated by a straight line with a 34 degree angle from the surface. The slopes of these curves are a function of the stiffness and thickness of the layers. Site 8, shown in Figure 45, has stiff and thick upper layers. The stress distribution in the upper part of the pavement model is therefore very flat. From the position of this curve, it is obvious that only the first two sensors measure any deflection that occurs in the base and surface layer. From the seven deflection sensors, spaced one foot apart, five sensors measure deflections that originate purely in the subgrade. For the thinner pavement section shown in Figure 46, the situation is worse, with even

1 The two-thirds rule is based on the tangent of 34 degrees which is about 0.67.

more of the geophones measuring purely deflections occurring in the subgrade. The evaluation of the surface and base stiffness primarily depends on the inner sensors. Deflection testing and analysis will greatly benefit by placing more sensors near the loadplate. A geophone configuration with more sensors positioned close to the load are used by several highway testing agencies (SHRP 1989) in the United States.

THE USE OF AN APPARENT RIGID LAYER TO MODEL SECTIONS WITH INCREASING SUBGRADE STIFFNESS WITH DEPTH

As illustrated most subgrades increase in stiffness with depth. The fine grained soils are only slightly affected while the sandy soils show a considerable increase in stiffness due to geostatic pressures. This change in stiffness is not accounted for in layered elastic backcalculation procedures. Deflection analysis based on layered elastic concepts are therefore inaccurate.

To model a subgrade with increasing stiffness with depth, the use of a rigid layer underlying the subgrade is suggested. The rationale for this technique is illustrated in Figure 48. Systems A and B have been selected such that their surface deflections under a 9000 lb. FWD load, as predicted using the layered elastic program BISAR, are similar. As shown, their deflection vs. 1/r plots are very similar. If the deflections of the hypothetical structure A were analyzed using the technique developed in Chapter IV, a rigid layer would be predicted at a depth of 18.4 feet. By using this depth in a backcalculation model, the subgrade as shown in system B will be obtained. This subgrade modulus is more representative than the subgrade shown in system C, the product of backcalculation using an infinitely thick subgrade.

The predicted rigid layer depth is a function of how much the subgrade stiffness changes with depth. The more rapid the stiffness increases, the shallower the rigid layer required to represent this increase. The systems D and E are also equivalent in terms of surface deflection. To account for the rapid increase in subgrade stiffness of system D, a rigid layer at an apparent depth of 11.47 feet is required. The subgrade modulus backcalculated using the apparent rigid layer

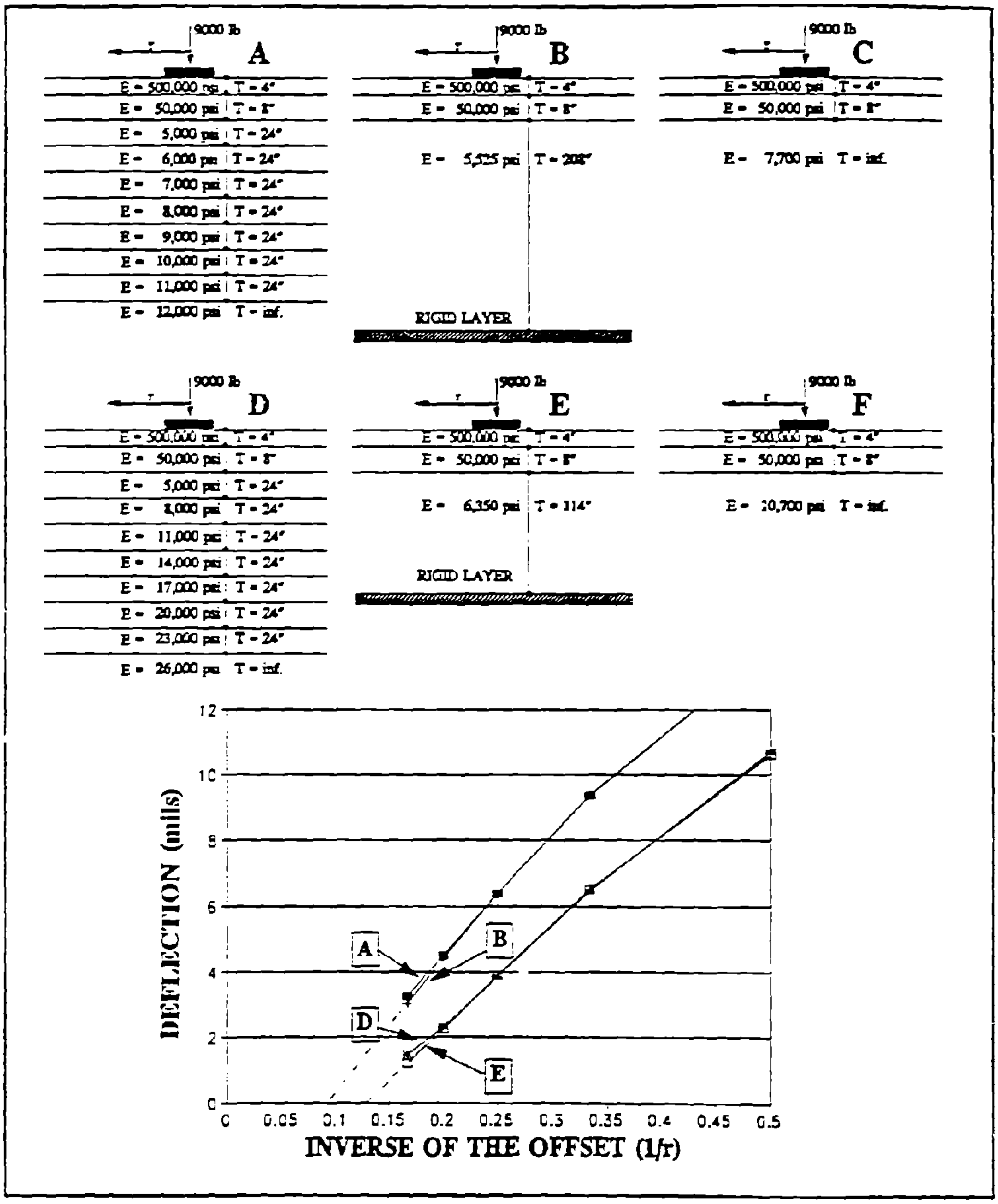

Figure 48. Hypothetical Pavement Structures to Illustrate How a Three Layer System and a Rigid Layer Can Be Used to Model a Subgrade With Increasing Stiffness with Depth.

approach is again more representative than the results assuming an infinitely thick subgrade as shown in system F.

To verify that the apparent rigid layer depth predicted from surface deflections is related to the type of subgrade, FWD deflections collected on sites 1 through 12 were analyzed and the apparent depth to a stiff layer at each site was estimated using the technique described in Chapter IV. On each site, deflection data collected monthly at position 01 were used. The apparent depth estimated from each deflection bowl were then statistically analyzed. The predictions within the 90 percent confidence interval were used to calculate the average rigid layer depth:

$$H_{avg} = n \left[\frac{1}{\sum_{i=1}^{n} \left[\frac{1}{H_i} \right]} \right] \tag{5.1}$$

where:

H_i = The Estimated Rigid Layer Depth from the i^{th} deflection bowl (from equations 4.4 to 4.7);

n = Number of apparent rigid layer predictions.

The results of this analysis are shown in Table 16.

With the exception of sites 2 and 4, a distinct trend is obvious in the apparent rigid layer depths predicted for the ten sections analyzed. For the sandy sections, the apparent rigid layer depth is in the order of ten feet. On the sandy clay section, a depth of 12 feet was found and on the clay subgrades the apparent rigid layer depth is in the order of twenty feet. This trend can be explained by the change in stiffness found in subgrades with depth, as discussed above.

MODIFICATIONS TO THE SYSTEM MODULUS 2.0

In addition to the inclusion of an apparent rigid layer in the backcalculation process, two changes were made to the program MODULUS 2.0. The first change involves the weight assigned to each deflection sensor during the search process to match the measured deflection bowl. The second change involves the number of sensors used in the

Table 16. The Apparent Rigid Layer Depth Predicted for the 10 Test Sites.

Site	Subgrade*	No. of Deflection Bowls	No. of Deflection Bowls in 90% Confidence Interval	Apparent Rigid Layer Depth (feet)
1	Sandy	92	88	6.9
12	Sandy	93	89	8.0
4	Clay	76	72	9.4
7	Clay **	86	80	9.7
11	Sandy	91	86	11.3
5	Sandy Clay	92	88	12.3
8	Clay **	82	80	15.7
2	Sandy	92	87	18.8
9	Clay	92	88	20.5
6	Clay	86	81	21.4

* A More Detailed Subgrade Characterization Is Shown in Appendix B
** Distinct Rigid Layer Found Through Penetration Testing

backcalculation process. Both these changes are made in an attempt to increase the influence of the inner sensors during deflection analysis.

The objective of most backcalculation procedures is to minimize the difference between the measured and calculated deflections. Two approaches are commonly used to evaluate the accuracy of this match, the arithmetic absolute sum of the percent error and the root mean square of the error (Irwin 1989).

The arithmetic absolute sum of the percent error (AASE) is defined as:

$$AASE = \sum_{i=1}^{n} \left[100 \frac{\delta_{ci} - \delta_{mi}}{\delta_{mi}} \right] \tag{5.2}$$

where:

δ_{mi} = The Measured Deflection of sensor i;

δ_{ci} = The Calculated Deflection of sensor i;

n = Number of sensors.

The second approach, the root mean square percent error (RMSE), is independent of the number of sensors used to characterize the deflection basin. This measure of error was defined in equation 4.1 and is repeated here for convenience:

$$RMSE = \sqrt{\frac{1}{n}\sum_{i=1}^{n}\left[\frac{\delta_{ci} - \delta_{mi}}{\delta_{mi}}\right]^2} \qquad (5.3)$$

In the pattern search technique used in the program MODULUS, the basin matching is reported in terms of the RMSE. During the search for the best matching deflection bowl, the following objective function is minimized:

$$\varepsilon = \sqrt{\sum_{i=1}^{n}\left[\left(\frac{\delta_{mi} - \delta_{ci}}{\delta_{mi}}\right)W_i\right]} \qquad (5.4)$$

where:

W_i = Weighing Factor Associated with Sensor i.

Deflection analyses results are normally reported in terms of error per sensor, and most specifications require deflection matching errors of less than 2% per sensor. In MODULUS 2.0 the recommended weighing factors (W_i) during deflection analysis is 1.0 for all sensors. This ensures that the program obtains the deflection bowl resulting in the least possible RMSE. However, in MODULUS the calculated subgrade modulus is a function of the whole deflection bowl, and the use of equal weighing factors for all sensors in the search routine, may not lead to the best results. For example, consider the set of backcalculation results shown in Table 17. If the weighing factors used for this deflection bowl were all equal, each sensor would have a $(1/\delta_{mi})^2$ influence during the search on the absolute difference between the measured and calculated deflection bowls. For example a 0.1 mil difference on the outer sensor between the

Table 17. Typical Deflection Matching Results.

Measured Deflections (δ_{mi})	30.60	21.19	12.25	7.48	5.16	3.61	2.89
Predicted Deflections (δ_{ci})	30.04	21.61	12.45	7.33	4.85	3.64	2.99
RMSE (Error/sensor) (percent)	1.83	-1.98	-1.63	2.01	6.01	-0.83	-3.46
Absolute Difference (δ_{mi}-δ_{mi})	0.56	-0.42	-0.20	0.15	0.31	-0.03	-0.10

measured and calculated deflection would have the same effect on the search routine as 1.06 mils difference on the sensor below the loading plate. In terms of absolute difference between the measured and calculated deflections, 31 percent of the search effort is placed on the outer sensor and only 2.9 percent on the inner sensor.

For several reasons it is believed that the closer the sensor to the load, the more its contribution should be in the MODULUS search routine. In general the closer the sensor to the loadplate, the more information it contains about the upper pavement layers. Unlike many backcalculation techniques where the subgrade is purely a function of the deflections measured at the outer sensors, MODULUS uses all sensors to predict the subgrade modulus. Due to the stress sensitive behavior of soils, as describes in Chapter II, the apparent subgrade stiffness is smaller below the load and increases in stiffness towards the outer sensors. By placing such a large emphasis on matching the outer sensor deflections, the subgrade modulus is generally over predicted. As described in Chapter III, the measuring accuracy of the geophones involves both a percentage and an absolute possible error. This implies that the smaller the deflection, the bigger the possible error in measurement. An additional reason for reducing the importance of the outer sensors during the deflection analysis, is the possibility of dynamic effects at the outer sensors. These dynamic effects are caused by refraction of waves and can lead to attenuation of the measures deflections (Roesset 1990). This effect is more likely at the outer sensors. Especially in the presence of rigid layers, this could lead to erroneous deflection measurements.

By setting the weighing factor at each sensor equal to the square of the measured deflection, the minimum absolute difference between measured and calculated deflection bowls can be obtained. This results in a situation where the deflection analysis is dominated by the magnitude of the inner sensors. The deflections at the outer sensors have very little influence on the backcalculation process. To prevent domination by either the inner or outer sensors in the deflection analysis, weighing factors proportionate to the magnitude of the measured deflection should be used. This has been incorporated in the new MODULUS 3.0, and as shown in Chapter VI, it leads to favorable results.

The second improvement involves a procedure to select the sensors to use in the deflection analysis. This involves using the sensors close to the load up to and including the first sensor that measures purely deflections in the subgrade. Bousinesq's equation for deflection under a point load (equation 4.2) is used to determine the surface location at which the measured deflection is purely originating in the subgrade. At each sensor the apparent Young's modulus E_r of the infinite half space is calculated:

$$E_r = \frac{P\,(1-\mu^2)}{\pi\, r\, D_r} \tag{6.4}$$

where:

D_r	=	Surface deflection at offset r due to load P;
P	=	Point load;
μ	=	Poisson's ratio;
r	=	Horizontal offset from the load.

By plotting the E_r at the various sensors, it is possible to determine the approximate offset at which the measured deflection is purely originating in the subgrade. The technique is illustrated in Figure 49. At the inner sensors, near position A, the calculated E_r is high due to the influence of the upper layers. With an increase in offset (point B in Figure 49), the apparent half space modulus reduces. The minimum apparent modulus occurs at position C. It is postulated that position C can be associated with the weakest modulus normally found near the top of the unmodified subgrade. Because most subgrades increase in stiffness with depth and distance from the load, the predicted E_r increases beyond this offset. The curve in Figure 49a is not continuous, and the actual minimum E_r might occur beyond position C. It is therefore suggested that the sensors up to and one beyond position C be used in deflection analysis. The other sensors do not measure the subgrade at its weakest position, and as a result the subgrade modulus is over predicted. By using only the selected sensors, and an apparent rigid layer to account for the increasing stiffness in the subgrade, the backcalculated subgrade modulus is more representative of the weakest part of the subgrade. As a result, deflection analysis is improved.

CONCLUSION

Due to the nature and origin of soils, the subgrade on which pavements are constructed is highly variable. During deflection testing and analysis, the highway engineer seldom has thorough knowledge about the stratigraphy of the subgrade. It usually changes drastically along the length of the road. The subgrade might consist of a fine grained or granular soil, and stiff layers might occur at shallow depths. Chapter IV illustrated how the depth of a rigid layer might be estimated from surface deflections. In this chapter it was shown that the predicted rigid layer depth might be representing a subgrade increasing in stiffness with depth.

The influence of stresses on the apparent stiffness of fine grained and granular materials is fundamentally different. Fine grained soils are mainly influenced by the deviatoric stress, while sands and granular material are also influenced by the confining stress. As a result, sands significantly increase in stiffness with depth. The increase in apparent stiffness in the fine grained soils is generally less drastic.

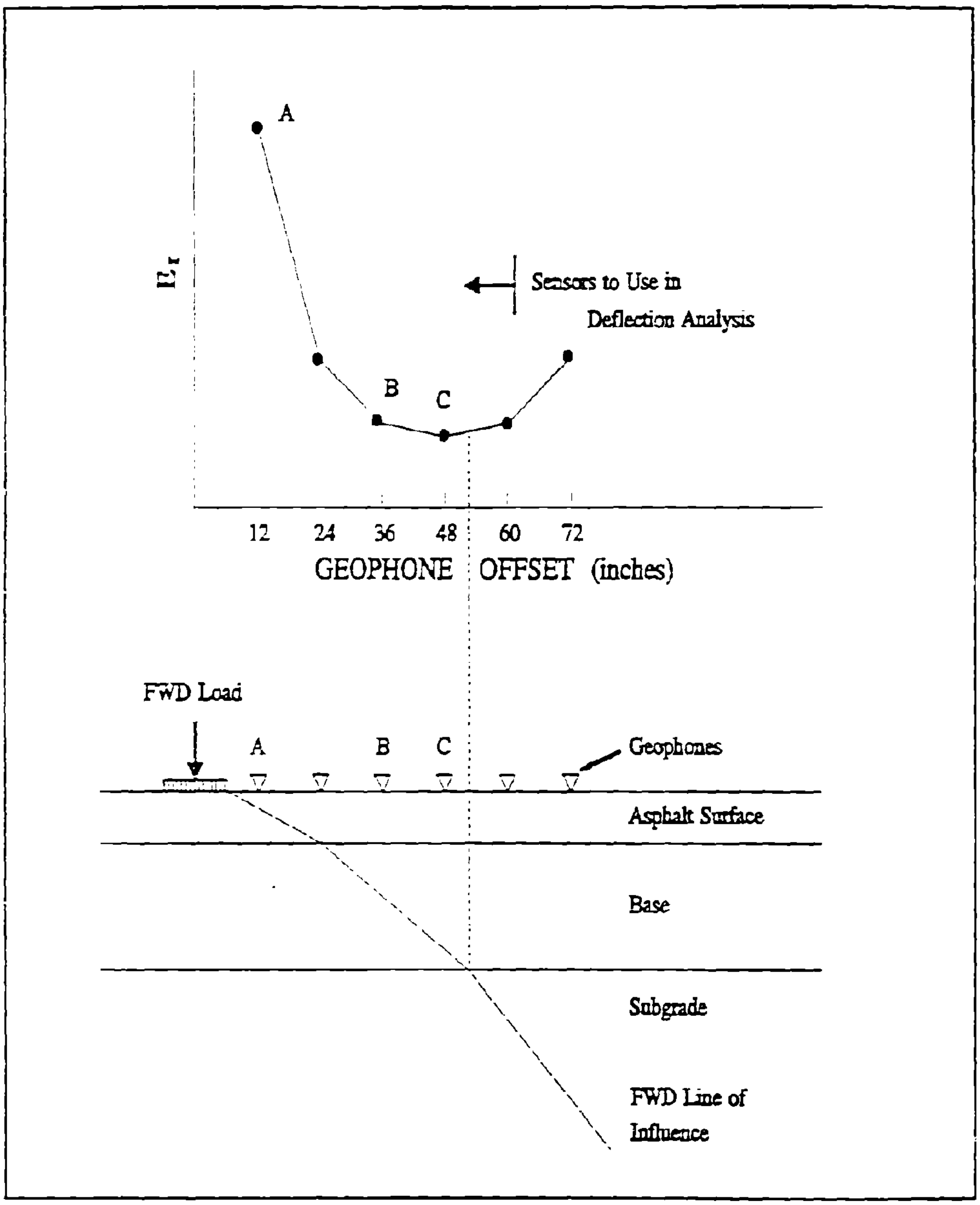

Figure 49. A Schematic Illustrating the Procedure to Select the Number of Sensors to Use During Deflection Analysis.

The fact that an apparent rigid layer can represent a stiff layer or increasing stiffness in the subgrade is highly significant. This allows the engineer to analyze deflections without knowledge of the subgrade stratigraphy. By including a rigid layer at the calculated depth, pavement modelling is improved. As a result, backcalculation results are more accurate, as illustrated in the next chapter. This improves the overall design process.

CHAPTER VI
EVALUATION OF A DEFLECTION ANALYSIS PROCEDURE THAT ACCOUNTS FOR SUBGRADE CHANGES WITH DEPTH

As discussed in the preceding chapters, the methods to account for changes in the subgrade stiffness with depth were evaluated on a number of test pavement sections throughout the state of Texas. The new backcalculation model using an apparent rigid layer to account for changes in subgrade stiffness with depth in the backcalculation process was used in parallel with existing backcalculation procedures. The results are compared and evaluated in terms of the available laboratory data. The detailed results of this analysis have been documented in Research Report 1123-3 (Rhode and Scullion, 1990). The technique was also evaluated on two instrumented pavement sections. Deflections were measured in the asphalt, base and subgrade under a FWD load. These were compared to deflections predicted using layered elastic theory and moduli from the improved backcalculation procedure.

ANALYSIS OF SURFACE DEFLECTION DATA

To evaluate the use of an apparent rigid layer to model a pavement in which the subgrade stiffness changes with depth, the deflection data collected on ten in-service pavement structures were analyzed. This analysis included approximately 96 deflection tests conducted at position 01 of each test site. The tests were conducted monthly over the duration of one year as described in Chapter III. In analyzing the deflection data, three backcalculation models were used. The results were compared to that obtained through laboratory testing.

Comparison of Three Backcalculation Models

The analysis of the deflection data was completed using the layered elastic backcalculation program MODULUS. The data were analyzed using three backcalculation models. In the first, the subgrade was assumed infinitely thick. All seven deflection readings were used in the analysis. In the second model a rigid layer was placed at a depth of 20 feet, and again all seven deflections were used to determine the layer moduli. In the third model a rigid layer was placed at the depth predicted using the procedures developed in Chapters IV and V. The geophones used in the deflection analysis were selected and assigned weighing factors as described in Chapter V.

For the pavement structures with a thin asphalt surface of less than two inches, the modulus of the surface layer was not backcalculated but assigned a fixed modulus. A pavement layer this thin has little structural value and an arbitrary chosen stiffness of 100,000 psi was used throughout the year. On these sections, only the base and subgrade moduli were backcalculated.

On sites 1, 4, 5, 7, 11, and 12 the use of an infinitely thick subgrade (model 1) resulted in an inverse pavement structure (i.e., the backcalculated base modulus is lower than the subgrade modulus) for several months of the year. The cause of the overpredicted subgrade and underpredicted base moduli are twofold. First, the uniformly stiff subgrade was assumed too thick, and in order to match the same surface deflections, the subgrade stiffness was overpredicted. By including an apparent rigid layer to account for any changes in subgrade stiffness with depth, in model 3, the results were significantly improved. No more inverse pavement structures were found and all moduli obtained were realistic. The results were also more compatible with the laboratory data as shown in the next section. The six sites mentioned are all sections where an apparent rigid layer was predicted at a depth of less than 15 feet, as shown in Table 16, Chapter V. This suggests either a rigid layer at shallow depth or a subgrade stiffening with depth. The second reason for the overpredicted subgrade is the high weight assigned to the outer sensors in the bowl matching process. The actual subgrade is not linear elastic, and for both sandy and fine grained subgrades, the apparent stiffness of the subgrade increases toward the outer sensors. By including all sensors in the analysis, and by forcing the calculated deflection bowl through the measured deflection bowl at the outer sensors, an elastic analysis will find a subgrade modulus higher than that occurring beneath the load. This is a problem with all layered elastic procedures, but the influence can be reduced by using only the sensors required to obtain a representative subgrade as described in Chapter V.

On sections 2, 6, 8, and 9, the base moduli values determined using the infinite subgrade were lower than expected. On these sections where the apparent rigid layer predicted was in excess of 15 feet, both models 2 and 3 lead to reasonable results. On all sections the third model, which includes a rigid layer at the predicted depth, provides reasonable results. This observation is substantiated by comparing the backcalculation results to those obtained from laboratory testing.

Comparison of Backcalculation Results to Laboratory Data

The backcalculation results were further evaluated by comparing them to available laboratory data. As discussed in Chapter III, the laboratory testing consisted of indirect tension tests on asphalt surface cores and resilient modulus tests on samples of the base and subgrade materials. The laboratory and backcalculated moduli for each of the ten sections has been compared. This results are also shown in Report 1123-3 (Rohde and Scullion 1990).

When comparing laboratory and backcalculated moduli no perfect agreement should be expected. As discussed in Chapter IV, the laboratory tests are only simulating stress conditions expected in the pavement under repeated loads. Furthermore, the material samples are disturbed and in some cases even remolded. The results from the backcalculation on the other hand, are model properties rather than material properties. Using a layered elastic approach a single stiffness per pavement layer is obtained. This is only an apparent stiffness for the whole layer. Actually the stiffness of each pavement layer changes vertically and horizontally. As a result, the laboratory data and backcalculated layer moduli should not show a perfect agreement. They should show the same trends. For example, the results from both methods should show that asphalt stiffness reduces with an increase in temperature, or subgrade stiffness reduces with increased applied loads. The moduli should also be in the same general range.

The Subgrade

Most subgrades are stress sensitive, and in order to compare the backcalculated and laboratory moduli, the stress state at various depths in the subgrade is required. The stress state is defined by the confining pressure and the deviatoric stress. In order to calculate the confining pressure, the vertical overburden pressure was determined using equation 4.2, the unit weight of the soil and the moisture content. The confining stresses were determined using equation 4.3, the vertical overburden pressure, and K_o, the coefficient of lateral earth pressure. Next, the deviatoric stress was determined using the layered elastic program BISAR. Because all stresses in the layered elastic programs are load related, the vertical stress in the subgrade directly beneath the FWD load was taken to be the deviatoric stress. Using the stress-stiffness models developed from laboratory results (Tables 6 and 7), the stiffness at various depths in the subgrade was calculated and plotted against depth (Rohde and Scullion 1990).

On all the pavement sections, with the exception of site 1, backcalculation model 3 led to good subgrade stiffness predictions. This stiffness is most representative of the material in the top 18 to 24 inches of the subgrade. The curve representing the laboratory data is a best estimate of the stiffness of the material directly beneath the load where the apparent subgrade stiffness is at its softest. This area is normally the weakest link in the pavement structure. It should therefore be used for design purposes. Toward the outer sensors the subgrade stiffness increases. On the sand sections, there is a significant improvement in results from model 2 to model 3. On the clay sections where little change in stiffness with depth is expected, both models 2 and 3 tend to provide satisfactory results.

The Base

The characterization of granular materials are extremely complex for several reasons (Witczak and Uzan 1988). The stress strain behavior of granular bases depends on the confining stress, shear strain amplitude, the compaction history, and the stress path during loading.

In addition gradation, particle orientation, suction, and compaction all influence the stiffness of a granular base. These factors are significantly different between the laboratory compacted base samples placed in a repeated load triaxial device and the actual base layer subjected to a FWD impulse load.

By modeling the pavement using a layered elastic or finite element program, tensile stresses are predicted at the bottom of the base layer. It is still an unanswered question whether these stresses actually exist. Possible reasons for the resistance of granular soils to tensile forces are suction, cementation and aggregate interlock. Heukelom and Klomp (1962) suggested that a granular material might be able to handle tensile bending forces due to interlocking of granules caused by forces perpendicular to the radial bending stress. This behavior of granular soils is not found in triaxial testing. Most granular soils have no strength in the unconfined state (Raad and Figueroa 1980). To overcome the problem of tensile forces, Raad and Figueroa (1980) developed a procedure to adjust the stress state in the base materials to stay within the Mohr-Coulomb failure envelope. Uzan (1985) suggested that residual stresses that develop due to compaction and loading should be incorporated in granular base modelling. In 1988 Witczak and Uzan added an arbitrary 2 psi residual stress to the base layer before adjusting stresses to comply with the Mohr-Coulomb failure envelope. In 1990, Uzan and Scullion presented a model to include dilation effects when the major to minor principle stress ratio exceeds a given value. This behavior was verified through in-depth deflection testing.

It is obvious that base characterization is extremely complex. Any comparison between laboratory and backcalculated base moduli must include a great deal of correction of stresses and assigning of material properties. Because the results of any of the three models can be supported by assigning a different set of properties, it is believed that such an exercise does not serve any purpose.

The backcalculated base moduli were also evaluated in terms of the base to subgrade stiffness ratio. Several design procedures (Izatt et al. 1967, Barker and Brabston 1977, Uzan et al. 1989) have used a method in which the base stiffness is a function of both the subgrade stiffness and the base thickness. This ratio has been calculated for the deflection bowls analyzed and is shown in Report 1123-3 (Rohde and Scullion 1990). Several of the ratios found using Model 1 are less than one suggesting a weaker base than subgrade. According to field observations made at these test sites, this is unrealistic. On all sections, the base was in good condition. The ratios obtained using models 2 and 3 are reasonable; although, on a few sites, the ratios obtained from model 2 are believed to be too high. According to Barker and Brabston (1977), a ratio of between 1.9 and 4.3 can be expected for a base founded on a subgrade with a stiffness of between 20 and 3 ksi. With the exception of sites 1, 5, and 8, the ratios obtained from model 3 are within the expected range. The high ratio obtained for site 8 can be explained by its thickness of 13 inches. This layer can be subdivided into two 6.5 inch layers where the stiffness of the top half is a function of the stiffness of the bottom 6.5 inches.

The Asphalt Surface

As discussed in Chapter III, the stiffness of asphalt concrete is influenced by the temperature and loading frequency. In Report 1123-X the laboratory results from the indirect tension test are plotted for various temperatures and loading frequencies. The backcalculated moduli were plotted against the asphalt temperature measured in the asphalt layer during the time of testing.

With the exception of sites 1 and 4, the backcalculated surface moduli from backcalculation model 3 were in good agreement with the laboratory data. At lower temperatures, backcalculation model 3 led to better agreement with the laboratory data than models 1 and 2. The good agreement over a whole range of temperatures is remarkable because the uppermost layer in the pavement system is the most difficult to backcalculate (Lytton et al. 1990). In both sections 1 and 4, the backcalculated asphalt moduli were considerably less than the laboratory results. Although backcalculation model 1 on these sections seems to provide results consistent with the laboratory data, the results are not reliable because the base stiffness reached the lower limit of 5,000 psi during backcalculation. The low surface moduli, backcalculated using model 2 and 3, might be explained by a loss in stiffness due to cracking in the asphalt concrete surface. The loss of structural integrity due to cracking does not always show up in the laboratory testing of a 6 inch diameter core.

SUMMARY

In this chapter FWD deflection data collected on ten in-service pavement structures were analyzed using various backcalculation models. The results were compared and evaluated in terms of available laboratory data. Three backcalculation models were used in the comparison. The first two are existing methods of analyzing deflection data while the third model incorporates an apparent rigid layer to account for subgrade stiffness changes with depth.

The first backcalculation model, a three layer linear elastic system with an infinitely thick subgrade, led to poor results on the majority of pavement sections analyzed. The second backcalculation model, incorporating a rigid layer at a depth of 20 feet, resulted in favorable moduli only on the thick clay sections. The use of an apparent rigid layer, as proposed in this study, lead to reasonable results on nearly all pavement sections.

As expected, the backcalculated moduli did not match the laboratory data. The laboratory tests are conducted on disturbed samples under simulated stress conditions. Although the backcalculated moduli can give an indication of the material stiffness under actual load conditions, the backcalculated moduli are model dependant. No perfect agreement between the laboratory data and backcalculation results should therefore be expected. It was found that the backcalculation model, incorporating an apparent rigid layer, led to subgrade moduli representative of the subgrade stiffness in the top 18 to 24 inches of the subgrade. The backcalculated subgrade stiffness for the other models was stiffer. The backcalculated stiffness for the asphalt concrete compared remarkably well with that found in the laboratory.

CHAPTER VII
CONCLUSION AND RECOMMENDATIONS

This study addresses the analysis of deflection data on sections in which the subgrade stiffness changes with depth. This occurs beneath the majority of flexible pavement sections. It is caused by rigid layers below the subgrade, physical changes in the subgrade soil, and an apparent increase in stiffness due to the stress sensitive behavior of soils. In the past these changes were often ignored, and during deflection analysis the pavement was modelled as being founded on a uniformly stiff and infinitely thick subgrade. This study improves the state-of-the-art by accounting for increasing stiffness in subgrades during analysis of nondestructive deflection data.

IMPLEMENTATION OF THE NEW PROCEDURE

The use of an apparent rigid layer to account for changes in subgrade stiffness with depth can be incorporated into any layered elastic backcalculation method. First, the deflection data should be analyzed to determine the apparent depth to a rigid layer. This is done by using equations 4.4 through 4.7 and the technique described in Chapter IV. The measured deflections are then analyzed using a three layer linear elastic model with a rigid bottom at the calculated depth. In this analysis the outermost sensors of the FWD are ignored, and only a selected number of sensors are used in the analysis as discussed in Chapter V.

The backcalculated subgrade modulus, as determined using this procedure, will be representative of the weakest part of the subgrade. This critical stiffness can be used as design value for the subgrade in both new and rehabilitation designs. The backcalculated base modulus will be a representative stiffness for use in rehabilitation design.

CONCLUSIONS

The following conclusions are based on this study:

1. The assumed subgrade thickness during deflection analysis significantly influences the backcalculation of layer moduli.

As a result, the predicted performance based on these properties is not accurate unless this thickness is considered. An overprediction of the rigid layer depth leads to overpredicted subgrade moduli, resulting in unconservative designs.

2. The depth to an apparent rigid layer can be predicted from the shape of the deflection bowl. This technique was verified by comparing predicted rigid layer depths to those determined through penetration testing and seismic refraction analysis. This technique improves the pavement evaluation process because the depth to a rigid layer can be predicted and accounted for at every test position.
3. The use of a nonlinear elastic backcalculation technique is the most accurate model to account for vertical and horizontal changes in subgrade stiffness. However, it requires considerable computational power and detailed material characterization. It is useful for research applications, but in routine highway testing the subgrade materials changes continuously and computer equipment and time limitations make this technique impractical. Furthermore, most design programs are based on a layered elastic model necessitating the use of a layered elastic model during deflection analysis.
4. The apparent rigid layer, as predicted from surface deflections, can be used with a layered elastic model to represent increasing subgrade stiffness with depth. This increase in apparent stiffness is small on clay subgrades and more drastic on sandy and gravel materials. As a result the apparent rigid layer, that accounts for the stiffening subgrade, is in the order of 10 feet deep for sandy subgrades and 20 feet deep for clay subgrades. The fact that a rigid layer, predicted from surface deflections, can represent changes in subgrade stiffness with depth is highly significant. It allows the engineer to analyze deflections without knowledge of the subgrade stratigraphy.
5. The use of an apparent rigid layer in the backcalculation model

can lead to considerable improvements in deflection analysis. This was evident from the comparative study documented in Research Report 1123-3 (Rohde and Scullion, 1990) and summarized in Chapter 6. The layer moduli obtained using the new procedure were more consistent with the laboratory results than the models previously in use. The use of an infinite halfspace led to results in which the calculated base moduli were lower than the subgrade moduli in several structures tested. The use of a three layer linear elastic model led to reasonable results only on the thick clay subgrades, while the newly developed technique resulted in satisfactory results on nearly all test sections.

6. The analysis of in-depth deflection on two instrumented pavement sections, documented in Research Report 1123-3, identified the need for more FWD geophones close to the loadplate. This will lead to better characterization of, and distinction between, the surface and base stiffnesses.
7. On sections where the apparent rigid layer depth is predicted at a shallow depth, a rapid increase in stiffness with depth can be expected. The use of a backcalculation model with the top 24 inches of the subgrade treated as an individual layer leads to better deflection analysis.
8. The use of an apparent rigid layer to account for stiffness changes in subgrade with depth improves the analysis of deflection data and has been included into the MODULUS 4.0 backcalculation program.

RECOMMENDATIONS

The following areas are recommended for further research:

1. The method to predict the depth to an apparent rigid layer should be evaluated on a pavement structure incorporating a stabilized layer. Although the set of equations to predict this depth was developed to incorporate stiff upper layers, the evaluation conducted in Chapter 3 did not include any pavement systems with stabilized layers.

2. The existing models used to explain the nonlinear behavior of subgrades are based on laboratory results. The range of deviatoric stresses over which these tests are conducted are often higher than found within the subgrade under surface loads. Due to physical limitations the resilient modulus test cannot be conducted at the low stress levels found deep in the subgrade. The use of multidepth deflectometers and finite element models offer the opportunity of studying the insitu nonlinear elastic behavior of subgrades at low stress levels. This will require modifications to the MDD system to place the anchor deeper and to install more LVDTs within the subgrade.
3. It has been identified that a change in the FWD geophone configuration can improve the analysis of deflection data. A study should be conducted to determine the "best" sensor spacing for analysis of deflection data collected on typical Texas pavement cross sections. Although each pavement section tested will have a unique "best" sensor spacing, an optimum spacing for all flexible pavements should be determined.

CHAPTER VIII

REFERENCES

AASHTO guide for design of pavement structures. (1986). American Association of State Highway and Transportation Officials, Washington, D.C.

Ahlborn, G. (1972). *Elastic layered systems with normal loads*, Institute of Transportation and Traffic Engineering, University of California at Berkeley, California.

Allen, J.S., and Thompson, M.R. (1984). "Significance of variable confined triaxial testing." *J. Transp. Engrg.*, ASCE, 100(4), 827-843.

ASTM. (1987). *Annual book of ASTM standards.* American Society of Testing Materials, Philadelphia, Penn., Vol. 04.03. Road and Paving Materials, D4694 & D4695.

Barker, W.R., and Brabston, W.N. (1975). "Development of a structural design procedure for flexible airport pavements." *TR S-75-17*, US Army Engineering WES, Vicksburg, Mississippi.

Barksdale, R.D. (1969). *Analysis of layered systems*, Project B607, National Science Foundation Grant No. GK-1583, Georgia Inst. of Technology.

Barksdale, R.D., and Hicks, R.G. (1973). "Material characterization and layered theory for use in fatigue analysis." *Special Report #140*, Highway Res. Board, Washington, D.C.

Basson, J.E.B., Wijnberger, O.J., and Skultety, J. (1981). *The multi-depth deflectometer: a multistage sensor for the measurement of resilient deflections and permanent deformations at various depths in road pavements*, NITRR Tech. Report RP/3/81, Council for Scientific and Industrial Research, Pretoria, South Africa.

Briggs, R.C., and Nazarian, S. (1989). "Effects of unknown rigid subgrade layers on backcalculation of pavement moduli and projections of pavement per-formance." *Transp. Res. Record 1227*, Transp. Res. Board, Washington, D.C., 183-193.

Brown, S.F., and Pappin, J.W. (1981). "Analysis of pavements with granular bases." *Transp. Res. Record 810*, Transp. Res. Board, Washington, D.C., 17-23.

Burmister, D.M. (1943). "The theory of stresses and displacements in layered systems and applications to the design of airport runways." *Proc. Highway Res. Board*, Vol. 23, 126-148.

Bush, A.J. (1980). "Nondestructive testing for light aircraft pavements; phase II, development of the nondestructive evaluation methodology." *Report FFA-RD-80-9-II*, U.S. Department of Transportation, Washington, D.C.

Bush, A.J., and Alexander, D.R. (1985). "Pavement evaluation using deflection basin measurements and layered theory." *Transp. Res. Record 1022*, Transp. Res. Board, Washington, D.C., 16-29.

Chou, Y. (1989). *Development of an expert system for nondestructive pavement structural evaluation*, PhD Dissertation, Texas A&M University, College Station, Texas.

Claessen, A.I.M., Valkering, P., and Ditmarsch, R. (1976). "Pavement evaluation with the Falling Weight Deflectometer." *Proc. Association of Asphalt Paving Technologists*, Vol. 45, 122-157.

Crockford, W.W., Bendana, L.J., Yang W.S., Rhee, S.P., and Senadheera, S.P. (1990). "Modeling stress and strain states in pavement structures incorporating thick granular layers." *Report F08635-87-C-0039*, Texas Transp. Institute, Texas A&M University, College Station, Texas.

De Beer, M., Horak, E., and Visser, A.T. (1989). "The multidepth deflectometer (MDD) system for determining the effective elastic moduli of pavement layers." *Nondestructive testing of pavements and backcalculation of moduli*, ASTM STP 1026, American Society for Testing and Materials, Philadelphia, 70-89.

Dehlen, G.L. (1962). "A simple instrument for measuring the curvature induced in a road surfacing by a wheel load." *Transactions of the South African Inst. for Civil Engineers*, 4(9), 189-194.

De Jong, D.L., Peutz, M.G.F., and Korswagen, A.R. (1973). "Computer program BISAR: layered systems under normal and tangential surface loads." *External Report AMSR 0006.73*, Koninklijke/Shell Laboratorium, Amsterdam, the Netherlands.

Duncan, J.M., Monismith, C.L., and Wilson, E.L. (1968). "Finite element analysis of pavements." *Highway Res. Record No. 228*, Highway Res. Board, Washington, D.C., 18-33.

Ford, M.C., and Bisselt, J.R. (1962). "Flexible pavement performance studies in Arkansas." *Bulletin No. 321*, Highway Res. Board, Washington, D.C., 1-15.

Hicks, R.G. (1970). *Factors influencing the resilient properties of granular materials*, PhD Dissertation, Inst. of Transp. and Traffic Engineering, Berkeley, California.

Hicks, R.G., and Finn, F.N. (1970). "Analysis of results from the dynamic measurements program on the San Diego test road." *Proc. Association of Asphalt Paving Technology.*

Hicks, R.G., and Monismith, C.L. (1971). "Factors influencing the resilient response of granular materials." *Highway Res. Record 345*, Highway Res. Board, Washington, D.C., 15-31.

Hoffman, M.S. (1983). "Loading mode effect on pavement deflections." *J. of Transp. Engrg*, ASCE, 109(5), 651-668.

Hoffman, M.S., and Thompson, M.R. (1981a). "Mechanistic interpretation of nondestructive pavement testing deflections." *Transp. Engrg. Series No. 32*, Illinois Cooperative Highway and Transportation Res. Program, Series No. 190, University of Illinois, Urbana-Champaign, Illinois.

Hoffman, M.S., and Thompson. (1981b). "Nondestructive testing of pavements field testing program summary." *Transp. Engrg. Series No. 31*, Illinois Cooperative Highway and Transportation Res. Program, Series No. 190, University of Illinois, Urbana-Champaign, Illinois.

Hoffman, M.S., and Thompson, M.R. (1982). "Backcalculating nonlinear resilient moduli from deflection data." *Transp. Res. Record 852*, Transp. Res. Board, Washington, D.C.

Hooke, R., and Jeeves, T.A. (1962). "Direct search solution of numerical and statistical problems." *J. for the Association of Comp. Mach.*, 8(2), 212-229.

Horak, E. (1988). "Application of equivalent-layer thickness concept in a mechanistic rehabilitation design procedure." *Transp. Res. Record 1207*, Transp. Res. Board, Washington D.C., 69-75.

Hudson, W.R., Elkins, G.E., Uddin. W., and Reilley, K.T. (1987). "Evaluation of pavement deflection measuring equipment." *Report No. FH 67/1*, Austin Res. Engineers, Austin, Texas.

Hung, J.T., Briaud, J.L., and Lytton, R.L. (1982). "Layer equivalency factors and deformation characteristics of flexible pavements." *Res. Report 284-3.* Texas Transp. Institute, Texas A&M University, College Station, Texas.

Husain, S., and George, K.P. (1985). "In-situ pavement moduli from Dynaflect deflection." paper presentation at the 64th annual TRB Meeting, Washington D.C.

Hveem, F.N. (1954). "Pavement deflection and fatigue failure." *Bulletin No. 114*, Highway Res. Board, Washington, D.C., 32-44.

ILLI-PAVE user's manual. (1982). Transportation Facilities Group, Civ. Engrg. Dept., University of Illinois, Urbana-Champaign, Illinois.

Irwin, L.H. (1983). *User's guide to MODCOMP2*, Version 2.1. Local Roads Program, Cornell University, Ithaca, New York.

Izatt, J.O., Lettier, J.A., and Taylor, C.A. (1967). "The shell group methods for thickness design of asphalt pavements." paper presented at the annual meeting of the National Asphalt Paving Association, San Juan, Puerto Rico.

Jakosky, J. (1950). *Exploration geophysics*, Trija Publishing Company, Los Angeles, California.

Jordahl, P. (1985). *ELSDEF users guide*, Brent Rauhut Engineers, Austin, Texas.

Kashyapa, A.S., and Lytton, R.L. (1988). "A simplified mechanistic rut depth prediction procedure for low-volume roads." *Res. Report 473-1*, Texas Transp. Institute, College Station, Texas.

Kenis, W.J. (1977). "Predictive design procedures - a design method for flexible pavements using the VESYS structural subsystem." *Proc. Fourth Int. Conf. on Struct. Design of Asphalt Pavements*, Vol. I. The University of Michigan.

Khedr, S.A., Kraft, D.C., and Jenkins, J.L. (1985). "Automated cone penetrometer: a nondestructive field test for subgrade evaluation." *Transp. Res. Record No. 1022*, Transp. Res. Board, Washington, D.C., 108-115.

Kinchen, R.W., and Temple, W.H. (1980). "Asphaltic concrete overlays of rigid and flexible pavements." *Report No. FHWA/LA-80/147*, Louisiana Department of Transportation and Development.

Klomp, A.J.G., and Niesman, T.W. (1967). "Observed and calculated strains at various depths in asphalt pavements." *Proc. Second Int. Conf. on the Struct. Design of Asphalt Pavements*, Michigan.

Kung, K.Y. (1967). "A new method in correlation studies of pavement deflection and cracking." *Proc. Second Conf. on the Struct. Design of Asphalt Pavements*, University of Michigan, Ann Arbor, 1037-1046.

Kuo, S.S. (1979). "Development of base layer thickness equivalency." *Res. Report No. R-1119*, Res. Laboratory Section, Testing and Res. Division, Michigan Department of Transportation, Lansing, Michigan.

Lambe, T.W., and Whitman, R.V. (1969). *Soil Mechanics*, John Wiley & Sons, Inc., New York.

Lytton, R.L. (1989). "Backcalculation of pavement layer properties." *Nondestructive testing of pavements and backcalculation of moduli*, ASTM STP 1026, American Society for Testing and Materials, Philadelphia, 7-38.

Lytton, R.L., Germann, F., and Chou, Y.J. (1990). "Determination of asphaltic concrete pavement structural properties by nondestructive testing." *NCHRP Report 10-27 - Phase II*, National Cooperative Highway Res. Program, Transp. Res. Board, Washington, D.C.

Lytton, R.L., and Michalak, C.H. (1979). "Flexible pavement deflection using elastic moduli and field measurements." *Res. Report 207-7F*. Texas Transp. Institute, Texas A&M University, College Station, Texas.

Lytton, R.L., Robert, F.L., and Stoffels, S. (1987). "Determination of asphaltic concrete pavement structural properties by nondestructive testing." *NCHRP Report 10-27 - Phase I*, National Cooperative Highway Res. Program, Transp. Res. Board, Washington, D.C.

Magnuson, A. (1988). "Computer analysis of Falling Weight Deflectometer data, part I: vertical displacement computation on the surface of a uniform half-space due to an oscillating surface pressure distribution." *Report FHWA/TX-88/1215-1F*, Texas Transp. Institute, Texas A&M University, College Station, Texas.

Mamlouk, M.S. (1987). "Dynamic analysis of multilayered pavement structures - theory, significance, and verification." *Sixth Int. Conf. on the Structural Design of Asphalt Pavements*, Ann Arbor, Michigan, Vol. I, 466-474.

Marchionna, A., Cesarini, M., Fornaci, M.G., and Malgarini, M. (1985). "Pavement elastic characteristics measured by means of tests conducted with the falling weight deflectometer." *Transp. Res. Record 1007*, Transp. Res. Board, Washington, D.C.

Mahoney, J.P., Coetzee, N.F., Stubstad, R.N., and Lee, S.W. (1989). "A performance comparison of selected backcalculation computer programs." *Nondestructive testing of pavements and backcalculation of layer moduli*, ASTM STP 1026, American Society for Testing and Materials, Philadelphia, 452-467.

McVay, M., and Taesiri, Y. (1985). "Cyclic behavior of pavement base materials." *J. of Geotechnical Engrg.*, ASCE, 3(1), 1-17.

Mooney, H. (1977). *Handbook of engineering geophysics*, Bison Instruments Inc., Minneapolis, Minnesota.

Odemark, N. (1949). *Investigations as to the elastic properties of soils design of pavements according to the theory of elasticity.* Staten Vaeginstitut, Stockholm, Sweden.

Pappin, J.W., and Brown, S.F. (1980). "Resilient stress-strain behavior of a crushed rock." *Int. Symposium on soils under cyclic and transient loading*, Swansea, England, Vol. I, 169-177.

Peffer, J.R., and Robelen, P.G. (1983). "Affordable : overburden mapping using new geophysical techniques." *Pit and Quarry*, August.

Peterson, D.E. (1976). "Asphalt overlays and pavement rehabilitation - evaluating structural adequacy for flexible pavement overlays." *Report No. 8-996*, Utah Department of Transportation, Utah.

Peterson, G., and Shephard, L.W. (1972). *Deflection analysis of flexible pavements.* Final Report, Materials and Test Division, Utah State Department of Highways.

Raad, L., and Figueroa, J.L. (1980). "Load response of transportation support system." *J. of Transp. Engrg.*, ASCE, 106, 111-128.

Ralston, A., and Rabanowitz, P. (1978). *A first course in numerical analysis.* McGraw-Hill, New York.

Richart, F.E., Hall, J.R., and Woods, R.D. (1970). *Vibrations of soils and foundations.* Prentice-Hall International Series in Theoretical and Applied Mechanics, Prentice-Hall, New Jersey.

Robertson, P.K., and Campanella, R.G. (1983). "Interpretation of Cone Penetration Tests." *Canadian Geotechnical Journal*, 20(4).

Robertson, P.K., and Campanella, R.G. (1984). *Guidelines for use and interpretation of the electronic cone penetration test.* The University of British Columbia.

Rodriguez, A.R., Castillo, H. del., and Sowers, G.F. (1988). *Soil mechanics in highway engineering.* Trans Tech Publications, Clausthal-Zellerfeld, Federal Republic of Germany.

Roesset, J.M. (1990). "Development of dynamic analysis techniques for Falling Weight Deflectometer data." Summary report for project 2/3-18-88-1175 presented at the SDHPT area II research committee meeting, Victoria, Texas.

Roesset, J.M. (1987). *Computer Program UTFWIBM*, The University of Texas at Austin, Austin, Texas.

Roesset, J.M., and Shao, K. (1985). "Dynamic interpretation of Dynaflect and Falling Weight Deflectometer tests." *Transp. Res. Record 1022*, Transp. Res. Board, Washington, D.C., 7-16.

Rohde, G.T., and Scullion, T. (1990). *MODULUS 4.0: Expansion and Validation of the MODULUS Backcalculation System.* Res. Report 1123-3. Texas Transp. Institute, College Station, Texas.

Rohde, G.T., Smith, R.E., Lytton, R.L., and Uzan, J. (1989). "A microcomputer based pavement design program." *Proc. Third Int. Conf. on Microcomputers in Transp.*, San Francisco, California.

Rwenbangira, R., Hicks, R.G., and Traube M. (1987). "Sensitivity analysis of selected backcalculation procedures." *Transp. Res. Record 1117*, Transp. Res. Board, Washington, D.C., 25-37.

Scullion, T., Uzan, J., Yazdani, J.I., and Chan, P. (1988). *Field evaluation of the multi-depth deflectometers.* Res. Report 1123-2. Texas Transp. Institute, College Station, Texas.

Sharpe, G.W., Southgate, H.F., and Dean, R.C. (1979). "Pavement evaluation by using dynamic deflections," *Transp. Res. Record No. 700*, Transp. Res. Board, Washington, D.C., 34-45.

Shiffman, R.L. (1962). "General analysis of stresses and displacements in layered elastic systems." *Proc. Int. Conf. on the Structural Design of Asphalt Pavements*, University of Michigan, Vol. I, Ann Arbor, 710-721.

Shook, J.F., Finn, F.N., Witczak, M.W., and Monismith, C.L. (1982). "Thickness design of asphalt pavements - the asphalt institute method." *Fifth Int. Conf. on the Structural Design of Asphalt Pavements*, Delft, the Netherlands, Vol. I, 17-44.

Shrivner, F.H., Moore, W.M., McFarland, W.F., and Carey, G.R. (1968). "A system approach to the flexible pavement design problem." *Res. Report no. 32-11*, Texas Transp. Institute, College Station, Texas.

SHRP. (1989). *SHRP-LTPP manual for FWD testing version 1.0.* Operational field guidelines prepared for the Strategic Highway Res. Program, Washington, D.C.

Smith, R.E., and Lytton, R.L. (1984). "Synthesis study of nondestructive testing devices for use in overlay thickness design of flexible pavements." *FHWA/RD-83/097*, FHWA, U.S. Department of Transportation.

Sneddon, R.V. (1988). "Resilient modulus testing of 14 Nebraska soils." *Report Project No. RESI (0099) P404*, University of Nebraska-Lincoln, Lincoln, Nebraska.

Sorensen, A., and Hayven, M. (1982). "The Dynatest 8000 Falling Weight Deflectometer test system." *Int. Symposium on Bearing Capacity of Roads and Airfields*, Trondheim, Norway.

Southgate, H.F., Sharpe, G.W., and Deen, R.C. (1978). "A rational thickness design system for asphaltic concrete overlays." *Res. Report 507*, Division of Research, Bureau of Highways, Department of Transportation, Commonwealth of Kentucky.

Stewart, M., and Beaven, P.J. (1980). "Seismic refraction surveys for highway engineering purposes." *Report 950*, Transp. and Road Res. Laboratory, Chrowthorne, Berkshire.

Stock, A.F., and Yu, J. (1984). "Use of surface deflection for pavement design and evaluation." *Transp. Res. Record No. 930*, Transp. Res. Board, Washington, D.C., 64-69.

Stubstad, R.N. (1988). *The use of and users guide for the Dynatest ISSEM4 computer program*, Unpublished Dynatest Group Documentation for ISSEM4 Users.

Thompson, M.R. (1989a). "Calibrated mechanistic structural procedures for pavements." *NCHRP Report 1-26*, National Cooperative Res. Program, Transp. Res. Board, Washington, D.C.

Thompson, M.R. (1989b). "Factors affecting the resilient moduli of soils and granular materials." paper presented at the workshop on resilient modulus testing. Oregon State University, Corvallis, Oregon, March 28-30.

Thompson, M.R., and Robnett, Q.L. (1976). "Resilient response of subgrade soils." *Civil Engrg. Studies Series No. 160*, University of Illinois, Urbana-Champaign, Ill.

Thrower, E.N., Lister, N.W., and Potter, J.F. (1972). "Experimental and theoretical studies of pavement behavior under vehicular loading in relation to elastic theory." *Proc. Third Int. Conf. on the Structural Design of Asphalt Pavements*, Michigan.

Uddin, W., and McCullough, B.F. (1989). "In situ material properties from dynamic deflection equipment." *Nondestructive testing of pavements and backcalculation of moduli*, ASTM STP 1026, American Society for Testing and Materials, Philadelphia, 278-290.

Uddin, W., Meyer, A.H., and Hudson, W.R. (1986). "Rigid bottom considerations for nondestructive evaluation of pavements." *Transp. Res. Record 1070*, Transp. Res. Board, Washington, D.C., 21-29.

Ullitz, P. (1973). "The use of dynamic plate loading tests in design of overlays." *Proc. Conf. of Road Engrg. in Asia and Australia*, Kuala Lumpur.

Ullitz, P. (1987). *Pavement Analysis.* Developments in Civil Engineering No. 19, Elsevier, New York.

Ullidtz, P., and Stubstad, R.N. (1985). "Analytical-empirical pavement evaluation using the Falling Weight Deflectometer." *Transp. Res. Record 1022*, Transp. Res. Board, Washington, D.C., 36-43.

Uzan, J. (1985). "Characterization of granular materials." *Transp. Res. Record 1022*, Transp. Res. Board, Washington, D.C., 52-59.

Uzan, J., Lytton, R.L., and German, F.P. (1989). "General procedure for backcalculating layer moduli." *Nondestructive testing of pavements and backcalculation of moduli*, ASTM STP 1026, American Society for Testing and Materials, Philadelphia, 217-228.

Uzan, J., Rohde, G.T., Smith, R.E., and Lytton, R.L. (1989). "The new Texas flexible pavement design system." *Res. Report 2455*, Texas Transp. Institute, College Station, Texas.

Uzan, J., and Scullion, T. (1990). "Verification of backcalculation procedures." *Proc. Third Int. Conf. on the Bearing Capacity of Roads and Airfields,* Trondheim, Norway.

Uzan, J., Scullion, T., Michalek, C.H., Parades, M., and Lytton, R.L. (1988). "A microcomputer based procedure to backcalculate layer moduli from FWD data." *Res. Report 2-18-87-1123-1*, Texas Transp. Institute, College Station, Texas.

Vaswani, N.K. (1971). "Method for seperately evaluating structural performance of subgrades and overlying flexible pavements." *Highway Res. Record 362*, Highway Res. Board, 48-62.

"The WASHO road test." (1954). *Special Report 18*, Highway Res. Board, National Academy of Sciences, Washington D.C.

Wilson, E.L. (1965). "Structural analysis of axisymmetric solids." *J. AIAA*, 3(12).

Witczak, M.W., and Uzan, J. (1988). *The universal airport pavement design system, report I of IV : granular material characterization*, Dept. of Civil Engrg., University of Maryland, College Park, Maryland.

Yang, N.C. (1972). *Design of functional pavements.* McGraw-Hill Book Company, New York.

Yang, W. (1988). *Mechanistic analysis of nondestructive pavement deflection data.* PhD Dissertation, Cornell University, Ithaca, New York.

Yazdani, J.I. (1989). *Using the multi-depth deflectometer to study pavement response.* MSc Thesis. Texas A&M University, College Station, Texas.

Yoder, E.J., and Witczak, M.W. (1975). *Principles of pavement design.* Second Edition, John Wiley and Sons, New York.

Zienkiewicz, O.C., and Cheung, Y.K. (1967). *The finite element method in structural and continuum mechanics.* McGraw-Hill, London.

APPENDIX A

LABORATORY RESULTS

Table A1. The Laboratory Results for Site 1.

LABORATORY RESULTS FOR SITE 1								
ASPHALT			BASE			SUBGRADE		
Freq (Hz)	Temp (°F)	M_R (ksi)	σ_3 (psi)	σ_d (psi)	M_R (ksi)	σ_3 (psi)	σ_d (psi)	M_R (ksi)
TOP			1	5.0	18.5	0	2.05	19.1
10	0	1770	5	5.0	46.1	3	2.21	42.2
10	32	1090	1	9.8	16.5	0	3.90	16.8
10	77	710	5	9.9	27.7	3	3.80	23.2
10	100	140	10	9.9	44.8	6	3.90	29.1
20	0	1890	15	9.7	64.6	0	7.80	12.3
20	32	1480	25	9.9	104.2	3	7.80	17.5
20	77	650	1	14.8	18.3	6	7.89	16.1
20	100	220	5	14.7	27.6	0	10.13	12.9
BOTTOM			10	14.6	38.3	3	10.07	15.4
10	0	1790	15	14.7	52.9	6	10.00	17.5
10	32	1210	25	14.5	64.4			
10	77	720	10	24.6	37.0			
10	100	240	15	25.2	46.8			
20	0	1990	25	25.5	67.0			
20	32	1850	15	39.3	52.6			
20	77	970	25	37.9	75.8			
20	100		25	48.8	78.4			
* Test not Successful								

Table A2. The Laboratory Results for Site 2.

LABORATORY RESULTS FOR SITE 2								
ASPHALT			BASE			SUBGRADE		
Freq (Hz)	Temp (°F)	M_R (ksi)	σ_3 (psi)	σ_d (psi)	M_R (ksi)	σ_3 (psi)	σ_d (psi)	M_R (ksi)
TOP			1	9.8	14.8	0	1.86	5.3
10	0	2240	5	10.2	18.4	3	1.86	7.0
10	32	1370	10	10.3	28.8	6	1.71	9.3
10	77	670	20	10.2	41.4	0	3.74	4.5
10	100	250	30	10.8	47.4	3	3.74	5.8
20	0	2160	5	16.6	7.6	6	3.81	7.6
20	32	1510	10	20.7	23.6	3	7.56	3.3
20	77	710	20	21.0	36.7	6	7.96	6.0
20	100	280	30	21.0	44.0			
BOTTOM			20	36.5	32.5			
10	0		30	36.6	39.5			
10	32		20	46.7	36.5			
10	77		30	47.0	43.6			
10	100		20	62.6	34.9			
20	0		30	63.3	44.6			
20	32							
20	77							
20	100							

Table A3. The Laboratory Results for Site 4.

LABORATORY RESULTS FOR SITE 4								
ASPHALT			BASE			SUBGRADE		
Freq (Hz)	Temp (°F)	M_R (ksi)	σ_3 (psi)	σ_d (psi)	M_R (ksi)	σ_3 (psi)	σ_d (psi)	M_R (ksi)
TOP			1	4.9	13.4	0	1.95	11.4
10	0	2010	5	5.1	22.1	3	2.04	12.4
10	32	1170	10	4.9	31.4	6	1.98	12.4
10	77	510	15	5.1	35.1	0	3.86	6.7
10	100	70	20	5.1	39.3	3	3.92	7.3
20	0	1900	1	10.0	10.4	6	3.83	7.4
20	32	1330	5	10.0	15.6	0	7.79	3.3
20	77	460	10	10.0	21.1	3	7.86	3.5
20	100	90	15	19.9	27.1	6	7.63	4.5
BOTTOM			20	9.9	36.1	0	9.68	2.9
10	0	1580	1	14.7	9.2	3	9.74	3.6
10	32	990	5	14.7	14.5	6	9.90	2.1
10	77	330	10	14.8	19.2			
10	100	60	15	14.8	25.0			
20	0	1560	20	14.8	31.5			
20	32	1190	10	25.0	15.9			
20	77	400	15	24.8	17.9			
20	100	100	25	24.8	26.0			
			15	39.7	16.9			
			25	40.3	19.6			
			25	49.6	22.5			

Table A4. The Laboratory Results for Site 5.

LABORATORY RESULTS FOR SITE 5								
ASPHALT			BASE			SUBGRADE		
Freq (Hz)	Temp (°F)	M_R (ksi)	σ_3 (psi)	σ_d (psi)	M_R (ksi)	σ_3 (psi)	σ_d (psi)	M_R (ksi)
TOP			1	4.9	12.9	0	1.99	7.5
10	0	2040	5	4.8	69.9	3	2.06	8.6
10	32	960	1	9.6	8.7	6	1.96	9.6
10	77	320	5	9.6	23.3	0	3.73	5.7
10	100	60	10	9.8	54.0	3	3.86	7.1
20	0	2220	15	9.8	84.3	6	3.86	7.9
20	32	1490	1	14.9	8.3	0	7.60	3.7
20	77	360	5	14.6	13.9	3	7.63	4.4
20	100	90	10	14.7	26.1	6	7.82	5.0
BOTTOM			15	14.8	45.0	0	9.61	2.7
10	0		25	14.9	77.6	3	9.84	3.2
10	32		10	24.4	19.2	6	9.97	4.2
10	77		15	24.6	26.9			
10	100		25	24.6	41.4			
20	0		15	39.2	21.6			
20	32		25	39.2	30.3			
20	77		25	47.8	28.4			
20	100							

Table A5. The Laboratory Results for Site 6.

LABORATORY RESULTS FOR SITE 6								
ASPHALT			BASE			SUBGRADE		
Freq (Hz)	Temp (°F)	M_R (ksi)	σ_3 (psi)	σ_d (psi)	M_R (ksi)	σ_3 (psi)	σ_d (psi)	M_R (ksi)
TOP			1	10.2	13.8	0	2.14	21.2
10	0		5	10.1	20.3	3	2.11	22.7
10	32		10	10.3	22.0	6	2.07	28.3
10	77		20	10.7	32.6	0	3.89	9.9
10	100		30	10.8	40.4	3	3.83	10.7
20	0		5	20.2	14.6	6	4.09	12.3
20	32		10	21.0	20.8	0	7.82	2.7
20	77		20	21.4	29.5	3	8.05	5.4
20	100		30	21.5	36.7	6	8.44	6.3
BOTTOM			10	35.6	17.9	0	9.83	2.5
10	0		20	36.8	27.8	3	9.90	3.3
10	32		30	37.1	39.0	6	9.77	4.6
10	77		20	47.3	32.6			
10	100		30	47.9	42.7			
20	0		30	63.9	42.0			
20	32							
20	77							
20	100							

Table A6. The Laboratory Results for Site 7.

LABORATORY RESULTS FOR SITE 7								
ASPHALT			BASE			SUBGRADE		
Freq (Hz)	Temp (°F)	M_R (ksi)	σ_3 (psi)	σ_d (psi)	M_R (ksi)	σ_3 (psi)	σ_d (psi)	M_R (ksi)
TOP			1	5.2	45.1	0	2.1	5.3
10	0	1710	5	5.3	91.6	3	2.0	6.3
10	32	1260	1	10.0	23.3	6	1.9	7.0
10	77	870	5	10.1	24.9	0	4.1	5.2
10	100	150	10	10.0	100.4	3	4.0	5.7
20	0	1970	1	15.0	21.7	6	3.9	5.8
20	32	1430	5	15.0	25.5	0	8.2	4.0
20	77	810	10	14.9	111.4	3	8.2	4.5
20	100	200	10	24.9	44.4	6	8.5	4.8
BOTTOM			15	24.7	84.2	0	10.3	3.5
10	0	1700	25	24.7	163.7	3	10.4	4.0
10	32	1030	15	39.6	51.9	6	10.3	4.2
10	77	600	25	40.0	154.0			
10	100	160	25	48.8	79.0			
20	0	1860						
20	32	-*						
20	77	600						
20	100	210						
* Test not Successful								

Table A7. The Laboratory Results for Site 8.

LABORATORY RESULTS FOR SITE 8								
ASPHALT			BASE			SUBGRADE		
Freq (Hz)	Temp (°F)	M_R (ksi)	σ_3 (psi)	σ_d (psi)	M_R (ksi)	σ_3 (psi)	σ_d (psi)	M_R (ksi)
TOP						0	1.9	13.9
10	0	1850				3	1.9	14.9
10	32	1220				6	1.9	19.3
10	77	610				0	3.9	9.9
10	100	200				3	4.0	11.0
20	0	2000				6	4.0	11.8
20	32	1580				0	6.4	4.7
20	77	650				3	6.3	5.5
20	100	220				6	6.3	6.1
BOTTOM						0	9.6	4.4
10	0	2010				3	9.4	5.7
10	32	1150				6	9.6	7.5
10	77	390						
10	100	120						
20	0	2330						
20	32	1510						
20	77	590						
20	100	150						

Table A8. The Laboratory Results for Site 9.

LABORATORY RESULTS FOR SITE 9								
ASPHALT			BASE			SUBGRADE		
Freq (Hz)	Temp (°F)	M_R (ksi)	σ_3 (psi)	σ_d (psi)	M_R (ksi)	σ_3 (psi)	σ_d (psi)	M_R (ksi)
TOP						0	1.9	25.5
10	0	1340				3	2.0	22.4
10	32	600				6	2.1	23.1
10	77	270				0	3.9	11.7
10	100	80				3	3.9	13.0
20	0	1780				6	3.9	13.9
20	32	1150				0	6.1	5.1
20	77	280				3	6.2	6.1
20	100	90				6	6.2	6.7
BOTTOM						0	9.7	5.3
10	0					3	9.7	6.7
10	32					6	9.7	7.8
10	77							
10	100							
20	0							
20	32							
20	77							
20	100							

Table A9. The Laboratory Results for Site 11.

LABORATORY RESULTS FOR SITE 11								
ASPHALT			BASE			SUBGRADE		
Freq (Hz)	Temp (°F)	M_R (ksi)	σ_3 (psi)	σ_d (psi)	M_R (ksi)	σ_3 (psi)	σ_d (psi)	M_R (ksi)
TOP			1	9.9	15.6			
10	0	1760	5	10.0	19.8			
10	32	890	1	14.9	13.0			
10	77	380	5	14.9	14.0			
10	100	220	10	14.8	17.6			
20	0	1750	15	14.9	21.5			
20	32	1020	25	14.9	74.2			
20	77	560	10	24.8	12.7			
20	100	260	15	24.8	14.7			
BOTTOM			25	24.7	31.2			
10	0	2220	15	39.8	19.9			
10	32	1260	25	39.5	22.8			
10	77	700	25	48.4	22.8			
10	100	430						
20	0	2110						
20	32	1770						
20	77	960						
20	100	510						

Table A10. The Laboratory Results for Site 12.

LABORATORY RESULTS FOR SITE 12								
ASPHALT			BASE			SUBGRADE		
Freq (Hz)	Temp (°F)	M_R (ksi)	σ_3 (psi)	σ_d (psi)	M_R (ksi)	σ_3 (psi)	σ_d (psi)	M_R (ksi)
TOP			1	9.8	24.7	1	2.1	35.9
10	0	2030	5	9.8	27.4	1	5.3	22.9
10	32	1140	5	18.5	17.4	1	8.1	19.3
10	77	580	10	10.3	48.7	1	11.6	16.3
10	100	190	10	21.1	31.7	4	5.2	29.7
20	0	2010	20	21.1	45.6	4	8.2	25.4
20	32	1330	20	35.5	51.7	4	11.8	21.9
20	77	560				8	5.2	46.3
20	100	210				8	8.2	31.0
BOTTOM						8	11.8	26.8
10	0							
10	32							
10	77							
10	100							
20	0							
20	32							
20	77							
20	100							

APPENDIX B

SUBGRADE INFORMATION

Table B1. Subgrade Information for Site 1.

SUBGRADE INFORMATION FROM THE DRILLERS LOG			
Depth from Surface (feet)	Material Description	Moisture Content (%)	Density (pcf)
2.30 - 5.30	Sandy Subgrade	14.9 14.9	104.7 108.0
5.30 - 8.30	Sandy Clay Subgrade	-	-
8.30 -12.00	Sandy Subgrade	-	-

SUBGRADE INFORMATION FROM SOIL SURVEY SERIES*	
Soil Name and Symbol	Nueces (Nu)
Description	Fine Sand (Top ±22 inches) Sandy Clay Loam (±22 - 76 inches)
Unified Soil Classification	SP-SM, SM, SM-SC, SC
AASHTO Soil Classification	A-2-4, A-3, A-2-6, A2-4

* Map Sheet 11 of the *Soil Survey of Willacy County Texas* as published by the US Department of Agriculture's Soil Conservation Service (December 1982)

Table B2. Subgrade Information for Site 2.

SUBGRADE INFORMATION FROM THE DRILLERS LOG			
Depth from Surface (feet)	Material Description	Moisture Content (%)	Density (pcf)
0.83 - 3.83	Sandy Subgrade	13.4 13.2	100.0 103.2
3.83 - 6.83	Sandy Subgrade	-	-
6.83 -	Sandy Subgrade	-	-

SUBGRADE INFORMATION FROM SOIL SURVEY SERIES*	
Soil Name and Symbol	Latia (Le)
Description	Sandy Clay Loam (Top ±04 inches) Sandy Clay Loam (±04 - 60 inches)
Unified Soil Classification	CL
AASHTO Soil Classification	A-4, A-6, A-7-6

* Map Sheet 14 of the *Soil Survey of Willacy County Texas* as published by the US Department of Agriculture's Soil Conservation Service (December 1982)

Table B3. Subgrade Information for Site 4.

SUBGRADE INFORMATION FROM THE DRILLERS LOG

Depth from Surface (feet)	Material Description	Moisture Content (%)	Density (pcf)
0.75 - 3.75	Clay Subgrade	24.5 24.6	88.4 93.4
3.75 - 9.75	Clay Subgrade	-	-
9.75 - 15.0	Clay Subgrade	-	-

SUBGRADE INFORMATION FROM SOIL SURVEY SERIES*

Soil Name and Symbol	Hildago (HoA)
Description	Sandy Clay Loam(Top ±42 inches) Clay Loam (±42 - 60 inches)
Unified Soil Classification	SC, CL
AASHTO Soil Classification	A-6, A-7-6

* Map Sheet 23 of the *Soil Survey of Willacy County Texas* as published by the US Department of Agriculture's Soil Conservation Service (December 1982)

Table B4. Subgrade Information for Site 5.

SUBGRADE INFORMATION FROM THE DRILLERS LOG

Depth from Surface (feet)	Material Description	Moisture Content (%)	Density (pcf)
1.00 - 4.00	Sandy Clay Subgrade	16.3 15.7	101.0 10.34
4.00 - 8.00	Sandy Clay Subgrade (more clayey)	-	-

SUBGRADE INFORMATION FROM SOIL SURVEY SERIES*

Soil Name and Symbol	Racombes (48)
Description	Sandy Clay Loam (Top ±13 inches) Sandy Clay Loam (±13 - 49 inches) Sandy Clay Loam (±49 - 72 inches)
Unified Soil Classification	CL, SC
AASHTO Soil Classification	A-4, A-6, A-7

* Map Sheet 78 of the *Soil Survey of Hidalgo County Texas* as published by the US Department of Agriculture's Soil Conservation Service (June 1981)

Table B5. Subgrade Information for Site 6.

SUBGRADE INFORMATION FROM THE DRILLERS LOG			
Depth from Surface (feet)	Material Description	Moisture Content (%)	Density (pcf)
0.75 - 3.75	Clay Subgrade	16.4 20.0 20.5	92.8 102.2 102.5
3.75 - 11.75	Clay Subgrade	-	-

SUBGRADE INFORMATION FROM SOIL SURVEY SERIES*	
Soil Name and Symbol	Hidalgo (28)
Description	Sandy Clay Loam (Top ±28 inches) Clay Loam (±28 - 80 inches)
Unified Soil Classification	SC, CL
AASHTO Soil Classification	A-6, A-7-6

* Map Sheet 68 of the *Soil Survey of Hidalgo County Texas* as published by the US Department of Agriculture's Soil Conservation Service (June 1981)

Table B6. Subgrade Information for Site 7.

SUBGRADE INFORMATION FROM THE DRILLERS LOG			
Depth from Surface (feet)	Material Description	Moisture Content (%)	Density (pcf)
1.75 - 4.75	Clay Subgrade	9.7 21.1 21.8	130.9 107.5 100.8
4.75 - 6.75	Clay Subgrade	-	-
6.75 - 9.75	Sandy Clay Subgrade	-	-

SUBGRADE INFORMATION FROM SOIL SURVEY SERIES*	
Soil Name and Symbol	Leeray (21)
Description	Clay (Top ±43 inches) Clay, Silty Clay (±43 - 65 inches)
Unified Soil Classification	CH, CL
AASHTO Soil Classification	A-7-6, A-6

* Map Sheet 7 of the *Soil Survey of Callahan County Texas* as published by the US Department of Agriculture's Soil Conservation Service (August 1981)

Table B7. Subgrade Information for Site 8.

SUBGRADE INFORMATION FROM THE DRILLERS LOG			
Depth from Surface (feet)	Material Description	Moisture Content (%)	Density (pcf)
1.75 - 4.75	Clay Subgrade	17.8 18.2	118.9 118.7
4.75 - 7.75	Clay Subgrade	-	-
7.75 - 12.5	Sandy Clay Subgrade	-	-

SUBGRADE INFORMATION FROM SOIL SURVEY SERIES*	
Soil Name and Symbol	Mangum (Ma)
Description	Silt Loam (Top ±09 inches) Silty Clay (±09 - 54 inches) Clay (±54 - 81 inches)
Unified Soil Classification	CH, CL
AASHTO Soil Classification	A-7-6, A-6, A-7

* Map Sheet 10 of the *Soil Survey of Taylor County Texas* as published by the US Department of Agriculture's Soil Conservation Service (December 1976)

Table B8. Subgrade Information for Site 9.

SUBGRADE INFORMATION FROM THE DRILLERS LOG			
Depth from Surface (feet)	Material Description	Moisture Content (%)	Density (pcf)
0.75 - 3.75	Clay Subgrade	7.7 8.5	133.2 127.1
3.75 -10.75	Clay Subgrade	-	-

SUBGRADE INFORMATION FROM SOIL SURVEY SERIES*	
Soil Name and Symbol	Sagerton (SaA)
Description	Clay Loam (Top ±11 inches) Clay (±11 - 33 inches) Clay Loam (±33 - 80 inches)
Unified Soil Classification	CL
AASHTO Soil Classification	A-6, A-4, A-7

* Map Sheet 25 of the *Soil Survey of Taylor County Texas* as published by the US Department of Agriculture's Soil Conservation Service (December 1976)

Table B9. Subgrade Information for Site 11.

SUBGRADE INFORMATION FROM THE DRILLERS LOG			
Depth from Surface (feet)	Material Description	Moisture Content (%)	Density (pcf)
1.92 - 4.92	Sand Subgrade	20.4	94.5
4.92 - 6.5	Sand Subgrade	19.5	95.2

SUBGRADE INFORMATION FROM SOIL SURVEY SERIES*	
Soil Name and Symbol	Tivoli (Tf)
Description	Fine Sand (±00 - 90 inches)
Unified Soil Classification	SP-SM
AASHTO Soil Classification	A-3

* Map Sheet 17 of the *Soil Survey of Mitchell County Texas* as published by the US Department of Agriculture's Soil Conservation Service (April 1969)

Table B10. Subgrade Information for Site 12.

SUBGRADE INFORMATION FROM THE DRILLERS LOG			
Depth from Surface (feet)	Material Description	Moisture Content (%)	Density (pcf)
0.75 - 3.75	Sand Subgrade	15.7	90.7
		14.6	96.8
3.75 - 6.75	Sand Subgrade	-	-
6.75 - 9.75	White Sandy Subgrade	-	-
9.75 - 12.0	White Sandy Subgrade	-	-

SUBGRADE INFORMATION FROM SOIL SURVEY SERIES*	
Soil Name and Symbol	Cobb (CmB)
Description	Fine Sandy Loam (Top ±08 inches)
	Sandy Clay Loam (±08 - 30 inches)
Unified Soil Classification	Sandstone (weakly cemented)
AASHTO Soil Classification	SM, SC, Cl
	A-4, A-2, A-6

* Map Sheet 25 of the *Soil Survey of Mitchell County Texas* as published by the US Department of Agriculture's Soil Conservation Service (April 1969)

APPENDIX C

SOIL SURVEY MAPS

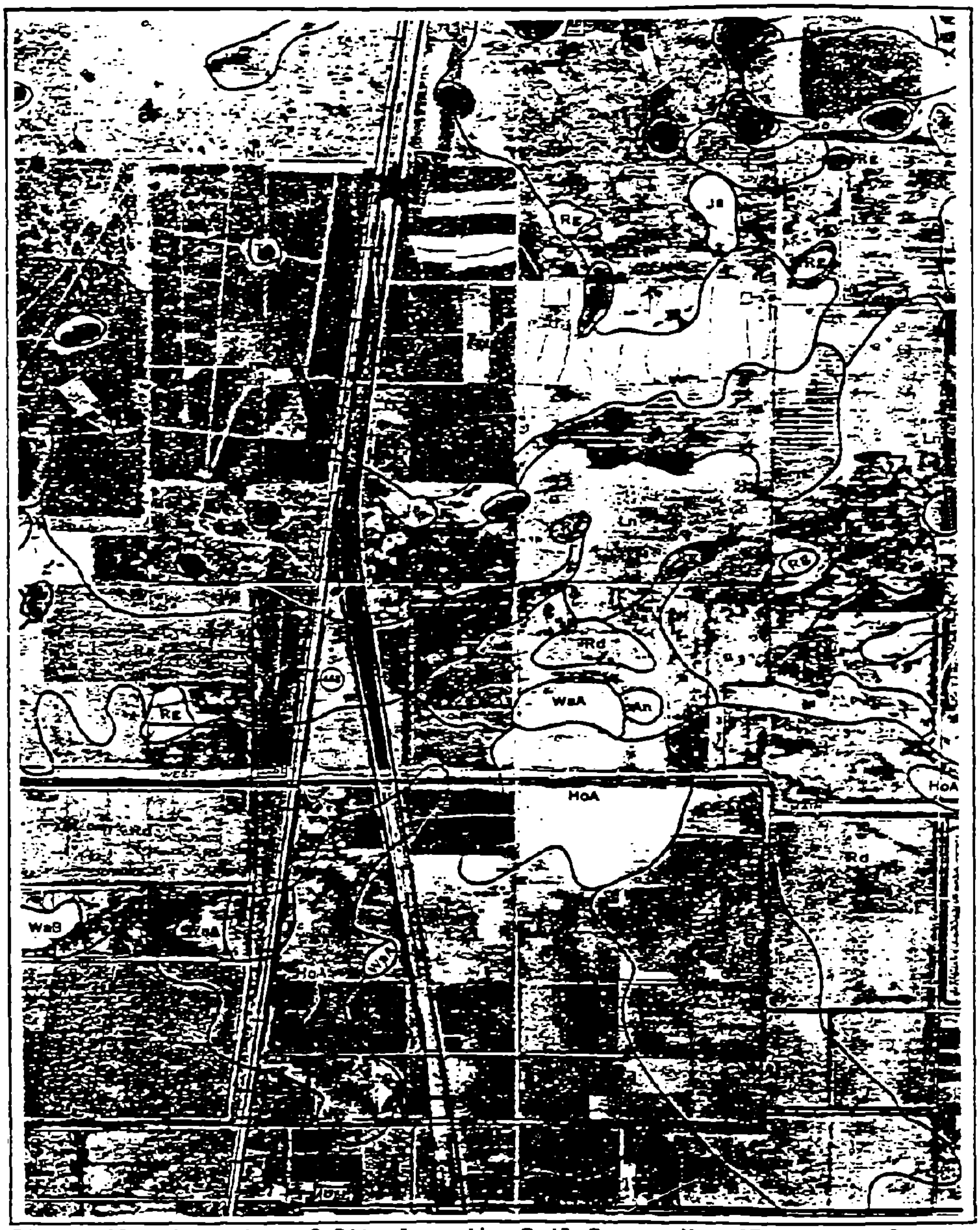

Figure C1. Location of Site 1 on the Soil Survey Map (Extracted from Sheet 11 of the *Soil Survey for Willacy County Texas* as published by the US Department of Agriculture's Soil Conservation Service).

Figure C2. Location of Site 2 on the Soil Survey Map (Extracted from Sheet 14 of the *Soil Survey for Willacy County Texas* as published by the US Department of Agriculture's Soil Conservation Service).

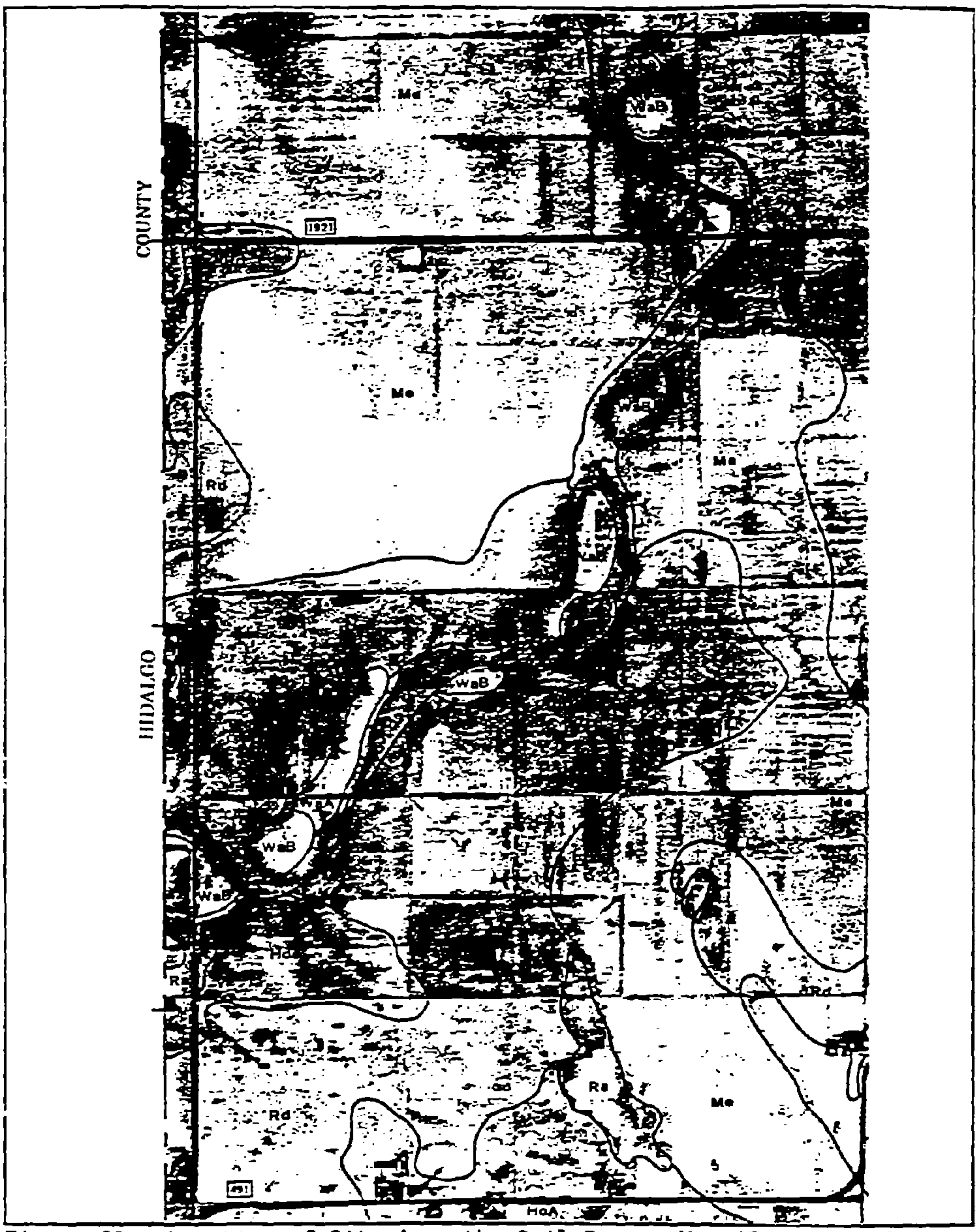

Figure C3. Location of Site 4 on the Soil Survey Map (Extracted from Sheet 23 of the *Soil Survey for Willacy County Texas* as published by the US Department of Agriculture's Soil Conservation Service).

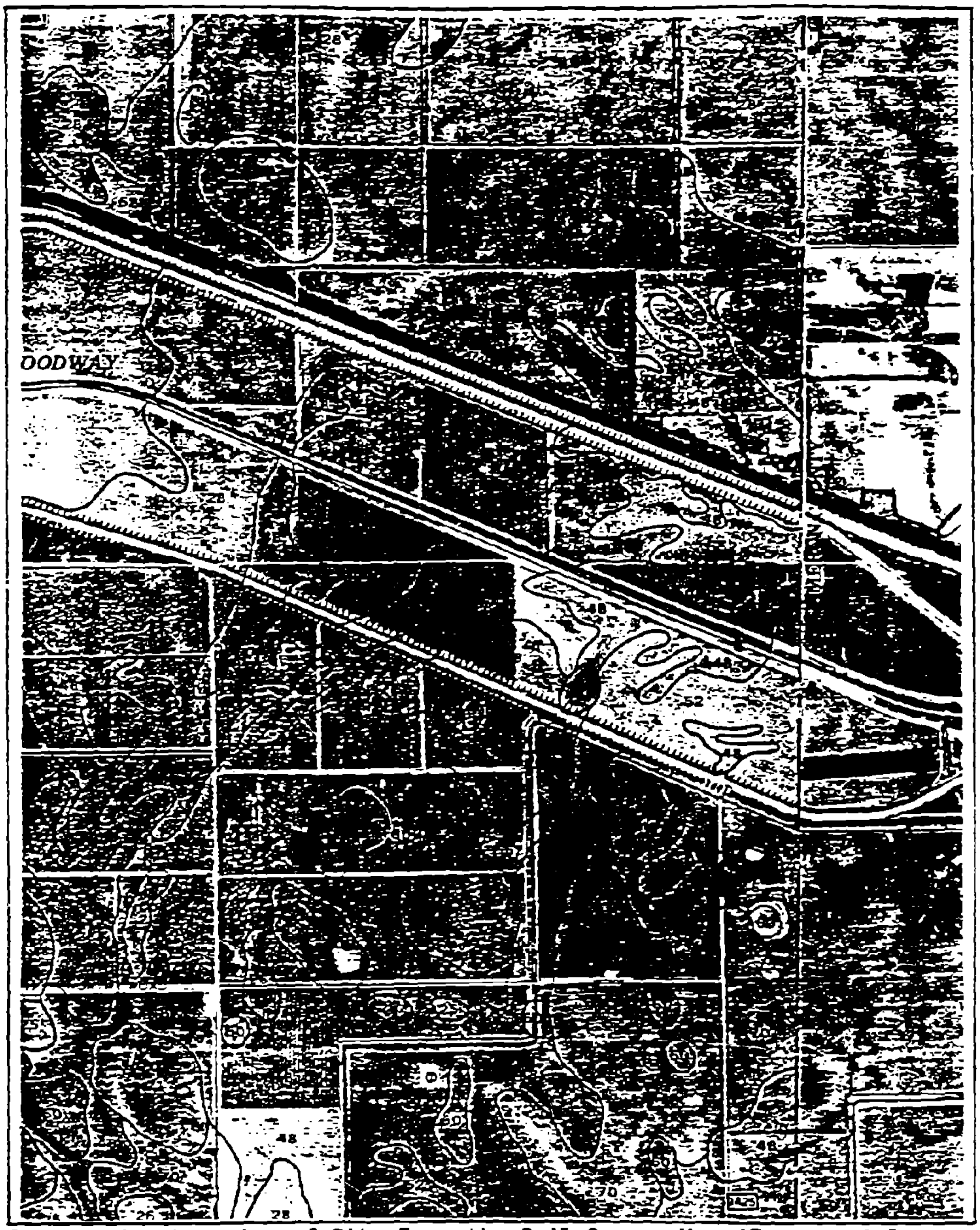

Figure C4. Location of Site 5 on the Soil Survey Map (Extracted from Sheet 78 of the *Soil Survey for Hidalgo County Texas* as published by the US Department of Agriculture's Soil Conservation Service).

Figure C5. Location of Site 6 on the Soil Survey Map (Extracted from Sheet 68 of the *Soil Survey for Hidalgo County Texas* as published by the US Department of Agriculture's Soil Conservation Service).

[redacted]

Figure C6. Location of Site 7 on the Soil Survey Map (Extracted from Sheet 7 of the *Soil Survey for Callahan County Texas* as published by the US Department of Agriculture's Soil Conservation Service).

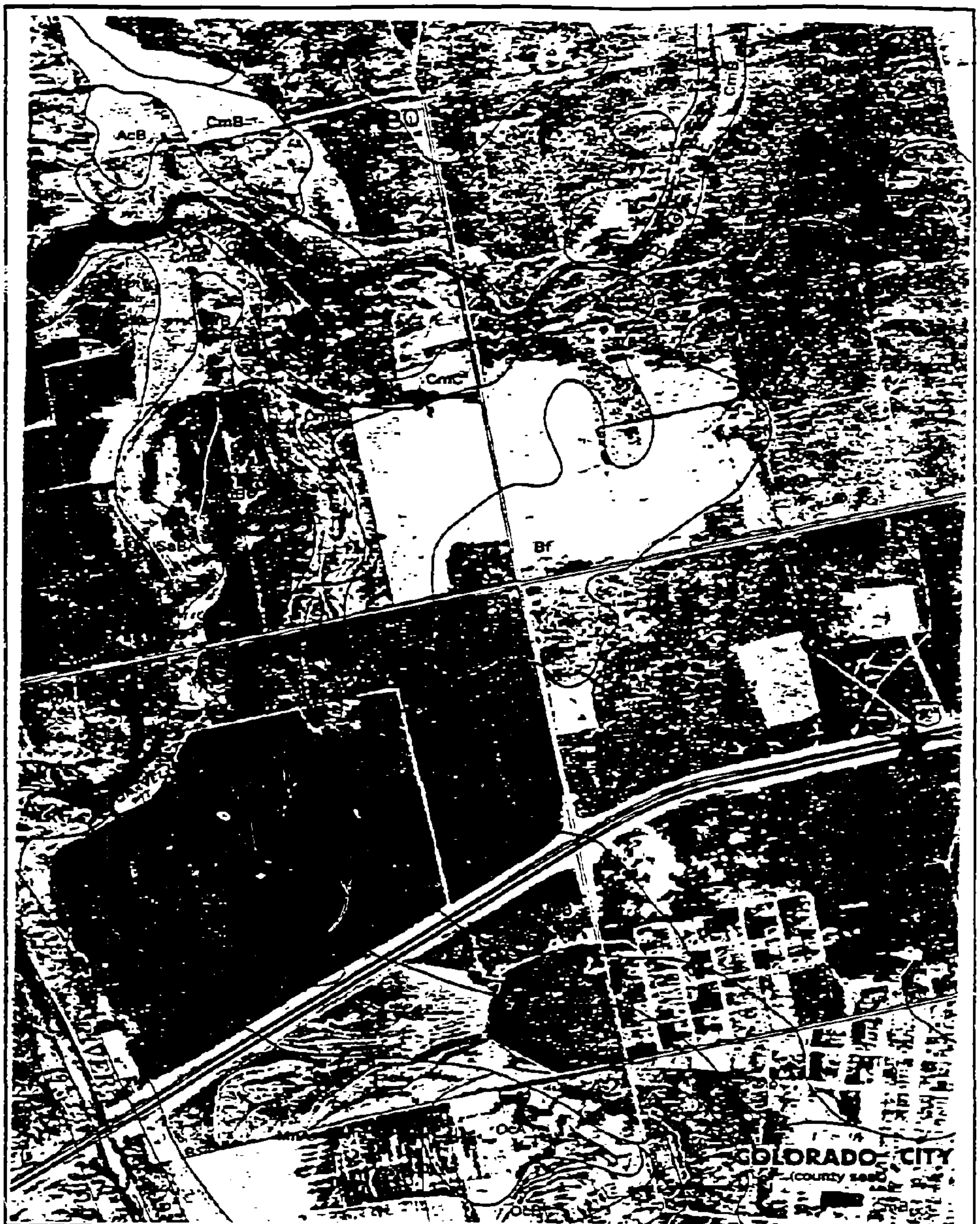

Figure C7. Location of Site 8 on the Soil Survey Map (Extracted from Sheet 10 of the *Soil Survey for Taylor County Texas* as published by the US Department of Agriculture's Soil Conservation Service).

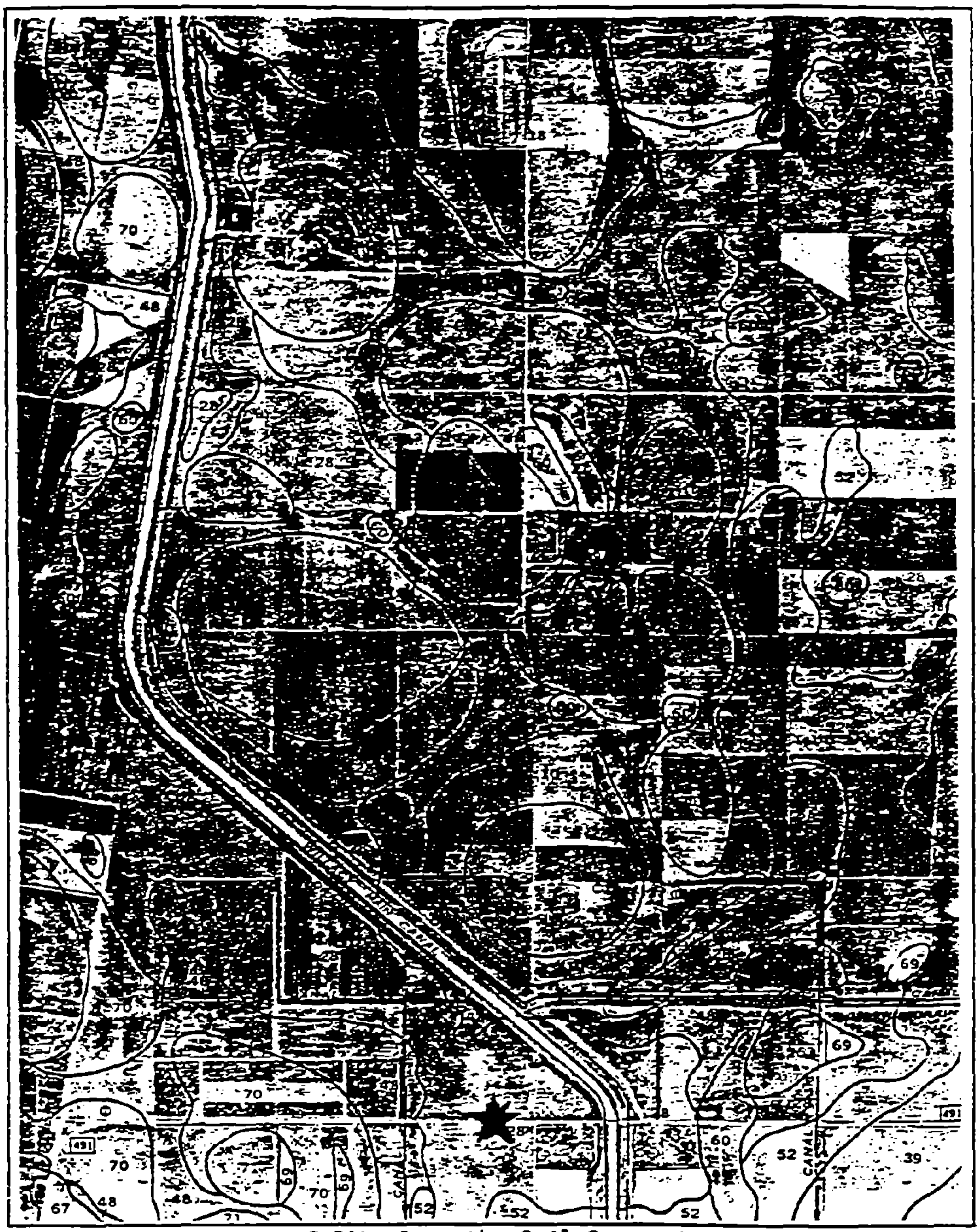

Figure C8. Location of Site 9 on the Soil Survey Map (Extracted from Sheet 25 of the *Soil Survey for Taylor County Texas* as published by the US Department of Agriculture's Soil Conservation Service).

Figure C9. Location of Site 11 on the Soil Survey Map (Extracted from Sheet 17 of the *Soil Survey for Mitchell County Texas* as published by the US Department of Agriculture's Soil Conservation Service).

Figure C10. Location of Site 12 on the Soil Survey ~~Map~~ Map (Extracted from Sheet 25 of the *Soil Survey for Mitchell County Texas* as published by the US Department of Agriculture's Soil Conservation Service).